FRICAULT, VALERIE JOY, M.S. Effects of Exposure to Aluminum Oxide (AL_2O_3) and Cerium Oxide (CeO_2) Nanoparticles on Human Alveolar Cells *in vitro*. (2018)
Directed by Dr. Ramji Bhandari. 100 pp.

Manufactured aluminum oxide and cerium oxide nanoparticles are regularly released into the environment, yet there are presently no regulations to monitor their non-acute effects on respiratory health. The present study, therefore, examined effects of aluminum oxide (AL_2O_3) and cerium oxide (CeO_2) nanoparticles on human alveolar cells *in vitro*. ATCC A549 human alveolar carcinoma cells were exposed to two different concentrations of these two different nanoparticles to test for cellular and molecular phenotypes, particularly cell viability, oxidative stress, disease marker gene expression and epigenetic responses. Samples were collected at 22 and 88 hours of incubation with and without nanoparticles, representing cells grown to one and four population doublings. Viability and cell health were measured using flow cell cytometry, a fluorescent alamarBlue® assay and total SOD assay. DNA and RNA were extracted from multiple cell samples at 22 and 88 hours of exposure. The extracted DNA was used to assess global DNA methylation and RNA was converted to cDNA to quantify gene expression. The mRNA levels of 15 genes, which are known to transcribe immunological and epigenetic traits, were measured by quantitative realtime PCR. The immunological genes assayed were *SOD*, *SESN*, *iNOS*, *IL-6*, *IL-33*, *HLA-B*, *IRF8*, *CD44* and *TNFα*. The epigenetic marker genes assayed were *DNMT1*, *DNMT3A*, *EZH1*, *KMT2D*, *EHMT1* and *DOT1*. Neither of the nanoparticle types nor concentrations affected viability of A549 cells, yet every experimental condition had effects on one or more gene transcript levels. The low concentration Al_2O_3 showed a decrease in global DNA methylation in 22 hours, while the high concentration showed an increase in 88 hours. *DNMT1* expression increased with exposure to AL_2O_3 with the high concentration in 22 hours suggesting an increased maintenance of genome DNA methylation during the first doubling of cells due to exposure. Conversly, two conditions of AL_2O_3 exposure caused a decrease in

DNMT3A, the *de novo* methylator. Histone methylation gene *DOT1L* decreased in the Low 88 group. Pro-inflammatory *HLA-B* transcripts increased in the High group in 88 hours. ROS reducing *SESN3* transcript levels decreased within 22 hours incubation. Cells exposed to varying concentrations of CeO_2 nanoparticles showed a tendency to increase both *DNMT1* and *DNMT3A* transcript levels as well as *HLA-B* and asthma exacerbation indicator *IL-6*. Similar to the response of AL_2O_3 exposed cells, there was a decrease in *DOT1L* expression and *SESN3* expression in CeO_2 exposed cells, suggesting that both Al_2O_3 and CeO_2 nanoparticles induce epigenetic modifications at various levels of biological organization. The present study, therefore, suggests that these nanoparticle exposures can lead to increased oxidative stress, activation of cancer and asthma related genes, and epigenetic alterations without affecting the viability of A549 alveolar cells.

EFFECTS OF EXPOSURE TO ALUMINUM OXIDE (AL_2O_3) AND CERIUM OXIDE (CEO_2) NANOPARTICLES ON HUMAN ALVEOLAR CELLS *IN VITRO*

by

Valerie Joy Fricault

A Thesis Submitted to
the Faculty of The Graduate School at
The University of North Carolina at Greensboro
in Partial Fulfillment
of the Requirements for the Degree
Master of Science

Greensboro
2018

Approved by

_____
Committee Chair

To my beloved husband, Mark Francis Fricault, my children Danielle Rae Fricault and Christopher Louis Fricault, my parents Louis Marion and Marguerite Joan Azbart and to my mother-in-law, Louise Mae Fricault and late father-in-law, Francis Edward Fricault. Thank you for your patience!

APPROVAL PAGE

This thesis written by Valerie Joy Fricault has been approved by the following committee of the Faculty of The Graduate School at The University of North Carolina at Greensboro.

Committee Chair _____

Committee Members _____

_____

_____
Date of Acceptance by Committee

_____
Date of Final Oral Examination

ACKNOWLEDGMENTS

For their ideas, guidance and review:

Ramji Bhandari, Ph.D. (Advisor)

Shyam Aravamudhan, Ph.D.

Zhenquan Jia, Ph.D.

For their contribution in providing supplies, assistance and training, many thanks to: Rebecca Malin, Steven Crawford, Lakshmi Beeravalli, Hamed Ghazizadeh, Jacob Cleary, Chelsea Smith, Xuegeng Wang, Ph.D., Victoria Akers, Bibhuti Timalaina, Megan Doldron and Leonette Griffin.

TABLE OF CONTENTS

Page

LIST OF TABLES vii

LIST OF FIGURES viii

CHAPTER

I. INTRODUCTION 1

II. MATERIALS AND METHODS 17

2.1 Cell Culture of ATCC® A549 17
2.2 Nanoparticle and Control Preparations 19
2.3 Cell Proliferation Reagent WST-1 (alamarBlue®) Assay 19
2.4 Flow Cell Cytometry 20
2.5 Superoxide Dismutase Assay 21
2.6 Nucleic Acid Extraction 22
2.7 Quantitation of Gene Expression 23
2.8 Quantitation of Methylated DNA 26

III. RESULTS 28

3.1 Aim 1 28
3.2 alamarBlue® Assay 28
3.3 Flow Cytometry 30
3.4 Total SOD Assay for AL_2O_3 Exposed Cells 32
3.5 Total SOD Assay for CeO_2 Exposed Cells 33
3.6 Expression of ROS Enzyme Gene *SOD1* in Al_2O_3 Exposed Cells 34
3.7 Expression of ROS Enzyme Gene *SOD1* in CeO_2 Exposed Cells 35
3.8 Aim 2 36
3.9 Expression of ROS Response Genes *SESN3* and *iNOS* in $A1_3O_2$ Exposed Cells 36
3.10 Expression of Asthmatic Response Genes *IL-6* and *IL-33* in Al_3O_2 Exposed Cells 38
3.11 Expression of Cancer Genes *HLA-B*, *IRF8*, *CD44* and *TNFα* in Al_3O_2 Exposed Cells 39
3.12 Expression of ROS Response Genes *SESN3* and *iNOS* in CeO_2 Exposed Cells 42
3.13 Expression of Asthmatic Response Genes *IL-6* and *IL-33* in CeO_2 Exposed Cells 44
3.14 Expression of Cancer Genes *HLA-B, IRF8, CD44* and *TNFα* in CeO_2 Exposed Cells 45
3.15 Global DNA Methylation and DNA Methylation Genes *DNMT1* and *DNMT3A* in Al_2O_3 Exposed Cells 48

3.16 Histone Methylation Genes *EZH1, KMT2D, EHMT1* and *DOT1L* in Al_2O_3 Exposed Cells 51
3.17 Global DNA Methylation and DNA Methyltransferase Genes *DNMT1, DNMT3A* in CeO_2 Exposed Cells 54
3. 18 Histone Methylation Genes *EZH1, KMT2D, EHMT1* and *DOT1L* in CeO_2 Exposed Cells 57

IV. DISCUSSION 61

REFERENCES 68

LIST OF TABLES

. Page

Table 1. Genes Regulating ROS Inhibition, Asthma Exacerbation and Cancer……24

Table 2. Genes Regulating Epigenetic Responses…….25

Table 3. Forward and Reverse Primer Sequences Designed for Human Alveolar Cells Genes 26

LIST OF FIGURES

Page

Figure 1. alamarBlue® Assay Comparison of Media vs Control Vehicle 29

Figure 2. alamarBlue® Assay Exposed Cells 29

Figure 3. Flow Cytometry with A549 Cells ..... .30

Figure 4. Flow Cytometry Anaylsis of Cell Populations 31

Figure 5. Inhibition of Total SODs Following Al_2O_3 Exposure 33

Figure 6. Inhibition of Total SOD Following CeO_2 Exposure 34

Figure 7. *SOD1* Gene Expression Following AL_2O_3 Exposure 35

Figure 8. *SOD1* Gene Expression Following CeO_2 Exposure 36

Figure 9. *SESN3* Gene Expression Following AL_2O_3 Exposure 37

Figure 10. *iNOS* Gene Expression Following AL_2O_3 Exposure 38

Figure 11. *IL-6* Gene Expression Following Al_2O_3 Exposure 38

Figure 12. *IL-33* Gene Expression Following Al_2O_3 Exposure 39

Figure 13. *HLA-B* Gene Expression Following AL_2O_3 Exposure 40

Figure 14. *IRF8* Gene Expression Following Al_2O_3Exposure 40

Figure 15. *CD44* Gene Expression Following Al_2O_3Exposure 41

Figure 16. *TNF*α Gene Expression Following Al_2O_3 Exposure 41

Figure 17. *SESN3* Gene Expression Following CeO_2 Exposure ..... .42

Figure 18. *iNOS* Gene Expression Following CeO_2 Exposure 43

Figure 19. *IL-6* Gene Expression Following CeO_2 Exposure 44

Figure 20. *IL-33* Gene Expression Following CeO_2 Exposure 45

Figure 21. *HLA-B* Gene Expression Following CeO_2 Exposure 45

Figure 22. *IRF8* Gene Expression Following CeO_2 Exposure 46

Figure 23. *CD44* Gene Expression Following CeO_2 Exposure 47

Figure 24. *TNF* α Expression Following CeO_2 Exposure 47

Figure 25. Global DNA Methylation in Cells Exposed to Al_2O_3 versus Control 48

Figure 26. *DNMT1* Gene Expression Following Al_2O_3 Exposure 49

Figure 27. *DNMT3A* Gene Expression Following Al_2O_3 Exposure 50

Figure 28. *EZH1* Gene Expression Following Al_2O_3 Exposure 51

Figure 29. *KMT2D* Gene Expression Following Al_2O_3 Exposure 52

Figure 30. *EHMT1* Gene Expression Following Al_2O_3 Exposure 52

Figure 31. *DOT1* Gene Expression Following Al_2O_3 Exposure 53

Figure 32. Global DNA Methylation in Cells Exposed to CeO_2 versus Control 54

Figure 33. *DNMT1* Gene Expression Following CeO_2 Exposure 55

Figure 34. *DNMT3A* Gene Expression Following CeO_2 Exposure 56

Figure 35. *EZH1* Gene Expression Following CeO_2 Exposure 57

Figure 36. *KMT2D* Gene Expression Following CeO_2 Exposure 58

Figure 37. *EHMT1* Gene Expression Following CeO_2 Exposure 59

Figure 38. *DOT1* Gene Expression Following CeO_2 Exposure 60

CHAPTER I

INTRODUCTION

Initial human exposure to most airborne nanoparticles, especially via combustion processes, is through inhalation. Inhaled particles travel from the nasopharangeal region to the tracheobronchial regions in the lungs. Because of the lungs' extensive 150 meter^2 epithelial surface area, these organs are the most susceptible to deposition and interaction with inhalants (Gehr *et al* 1978). Nanoparticles have been known to penetrate into the alveoli (McDowell *et al* 1978 *et al*, Oberdörster 2005). For years, it has been known that particulate matter increases morbidity and mortality and occupational and accidental nanoparticle inhalation has been linked with the exacerbation of existing cardiopulmonary diseases and increased inflammation (Peters *et al* 1997, Duffin *et al* 2007, Stone *et al* 1998, Li *et al* 2003, Pope and Dockery 1999). Exacerbated inflammation can damage the respiratory tissues, decreasing their capacity for gas exchange (Poland and Clift 2013). Additionally, airborne nanoparticles can cause the formation of reactive oxygen species (ROS), microglial activation and neuron loss, all of which can lead to disease states (Eom and Cho 2009, Wang *et al* 2017).

Some case studies have demonstrated that lung clearance of accumulated inhaled nanoparticles was hindered during chronic exposure (Moller *et al* 2008, Braydich-Stolle *et al* 2010). In 1998, human volunteers inhaled a single dose of 1.2 µm AL_2O_3 and were followed for 3 months. Most of the particles were cleared in 2-4 days post-exposure, but what remained was cleared very slowly by the kidneys, and the estimated half-life was 5.5 years (Priest *et al* 1998). Following exposure to "World Trade Center Dust", some first responder's lungs aged the equivalent of 10-12 years in the initial weeks following the attack due to the debris cloud

particles, and the effect on smokers and pre-existing asthma sufferers was even worse (American Lung Association 2016). To add further complications, a particle itself can also absorb ambient chemicals and protein molecules and once inhaled, due to the lung's thin-air/blood barrier, can translocate to the pleura and nervous, digestive and reproductive systems (Gates 2006, Saptarshi *et al* 2013, Kreyling *et al* 2002, 2006, McAuliffe and Perry 2007, Hankin and Poland 2013, Yang *et al* 2008).

Lung cancer is the leading cause of cancer death among both men and women (American Cancer Society 2018). In America, the risk of contracting lung cancer is 1 in 15 for men and 1 in 17 for women, regardless of tobacco use history. Presently, over 2 million Americans are active military or reserves, another 21.4 million Americans are surviving veterans and lung cancer rates are approximately the same for both military and civilian populations (DVA 2017, DOD 2018, Zhu *et al* 2009). It is currently unknown if the deteriorated respiratory health conditions have a link to their occupational exposure to nanoparticles. This study, therefore, focused on effects of aluminum (Al_2O_3) and cerium (CeO_2) nanoparticles on human alveolar cells (A549) *in vitro* with aims to identify phenotypic or epigenetic effects caused by exposure at two different concentration of human exposure relevance.

Aluminum is the most abundant metal and the 3rd most abundant element in the earth's crust (Greenwood and Earnshaw 1984). Acute and chronic aluminum metal exposure has been proven toxic to humans (Jeffery *et al* 1996). Aluminum attracts a natural oxide layer upon exposure to ambient air, forming energetic bonds; it is a pro-oxidant, naturally oxidizing in most forms (Exley 2004). Aluminum oxide nanoscale particles were initially manufactured in 2006 (Dlott 2006, Zamkov *et al* 2007). The first public mention of AL_2O_3 nanoparticles for military use appears in The Department of Defense 2008 Annual Report (Porter 2008). Aluminum nanospheres are used by the military as fuel additive catalysts to increase propellant combustion

speed, heat and stability and as a coating for artillery surfaces (Henz *et al* 2010). Aluminum metal occupational exposure suggests that pulmonary adsorption is possible (Sjögren and Ulfvarson 1985). In a study, a 4-69 nm mixed size aluminum slurry at a 500 ug/ml concentration decreased pneumocyte viability and altered phagocytic behavior (Braydich-Stolle *et al* 2010). Murine studies using 180 nm heat-treated aluminum nanoparticles decreased white blood cell number, increased neutrophil number, increased mucus production and enhanced secretion of interleukin 8 as well as BEABS lung cells toxicity (J.W. Park *et al* 2016). Human bronchial epithelial cells (BEAS-2B) suffered a significant increase in DNA strand breaks as measured by a comet assay, when exposed to 68-273 μg/ml of 50 nm AL_2O_3 nanoparticles for two hours (Kim *et al* 2009). AL_2O_3 nanoparticles can be found released airborne into the environment at multiple sizes, including this project's 30 nm size. Active military personnel and veterans are particularly vulnerable to this exposure although civilians living near military installations may also come into contact with airborne aluminum nano-sized particles.

Cerium is moderately toxic to living creatures and is the 26th most abundant element in the earth's crust (Greenwood and Earnshaw 1984). Nanoceria, or cerium dioxide nanoparticles, are used as a catalyst in diesel fuel worldwide, except for on-road vehicles in North America. The nanoceria-containing commercial fuel additive Envirox™, made by Oxonica, increases fuel economy in the catalytic converter and reduces particulate matter emissions and other pollutants at mg/liter (Zhang *et al* 2016). This oxygen containing nanofuel enhances the heat transfer characteristics of the original base fuel and is marketed as enhancing fuel consumption by 7% while decreasing CO_2 emmissions (Trovarelli 1996, Park *et al* 2008, Dale *et al* 2017, Energetics online advertising). This insoluble, reactive metal oxide is also used in industry as a polishing compound, glass manufacturing additive and pigment (Kilbourne 2004, Reinhardt and Winkler 2003). Nanoparticulate cerium oxide particles cycle between the more predominant Ce (III) and

the exceptional Ce (IV) valence states. These Ce^{3+} and Ce^{4+} mixed valence states allow the nanoceria to both periodically scavenge free radicals as a cellular antioxidant and to act as a pro-oxidant (Das *et al* 2007, Greenwood and Earnshaw 1984, Heckert *et al* 2008, Kitchin *et al* 2014, Ma *et al* 2010, Grulke *et al* 2014). CeO_2 nanoparticle toxicity has been examined *in vivo* in various organismal models. In the arthropod, *Daphnia magna*, there was no acute toxicity for 24 hours of exposure, but 29 nm CeO_2 nanoparticles were harmful to reproduction over a 21-day chronic test at the 10–100 mg/L concentration range, which includes this project's two concentrations. Algae growth inhibition was noticed at concentrations lower than the ones used in this experiment, but nanoparticles were not observed to be taken in cellularly (Van Hoeke *et al* 2009). In one earthworm study, the annelid showed histological changes at 400 times greater than this project's concentrations, but no survival or reproductive effects were sustained in another study using levels 100 times those used in this experiment (Lahive et al 2014, Roh *et al* 2010). In 2013, no developmental toxicity was found in zebrafish exposed to polymer-coated CeO_2 nanoparticles, however, the nanoparticles were able to penetrate the second generation embryonic chorions (Felix *et al* 2013). DNA strand breaks were measured electrophoretically in comet assays and found significant in two cell studies. One group exposed A549 cells for 4 hours to 40 ug/ml and 80 ug/ml concentrations of 4-25 nm CeO_2 spheres (Kain *et al* 2012). Another group exposed hepatic carcinoma ($HepG_2$) cells to a 500 μg/ml concentration of 16-22 nm CeO_2 nanoparticles (De Marzi *et al* 2013). One study using 2008 environmental level computer models did not consider Envirox^{TM} to pose an acute health risk (Park *et al* 2008).

At a diesel engine exhaust, 5–300 nm sized, near-spherical CeO_2 nanoparticles are released into the environment (Dale *et al* 2017, Stafford 2008). There are 1.2 billion cars and 377 million trucks on the world's roads today (Voelcker 2014, Smith 2016). Most medium and heavy trucks are diesel-powered due to the fact they are the most rugged and long-lasting internal

combustion engines. Diesel exhaust expels not only nanoparticle spray, but carbon dioxide, ozone and nitrogenous pollutants (USDOE 2014). Although diesel exhaust is ubiquitous and potentially dangerous to everyone, diesel fuel has long been the favorite power source of military and peacekeeping vehicles throughout the world and its particulate matter is, therefore, an additional threat to active duty military personnel (Anderson 2015).

As of the beginning of 2018, 1600 “nano-containing” consumer products were registered in the Nanotechnology Consumer Products Inventory (CPI); they are ubiquitous (Bierkandt *et al* 2018). However, real-world Human Particle Dose of AL_2O_3 and CeO_2 is currently unclear. Theoretically, exposure may occur via direct dermal contact (Korani *et al* 2013), ingestion (Szakal *et al* 2014) and inhalation of airborne particles (Oberdörster 2001, Kreyling *et al* 2009, Donaldson and Seaton 2012). Recently, testing concentration and effects of real-world exposure to engineered nanomaterials has been proposed (Serfozo *et al* 2018). For genotoxicity testing of nanomaterials, similar to those used for pharmaceutical testing, there is not yet a battery of tests that will adequately measure parameters (Elespuru *et al* 2018). Airborne particulate matter, a component of air pollution, was cited as the 9^{th} most hazardous factor for the global burden of disease in 2010 (Lim *et al* 2012). The addition of these nanoparticles to explosives and fuels have not yet been proven to cause acute effects to the health of current military or civilian personnel and their ability to induce molecular and epigenetic effects and likelihood of development of alveolar phenotypes has not been addressed. Although there are acute *in vitro* toxicological studies on aluminum and cerium nanoparticles, neither have been studied extensively for their possible silent epigenetic level effects, so potential transgenerational health and safety concerns are unknown (Choi *et al* 2009, E.JPark *et al* 2016). Epigenetic changes do not alter genotypes but do alter heritable phenotypic characteristics. The "epigenetic landscape" was first introduced in the 1940s by British embryologist Conrad Hal Waddington; the concept of

epigenetics literally means "above the gene" (Waddington 1942). Epigenetics is the study of heritable changes in gene expression which are not related to the sequence of nucleotides, but to the structure of the DNA molecule microenvironment itself, such as methylation of the cytosine base or histone modification. These alterations can persist as cells divide, even after the damaging initial stressor subsides, and these changes can be inherited through generations in the germ line (Head 2014). This is the basis for epigenetic studies.

Pre-mitotic chromatin can be modified by epigenetic factors such as DNA methylation, histone methylation, chromatin remodeling, higher order chromatin structure and noncoding RNA regulation (Chen and Huang 2015). One standard tool of epigenetics is the measurement of DNA methylation, where a methyl group is added to the 5 position of the cytosine pyrimidine ring to form 5-methylcytosine in the DNA molecule. This process was most certainly present since primordial eukaryotic evolution and nucleotide methylation is widespread in both the animal and plant kingdoms (Law and Jacobsen 2010, Chan *et al* 2005, Thirlwell *et al* 2010). DNA methylation doesn't alter the sequence of the DNA bases but does affect the conformation and thereby the activity of the double helix nucleic acid. Correct placement and timing of cytosine methylation is necessary for the normal development of an organism's embryonic maturation, chromosomal stability, gene expression/silencing in cell differentiation, x- chromosome inactivation in vertebrates and subsequently, carcinogenesis and ageing (Teschendorff *et al* 2013, Vandiver *et al* 2015, Chen and Riggs 2011, Feinberg 2018). Normal human adult DNA bases are approximately 1% methylated with 60-80% of all the CpGs in the human genome being methylated (Parente 2018, Smith and Meissner 2013). The process is reversible with ten-eleven translocation (TET) methylcytosine dioxygenases (Chen and Riggs 2011). Extensive DNA methylation at cytosine residues in the promoter and coding regions of genes can result in silencing of gene expression (Richards and Elgin 2002). The aberrant gene expression affected by

abnormal DNA methylation has been linked to disease states, including cancer, and Fragile X and Rett Syndromes. So, measurement of DNA global DNA methylation in experimental context presents overall methylation genomewide induced by treatment.

There are over 200 known post-translational histone modifications, including methylation of these spindles which help wind and organize DNA into nucleosomes. H3 is one of the four core histones, responsible for both packaging nucleosomes and for general gene suppression (Lorch *et al* 1987, Han and Grunstein 1988). Histone methylation by methyltransferases can either activate or repress transcription, depending on which amino acid is being methylated and nearby methyl or acetyl groups (Greer and Shi 2012, Petersen and Laniel 2004). The enzymes Histone H3 methyltransferase (DOT1L) Euchromatic Histone Lysine Methyltransferase 1 (EZH1), Histone-lysine N-methyltransferase 2D (KMT2D) and Euchromatic Histone Lysine Methyltransferase (EHMT1) can all methylate H3. Disease states associated with these methylations are numerous and include cancer, cell growth and neurological abnormalities (Chen and Armstrong 2015, Chen and Huang 2015, Soshnev *et al* 2016).

Environmental stressors can have serious effects on dynamic heritable epigenomes, including DNA and histone methylation. An increase in global DNA methylation may serve as an early marker to indicate heritable phenotypic abnormalities, and the resulting dysregulation of epigenetically modified enzymes due to environmental injury may explain heritable traits that can not otherwise be attributed to known genetic alleles. (Rose and Klose 2014, Kondo 2009, DeBaun *et al* 2002, Maegawa *et al* 2014, Vandiver *et al* 2015, Baedke 2018, Teschendoff *et al* 2013, Pujada and Feinberg 2012).

As of the beginning of 2018, 1600 “nano-containing” consumer products were registered in the Nanotechnology Consumer Products Inventory (CPI); they are ubiquitous (Bierkandt *et al* 2018). Theoretically, nanoparticle exposure may occur via direct dermal contact

(Korani *et al* 2013), ingestion (Szakal *et al* 2014) and inhalation of airborne particles (Oberdörster 2001, Kreyling *et al* 2009, Donaldson and Seaton 2012). Recently, testing concentrations and effects of environmentally relevant exposure to engineered nanomaterials have been proposed (Serfozo *et al* 2018). So far, in genotoxicity testing of nanomaterials, similar to those used for pharmaceutical testing, there is not yet a battery of tests that will adequately measure parameters (Elespuru *et al* 2018).

The innovation of this research is that it examined the epigenetic risk effects of nanoparticle exposure in alveolar epithelial cells and also examined if the cells that divide can maintain the same level of DNA methylation and gene expression patterns across three cell divisions. The goal was to better understand initial triggers in the expression of networks of interacting genes and associated epigenetic changes initiated by nanoparticle exposure. Initial expression patterns may differ from disease endpoints, but study of the first 22 hours following exposure and 4 cell divisions thereafter gives ideas about what pathways are being activated or silenced by the initial mode of action of these two nanoparticles at environmentally relevant concentrations.

In order to characterize effects of nanoaluminum and nanocerium exposure in the lung alveolar A549 cells, expression patterns of a suite of genes were examined. All the genes have some important functions in alveolar cells and are described below:

The enzyme superoxide dismutase (SOD) is abundant throughout the body, being synthesized in the cytosol. Naturally occurring cell process byproducts charge oxygen molecules and these toxic free radicals must be broken down or cell damage will result. *SOD1* is one of the three superoxide dismutase genes responsible for the breakdown of superoxide radicals. SOD1 binds to copper and zinc ions and converts superoxide radicals to normal, uncharged oxygen and hydrogen peroxide. The harmful hydrogen peroxide formed is further broken down by catalase

(McCord and Fridovich 1969, Fridovich 1995). Dysregulation of the SOD gene can contribute to a decrease in ROS scavenging, as seen in inflammatory bowel disease (Almenier *et al* 2012).

Sestrin 3 (SESN3) is a member of the sestrin family of stress-induced proteins. This protein makes possible an effective adaptive cellular response to a variety of environmental stresses. SESN3 reduces intracellular ROS levels, enables DNA repair, regulates pancreatic secretions and allows for adaptation in chronic disease states including cancer, diabetes, obesity, and chronic fatigue syndrome (Vakana *et al* 2013, Zamkova *et al* 2013, Lee *et al* 2013, Parmigiani and Budanov 2016). Dysregulation of this gene could allow for increased levels of harmful ROS.

Nitric oxide (NO) was the second biological ROS identified, after superoxide. It is formed in virtually all mammalian cells via oxidation of the amino acid L-arginine by a family of enzymes called nitric oxide synthases (Moncada *et al* 1987, Palmer *et al* 1987). Inducible nitric oxide synthase, or "iNOS", is one of three isoforms of the enzyme which produces nitric oxide, the smallest known cell signaling compound. Inducible NOS contributes to the pathophysiology of inflammatory diseases by regulating transcription, translation and neurotransmission (O'Dell *et al* 1991, Khan *et al* 1996, Schuman and Madison 1991). Rheumatoid arthritis is one disease characterized by increased NO production (Van'T Hof and Ralston 2001).

Secreted by T cells, adipocytes and macrophages at inflammation sites, interleukin 6 (IL-6) is both an anti-inflammatory cardiac myokine and a pro-inflammatory cytokine with receptors on a multitude of cell types, including B cells. This cytokine can also work with DNA methyltransferases to increase total DNA methylation (Kundakovic *et al* 2009). An IL-6 inhibitor, tocilizumab, has been clinically successful in the treatment of autoinflammatory diseases, although it is not yet approved for treatment by the FDA (Tanaka *et al* 2017). There appears to be a link between IL-6 mediated adipocytic inflammation and asthma exacerbation (Peters *et al*

2016). Both TNFα and IL-6 are involved in angiogenesis and can augment many steps of the cancer-related inflammation cascade (Upadhyay *et al* 2018).

Expressed by many cell types in its precursor form, interleukin 33 (IL-33) is an alarmin, released upon cell damage or necrosis, having both inflammatory and anti-inflammatory. It induces helper T cells, mast cells, eosinophils and basophils to produce type 2 humoral cytokines. Elevated levels of IL-33 are associated with asthma and clinical trials with an anti-IL-33 have proven promising for treating asthma (Bahrami *et al* 2015, Dinerello 2017).

There are hundreds of allelic versions of human leukocyte antigens (HLA). The HLA B27 class I molecule, also called HLA-B, is one of many of the major histocompatibility complex Class 1 glycoproteins. Although not yet fully understood, these molecules exist on the surface of most cells, presenting self antigens to cytotoxic T cells. They can increase or suppress inflammatory responses, thereby allowing for an increase in tumor incidence and metastastis of lung cancer (Bremnes *et al* 2011, Bowness 2015).

Interferon regulatory factor 8 is a transcription factor which regulates apoptosis and might be promising as a cancer therapy (Hu *et al* 2011). Studies indicate the *IRF8* gene promoter is hypermethylated in human colon carcinoma cells. This suggests that these cancer cells might use DNA methylation to silence *IRF8* expression to spur the development of the disease (McGough *et al* 2008, Yang *et al* 2007).

The Cluster of Differentiation 44 antigen (CD44**)** is a cell-surface glycoprotein expressed in many mammalian cell types. Hundreds of isoforms of CD 44 exist; it is a transmembrane receptor involved in lymphocyte and macrophage activation, cell adhesion, migration, protein assembly, resistance to apoptosis and tumor metastasis (Amash *et al* 2016, Alves *et al* 2008, Hanly *et al* 2005, Ponta *et al* 2003). Animal experiments have shown that targeting CD44 and CD44-soluble proteins reduces the malignant activities of various neoplasms (Naor *et al* 2002),

Tumor Necrosis Factor alpha (TNFα) is a cytokine capable of causing both systemic inflammation and immunosppression (Tanaka *et al* 2017). Many defensive cells, but mostly activated macrophages, can secrete this cell signaling pyrogen as part of the innate immune system's acute phase reaction. TNFα regulates apoptotic cell death and can both inhibit and stimulate tumorigenesis (Granger *et al* 1969, Carswell *et al* 1975, Lukas 2010).

Although details are only now emerging on the exact mechanism of action of transmembrane protease, serine 4 (TMPRSS4), it does degrade basement membrane, which anchors epithelial cells and the structural extracellular matrix. Most importantly for our research, TMPRSS4 facilitates a transformation from epithelial to mesenchymal multipotent cells leading to unchecked cell division. Understandably, upregulation of *TMPRSS4* is seen in many cancer cell lines, especially in lung cancer tissue (Valero-Jiminez *et al* 2018).

Chemokine 11 (CXCL11) is a small chemotactic cytokine secreted by monocytes, endothelial cells, fibroblasts and cancer cells. Receptors are enhanced by TNF α and exist on monocytes, activated T cells, natural killer, dendritic and cancer cells (Ohmori *et al* 1993, Ohmori *et al* 1997, Brightling *et al* 2005, Muehlinghaus *et al* 2005). It is moderately expressed in lung tissue (Cole *et al* 1998). Atherosclerosis can develop from dysregulation of CXCL11 (Dunn 2010).

Chitinase-3-like protein 1 **(**CHI3L1) is a glycoprotein associated with inflammation and asthma. Secretion of this substance may catalyze the AKT anti-apoptotic signaling pathway and direct neural cell migration. Expression of this gene can be induced by a variety of cancers which leads to metastasis (Ober *et al* 2008, Ma *et al* 2016). CHI3L1 drives hyperfibrosis in an exaggerated repair of epithelium to lung injury in Hermansky–Pudlak syndrome lung disease (Zhou *et al* 2018).

The binding of the membrane protein Cluster of Differentiation 86 (CD86) with Cluster of Differentiation 28 can stimulate T cell activation, although its binding with cytotoxic T-lymphocyte-associated protein 4 reverses this response. This immunoglobulin ligand can be expressed by monocytes, dendritic, T and B cells (Bugeon and Dallman 2000). Colon, rectal and adenoma polyps have an increased expression of *CD 86*. Adenoma polyps are initially benign tumors formed from glandular structures in epithelial tissue, including bronchi, which can transform into malignant growths over time (Peyravian *et al* 2017). Tumor suppressor genes are frequent targets of epigenetic processes, and the downregulation of them can lead to uncontrolled cell proliferation. Inappropriate transcriptional silencing or activation can result from epigenetic changes including DNA or histone methylation and can lead to a wide spectrum of disease states, including lung cancer (Kadar and Rauch 2012).

The family of DNA methyltransferases includes four DNA methylating members: DNMT1, DNMT3A, DNMT3B, and DNMT3L, and DNMT2, which methylates RNA (Goll *et al* 2006). DNA methylation (the CpG methylation of DNA) occurs at carbon 5 of cytosines in the mammalian CpG dinucleotide, but not in island-rich areas of the genome (Salert and Weber, 2013). The addition of methyl groups modifies the DNA into a more compact structure limiting the accessibility of the DNA to the binding of transcription factors necessary to convert DNA to RNA. Many transcription factors recognize sequences that contain CpGs (Deaton and Bird 2011) and some show a reduction in binding affinity when the cytosines in the sequence are methylated (Campanero *et al* 2000, Iguchi-Ariga and Schaffner 1989, Kim *et al* 2003).

Previously, it was observed that DNMT1 was active at DNA replication sites during S phase and on the partially methylated CpGs on one of the two DNA strands following replication, leading to the conclusion that DNMT1 is responsible for “maintenance” DNA methylation, copying the methylation pattern from an existing DNA strand to the newly synthesized DNA

strand and methylating hemimethylated DNA. DNMT1 is called the maintenance methyltransferase (Arand *et al* 2012, Leonhardt *et al* 1992). Conversely, DNMT3A is responsible for establishing *de novo* DNA methylation during development or adding a methyl group to a cytosine at a new location, not one already copied. DNMT3A is prevalent in differentiated cells and is called a *de novo* methyltransferases (Okano *et al* 1991).

The study of epigenetics also involves histone modification. The methylation, which is reversible, takes place on arginine and lysine residues within the histone tails. Five different types of histones spool DNA into nucleosomes: H1, H2A, H2B, H3 and H4. Four histone methylating genes were chosen for study: *EZH1*, *KMT2*d, *EHMT1*, and *DOT1*. When a histone is methylated, even slightly, it can cause either transcriptional repression or activation, depending on which of its amino acids are modified and to what extent the structure is altered (Greer and Shi 2012). A range of cancers and Kabuki syndrome are known diseases caused by dysregulation of histone methylation (Parente 2018).

DOT1L (Disruptor of Telomeric Silencing 1), also known as Histone H3K79 Methyltransferase, catalyzes the methylation of histone H3 lysine 79 (H3K79) in humans. This action regulates diverse cellular processes such as progression of G1 and S phases, mitosis, and meiosis and overall DNA damage response, differentiation, and proliferation (Vlaming and van Leeuwen 2016, Nguyen and Zhang 2011). *DOT1L* misregulation can lead to the development of cancer, especially mixed-lineage leukemia, and might serve as a cellular time clock (Wang *et al* 2016, Farooq *et al* 2016, McLean *et al* 2014, Soria-Valles *et al* 2014, Feinberg *et al* 2002*)*. Recent studies indicate DOT1 may chaperone histones in yeast, in addition to its methylation activities (Lee *et al* 2018).

Histone-lysine N-Methyltransferase 2D (KMT2D) is widely expressed in human tissue (Prasad *et al* 1997). More than 80% of lung cancer is categorized as non–small-cell lung cancer

(NSCLC), and small cell lung cancer (SCLC) accounts for the remaining 15% (Van Meerbeeck *et al* 2011, Chen *et al* 2014). *KMT2D* mutation is associated with reduced survival in NSCLC but not in SCLC (Ardeshir-Larijani *et al* 2018). *KMT2D* mutations have also been observed in other cancers, including non-Hodgkin lymphoma, medulloblastoma, prostate, renal, and bladder (Morin *et al* 2011, Lopez 2014, Grasso *et al* 2012, Dalgliesh *et al* 2010, Yang *et al* 2017, Ardeshir-Larijani *et al* 2018). Thus, epigenetic modification of histones via alteration of *KMT2D* gene may indicate onset of similar phenotypes in humans.

Euchromatic histone-lysine N-methyltransferase 1, also known as G9a-like protein (GLP), is a protein that is encoded by the *EHMT1* gene in humans. It methylates the lysine-9 position of histone H3 and MDC1, a mediator for DNA repair processes (Watanabe *et al* 2018). This enzyme plays a role in silencing transcription factors that regulate the cell division cycle G0 resting phase to the G1 cell size enlargement phase transition (Xiong *et al* 2017).

Histone-lysine N-Methyltransferase 1, also known as Enhancer of Zeste 1, or EZH1, is the human enzyme that is encoded by the *EZH1* gene (Abel *et al* 1997). *EZH1* expression is maintained throughout adulthood and is rich in the brain (Miller *et al* 2014). This methyltransferase affects stem cell maintenance, self-renewal and differentiation hematopoeisis differentiation. Not surprisingly, it has been associated with adenomas, neoplasms arising from glandular or secretory epithelial cells, including bronchi (Jung *et al* 2018). Using knockdown techniques, 70 other genes have been identified as altered in response to the decrease in this enzyme. These genes regulate neurons, axons, and neurotransmitter signaling. Phenotypic analysis of these genes showed complex associations with many learning and complex behavioral categories (Johnstone *et al* 2018). Since this gene is a universal regulator of H3K9me3 histone modification, the alteration of expression of this gene would indicate alteration in histones of closed chromatin states that results in gene silencing (short term or long term).

There are two aims to this study. Aim 1 was to evaluate phenotypic characterization in A549 cells when exposed to 0.05% Tween 80™, the nanoparticle Control Vehicle, known as Control, or exposed to both 25 μg/ml (Low) and 250 μg/ml (High) concentrations of AL_2O_3 and CeO_2 nanoparticles. Aim 1 focused on A549 cell viability using the alamarBlue® Assay, flow cytometry, SOD Assay and qPCR of gene *SOD1*. The alamarBlue® Assay measured the cells' ability to reduce the dye resazurin and flow cytometry descriptively differentiated dead from live cells in the total population. The health of the exposed cells was firther evaluated by measuring their ability to get rid of their microenvironment of superoxides. This was accomplished directly using a xanthine/xanthine oxidase method for total oxidase enzyme activity and indirectly using qPCR to measure the expression of the Super Oxide Dismutase 1 (*SOD1*) gene in Control cells and exposed cells.

Aim 2 was to examine the cells for molecular endpoints associated with disease states using qPCR quantitation of fifteen genes and ELISA for measurement of total DNA methylation. Changes in expression of Sestrin 3 (*SESN3*) and inducible Nitric Oxide Synthase (*iNOS*) genes indicate a change in their ability to reduce radical oxygen species breakdown. Exacerbated asthmatic conditions accompany dysregulation of Interleukin 6 (*Il-6*) and Interleukin 33 (*Il-33*), so measurement of these genes give insights into molecular conditions leading to the onset of asthmatic conditions. Cancer proliferation is often preceded by variations in transcription of Human Leukocyte Antigen B (*HLA-B*), Interferon 8 (*IRF8*), Cluster of Differentiation (*CD44*) and Tumor Necrosis Factor Alpha (*TNFα*), so alterations in these genes give insights into the ability of nanoparticles to tease gene networks relevant to carcinogenesis. Alterations in expression of epigenetic marker genes DNA (cytosine-5)-Methyltransferase 1(DNMT1) and DNA (cytosine-5)-Methyltransferase 3A (DNMT3A) were quantitated through qPCR methods and total DNA methylation in the cells via ELISA. The expression of histone modifications were

indirectly examined by qPCR quantitation of histone methylase enzyme genes encoding Euchromatic Histone Lysine Methyltransferase (*EZH1*), Histone-lysine N-Methyltransferase 2D (*KMT2D*), Euchromatic Histone Lysine Methyltransferase (*EHMT1*), and Histone H3K179 Methyltransferase (*DOT1*). Expression of EZH1 and EHMT1 genes indicate epigenetic silencing in place, whereas expression of DOT1 and KMT2D indicates epigenetic induction of gene expression in the A549 cells following exposure.

CHAPTER II

MATERIALS AND METHODS

2.1 Cell Culture of ATCC® A549

This line was derived from a human alveolar cell carcinoma (Lieber *et al* 1976). The properties are those of Type II alveolar epithelial cells, complete with surfactant secretion. The alveolar region is where gas exchange takes place (Ochs and Weibel 2008). In the human body, clearance in the non-ciliated alveolar region of the lungs is slower than in the upper respiratory system and relies on circulating macrophages. According to American Type Culture Collection of Manassas, VA, optimal A549 cultures can be established between 2000 and 10,000 viable cells/cm^2 in filter-sterilized Gibco's Ham's F-12K (Kaighn's) Medium with 10% fetal bovine serum (FBS) and 1% Penicillin, Streptomycin, Neomycin (PSN) antibiotic mixture stored in a 4°C refrigerator for up to one month. A549 cells are 10-15 μm (Jiang *et al* 2010). Confluency may reach 95% without complications.

First, adherent human lung ATCC® A549 epithelial carcinoma cells were cultured at 37°C, 5% CO_2. Adherent cells were detached with trypsin, dyed with 50% Trypan Blue and counted using an automated hemocytometer (BioRad TC-10) to determine density and viability percentage. Batches of cells were kept in liquid nitrogen and defrosted as passages aged. Cells from passages 6-12 were utilized for this study. Each well on a 6 well Tissue Culture Treated plate is a "T-9", that is, there is 9 cm^2 of cell adherent area, or "cell growth area" and the working well volume is 3 ml. Every doubling provides for mitosis and therefore, genetic revisions, predictive of an *in vivo* environment. The cells were allowed to double 4 times post-attachment, the maximum for the health of these cells due to confluency constraints.

Every plate was initially seeded with 12,000 cells per well in 3 ml of media or 1300/cm^2 to help reduce stress of overcrowding for five doublings. They were allowed to adhere for 22 hours at 37°C and 5% CO_2. Most cells adhered to the flat well bottoms and doubled in that time. Gibco TrypLE™ Express (12604013) was used to release adherent cells from the TCT flasks for counting and passaging. This ultrapure trypsin enzyme cleaves peptide bonds on the C-terminal sides of lysine and arginine adhesive proteins in the cell membrane and allows for cell dissociation. Cell densities were determined using a BioRad TC-10 automated cell counter. "Tissue-culture treated (TCT) plates" refers to their polystyrene surface having been made to become hydrophilic by increasing its negative charge through chemical and manufacturing treatments, which allows for cell adhesion. The cells were maintained from 6,000 to 60,000 cells/cm^2 but never exceeded 70,000 cells/cm^2. These cells doubled about every 22 hours and they were housed for 5 doublings, the maximum for this cell line at this concentration and volume.

12,000 → 24,000 → 48,000 → 96,000 →192,000 → 384,000 cells/ml media

1300 → 2600 → 5200 →10,400 → 20,800 → 41,600 cells/cm^2 flask surface

Seed → 0 hour → 22 hr → 44 hr → 66 hour → 88 hour exposures

Wells contained unexposed cell controls, with and without 0.05% Tween™ 80, and cells with added AL_2O_3 or CeO_2 nanoparticles. Exposure, still at 37°C and 5% CO_2, was terminated at five exposure time points: 0 day, 22 hours, 44 hours, 66 hours and 88 hours, chosen because the cell doubling time is approximately 22 hours. Collection times were +/- 1 hour. At the 5 time points, cells were scraped and pipetted into labeled, sterile, nuclease-free centrifuge tubes and centrifuged at 1400 g for 10 minutes. Supernatants and cell pellets were separated, and transported in dry ice to a -80°C freezer for storage and future manipulation and assay. This

completed 5 doublings of cells, 4 of which were exposed to nanoparticles. The scraped plates were discarded.

2.2 Nanoparticle and Control Preparations

Two separate stock solutions (1g/ml and 10 g/ml), one of AL_2O_3 and one of CeO_2 nanoparticles, were made in sterile distilled, deionized water and 0.05% Tween™ 80. The Al_2O_3 nanoparticles were 30 nm; the CeO_2 nanoparticles ranged from 15-30 nm. 75 µl of these stock solutions were added to each 3 ml well making a total 25 µg/ml or 250 µg/ml concentration exposure. The wells contained 0.0125% Tween™ 80 total. The nanoparticle stock solutions were stored in a 4°C refrigerator for the duration of the experiments and vortexed during application.

A solution of 0.05% Tween™ was prepared in sterile distilled, deionized water and was added to all Control (C) wells. The solution was stored in a 4°C refrigerator for the duration of the experiments.

2.3 Cell Proliferation Reagent WST-1 (alamarBlue®) Assay

The reducing potentials of healthy living cells enzymatically convert the alamarBlue® reagent (resazurin) into a fluorescent product (resorufin). The oxidized form of alamarBlue® is a dark blue color, whereas when taken into cells, the reduced dye becomes a highly fluorescent red, detectable at 570 nm. Because of this chain of events, this assay is used to measure cell viability (Ahmed *et al* 1994). The MTT assay was not used to test viability due to the published history of nanoparticles reacting with the substrate, and causing false negative results. The LDH release kits have a history of metallic-based nanoparticles inhibiting LDH release, indicating misleading necrotic cell totals (Belyanskaya *et al* 2007, Kroll *et al* 2009).

A549 cells were seeded onto 8 separate TCT 96-well plates, in sets of 6 replicates, at a density of 400 cells in a volume of 100 µl media/well. This was the same concentration as used

in the exposure studies. Only the 96 well plates' inner wells were utilized for optimal spectrophotometer readings. The cells were allowed to adhere for 24 hours at 37 °C under a 5% CO_2 atmosphere. After the 24 hour incubation, the media was pipetted off and replaced with 100 µl of warmed fresh media (M), media containing nanoparticles **(**high or low AL_2O_3 or CeO_2 concentrations) or media containing 0.05% Tween™ 80 vehicle (C). At each time point, (0, 22, 44, 66 and 88 hours), the wells were washed three times with warmed 1x PBS, then 100 ul of warmed media and 10 µl/well of WST-1 was added to each well without the light on in the hood. The plates were wrapped in foil and incubated at 37 °C under a 5% CO_2 atmosphere for 4 hours. Following incubation, the fluorescence of each well was measured at 570 nm with a background subtraction reference reading of the plain media and WST-1 at the same ratio as experimental plates. Values were graphed as percent of negative control.

2.4 Flow Cell Cytometry

A549 Cells were grown and exposed as previously described, but in 1 ml total volumes in 24 well TCT plates, in triplicate. Media was aseptically pipetted off at the key exposure times of 0, 22, 44, 66 and 88 hours. To disassociate the cells, 250 µl of Gibco TrypLE™ Express was added to each well followed by incubation at room temperature for 7 minutes. The cell mixtures were pipetted into microcentrifuge tubes and centrifuged at 1000 rpm for 7 minutes. The supernatants were discarded and 1 ml of Phosphate Buffered Saline (PBS), pH 7.4, was used to wash the cells, followed by centrifugation at 5000 rpm for 5 minutes. The supernatants were discarded and the cell pellets were resuspended in 100 µl of PBS. A 10% solution of this cell suspension and 90% Guava® ViaCount® Reagent (Guava Technologies 4000-0040) were mixed together and allowed to incubate at room temperature for at least five minutes wrapped in foil to protect the samples from light. To count the cells and differentiate between dead and living cells, the samples were well mixed, then read on a Guava EasyCyte™ Flow Cell Cytometer using

CytoSoft software containing the Guava® ViaCount module software using 1000 events, with the viability threshold set at x intercept 1.5142, 32.16 angle.

2.5 Superoxide Dismutase Assay

A free radical is any atom or molecule with a single unpaired electron. Biological radicals include reactive oxygen species (ROS) such as peroxides, superoxide, hydroxyl radical and singlet oxygen (Hayyan *et al* 2016*).* ROS are present in every aerobic organism, produced as a normal by-product of respiratory electron transport energy release and cytochome P450 reactions. At normal cellular levels, ROS regulate cell differentiation and proliferation, and are extremely important to both the innate immune response and the development of inflammation (Casas *et al* 2015). An increase in ROS, however, induces cell damage and is known as oxidative stress. One of the most important ROS, superoxide, is a very small, mobile and unstable radical first discovered widely distributed in human tissue in 1968 (Mccord and Fridovich, 1969). In 1990, it was found that that superoxide radicals could react with nitric oxide to form peroxynitrite ($ONOO^-$) which breaks down to nitrogen dioxide (NO_2) and hydroxyl radical (•OH), which damages DNA and protein (Beckman *et al* 1990).

Removal of excess superoxide is an important step in cellular defense and anti-inflammatory regulation. The antioxidant enzyme superoxide dismutase (SOD) decomposes superoxide anions into less harmful hydrogen peroxide and oxygen (Valko *et al* 2007). There are three families of SOD enzymes: cytosolic Cu/Zn (SOD1), mitochondrial Fe/Mn (SOD2), and the extracellular nickel type (SODNi) (Zelko *et al* 2002). The total of these three types of SOD enzymes was measured directly according to the method described by Kuthan (1986) using xanthine/xanthine oxidase. BioAssay System's EnzyChromTM Superoxide Dismutase Assay Kit (ESOD-100) was utilized according to the manufacturer's protocol. In the assay, superoxide (O_2^-) is provided by xanthine oxidase. Superoxide reacts with a WST-1 dye to form a colored product.

Since SOD catalyzes the conversion of the O_2^- to less damaging radicals, less O_2^- is available for the chromogenic reaction. The adherent cells were washed in PBS buffer, lysed (50 mM potassium phosphate, 0.1 mM EDTA, 0.5% Triton X-100, pH 7.4), scraped and centrifuged at 12,000 g for 5 minutes. The supernatants were frozen for three weeks at -80°C. As suggested by Cell Biolabs, Inc. technical support, 70 µl of sample supernatants were added to duplicate wells in a 96 well flat bottomed plate. A mixture of 10 µL Assay Buffer, 5 µL Xanthine and 5 µL WST-1 was added to each well. Plates were incubated at 37°C for one hour wrapped in foil, then read at OD 490 nm.

2.6 Nucleic Acid Extraction

DNA and RNA were extracted from the scraped and centrifuged cell pellets from the 22 and 88 hour incubation times as directed by the Zymo Research ZR-Duet DNA/RNA MiniPrep Kit. First, 300 µl of Digestion Buffer and 10 µl of Proteinase K were added to the approximate 50 µl volume lung cell pellets. Proteinase K is a broad spectrum serine protease which digests contaminating proteins and degrades any nucleases present. Samples were then placed into a 55℃ heat block for 30 minutes to further unfold proteins. RNA alcohol precipitation preceded a series of buffers which washed the nucleic acids adsorbed onto separate silica filters before elution. Quantitation and purity of both DNA and RNA were ascertained by Nano Drop spectrophotometer. Both nucleic acids absorb ultraviolet (UV) light at the 260 nm wavelength (λmax = 260 nm) due to the heterocyclic rings of the nucleotides, so that absorbance was used to calculate the concentration and purity of extractions. A 260/280 ratio is the ratio of absorbance at 260 nm and 280 nm. A ratio of ~1.8 is generally accepted as "pure" for DNA; a ratio of ~2.0 is generally accepted as "pure" for RNA. Samples displaying these approximate ratios were utilized.

2.7 Quantitation of Gene Expression

RNA samples were reverse-transcribed into complementary DNA (cDNA) with reverse transcriptase using the instructions in the High Capacity cDNA Reverse Transcription Kit by Applied Biosystems (4368814). Amplification of a gene transcript is necessary to detect and quantitate gene expression. The amount of an expressed gene in a cell can be measured by the number of copies of an RNA transcript of that gene present in a sample. High quality RNA is needed for quantitation of genetic expression.

With quantitative polymerase chain reaction (qPCR), the fluorescent Applied Biosystems™ SYBR™ Green I Dye specifically binds to the double-stranded DNA formed via DNA polymerase between the single-stranded sample cDNA and specific gene primers of interest during thermal cycles. SYBR™ Green I Dye only fluoresces when bound. Fluorescence is monitored during the whole PCR process (along 30 to 45 cycles). "Real-time" PCR instruments measure the accumulation of the fluorescence during the exponential phase of the doubling. The accumulation is directly proportional to the starting amount of DNA. The higher the initial number of DNA molecules in the sample, the earlier the detection and faster the fluorescence increases during amplification (Applied Biosystems Protocols). All qPCR wells contained cDNA concentrations resulting from 3 ng/3 µl of original RNA concentration measurements. The average relative fold mRNA levels were calculated using the $^{-\Delta\Delta}$Ct method.

Cytokines can be adsorbed onto the surface of nanoparticles, making cellular secretion direct quantitation inaccurate (Pailleux *et al* 2013), so it was decided to quantitate these signaling molecules, along with several enzymes, via gene expression rather than direct measurement. Thirteen genes responsible for proteins that respond to ROS threat, indicate asthmatic response and chronic inflammation, and therefore tissue damage, and control cancer proliferation were examined for possible downregulation and upregulation due to exposure to AL_2O_3 and CeO_2

nanoparticles via quantitative polymerase chain reaction (qPCR). Nine of the thirteen genes were successfully assayed:

Table 1. Genes Regulating ROS Inhibition, Asthma Exacerbation and Cancer

Gene Symbol	**Accession ID**	**Gene Name**	**Function**
SOD1	ENSG00000142168	Superoxide Dismutase 1	breaks down ROS O^{2-} in cytosol; cancer
SESN3	ENSG00000149212	Sestrin 3	a stress-induced protein which reduces ROS
iNOS	ENSG00000169592	Inducible Nitric Oxide Synthase	catalyzes NO from L-arginine, modulates vascular and airway tone, non-specific immune defense
IL-6	ENSG00000136244	Interleukin 6	inflammatory cytokine and anti-inflammatory myokine; allergic response
IL-33	ENSG00000137033	Interleukin 33	drives production of T helper cytokines, receptor for mast cells and lymphocytes; asthma
HLA-B	ENSG00000234745	Human Leukocyte Antigen B2 7	presents antigens to T cells during inflammation and apoptosis
IRF8	ENSG00000140968	Interferon Regulatory Factor 8	transcription factor regulates apoptosis in myeloid cells, possibly a tumor suppressor
CD44	ENSG00000026508	Cluster of Differentiation 44	cell-surface glycoprotein in cell–cell interactions, cell

			adhesion, migration, cancer
TNFα	ENSG00000232810	Tumor Necrosis Factor alpha	inflammatory cytokine

Six genes responsible for regulating epigenetic heritable traits were examined using quantitative polymerase chain reaction (qPCR) method:

Table 2. Genes Regulating Epigenetic Responses

Gene Symbol	**Accession ID**	**Gene name**	**Function**
DNMT1	ENSG00000130816	DNA (cytosine-5)-Methyltransferase 1	maintenance DNA methylation enzyme
DNMT3A	ENSG00000119772	DNA (cytosine-5)-Methyltransferase 3A	de novo DNA methylation enzyme
EZH1	ENSG00000108799	Euchromatic Histone Lysine N-Methyltransferase	enzyme may both activate certain genes important for cell development and act as a tumor suppressor
KMT2D	ENSG0000016754	Histone-lysine N-Methyltransferase 2D	large protein is 1 of a family of 6 methyltransferases necessary for cell differentiation and tumor suppression
EHMT1	ENSG00000181090	Euchromatic Histone Lysine Methyltransferase	methylates the histone protein, responsible for providing the structural basis for chromosomes.
DOT1L	ENSG00000104885	Histone H3K79 Methyltransferase	methylates core histone H3 to form H3K79me. It is needed for mitotic, meiotic,

			S1 and G cell phase progression

2.8 Quantitation of Methylated DNA

Denatured, single-stranded human lung DNA was assayed for global methylation via Zymo Research 5-mC DNA ELISA Kits (D5325). The 100 ng denatured DNA samples were incubated to coat 96 well plate surfaces, then anti-5-methylcytosine monoclonal antibody (Anti-5-mC mAb) and HRP-conjugated Secondary Antibody were added to make a "sandwich". Percent 5-mC in a DNA sample was quantified after addition of the kit's color HRP Developer and comparison to a 450 nm absorbance standard curve read on a Biotek Synergy 2 with Gen5 software. Calculations were then made against the CpG ratio of *E.coli* in the standards to the human CpG ratio.

Table 3. Forward and Reverse Primer Sequences Designed for Human Alveolar Cells Genes

Primer Name	Forward Primer Sequence	Reverse Primer Sequence
DNMT1	5'- AGA TCT AGC TGC CAA ACG GA -3'	5'-TGC GTC TCT TCT CCT CCT TT -3'
DNMT3A	5'- CTG GAA AAG GGA GGC TGA GA -3'	5'- CTC CAC CTT CTG AGA CTC CC -3'
EHMT1	5'- CAT GCA GCC AGT AAA GAT CCC -3'	5'- CTG CTG TCG TCC AAA GTC AG -3'
EZH1	5'- GTC ACT GAA CAC AGT TGC ATT G -3'	5'- TGC ACA AAA CCG TCT CAT CTT C3'
KMT2D	5'- GCA GAA CTG AAT CCC AAC TCG -3'	5'- GGA GCG GAT AGT CTG ACC TC -3'
CD44	5'- GCT GAT CAT CTT GGC ATC CC -3'	5'- TCT TCT GCC CAC ACC TTC TT-3'
CD86	5'- AGC TAC AGT CGA CAG GCA TT-3'	5'- TTC AGA GGA GCA GCA CCA G -3'
CHI3L1	5'- GAT TTT CAT GGA GCC TGG CG -3'	5'- CCC CAC AGC ATA GTC AGT GT-3'
CXCL11	5'- CAG TTG TTC AAG GCT TCC CC -3'	5'- TCT GCC ACT TTC ACT GCT TT- 3'
DOT1l	5'- CTG CCG GTC TAC GAT AAA CAT C -3'	5'- AGC TTG AGA TCC GGG ATT TCT-3'
HLA-B	5'- GGA GGA AGA GTT CAG GTG GA -3'	5'- TGA GAG ACA CAT CAG AGC CC -3'
IL-6	5'- TGT GAA AGC AGC AAA GAG GC -3'	5'- TTC ACC AGG CAA GTC TCC TC -3'
IL-33	5'- TGA ATC AGG TGA CGG TGT TG -3'	5'- TCC TTG TTG TTG GCA TGC AA -3'

iNOS	5'- CAG CGG GAT GAC TTT CCA A -3'	5'- AGG CAA GAT TTG GAC CTG CA -3'
IRF8	5'- CTG GCT GCG TGA ATG AAG TT -3'	5'- AAT CGT CCA CAG AAG GCT CC -3'
SESN3	5'- GGC AGC AAC TTT GGG ATT GT -3'	5'- GAC GCC TCT TCA TCT TCC CT -3'
SOD1	5'- ACT GGT GGT CCA TGA AAA AGC -3'	5'- AAC GAC TTC CAG CGT TTC CT-3'
TMPRSS4	5'- CAT GTG GTG GGC ATC GTT AG -3'	5'- AGC TCA GCC TTC CAG ACA TT-3'
TNF alpha	5'- AGC CCA TGT TGT AGC AAA CC -3'	5'- TGG TTA TCT CTC AGC TCC ACG -3'
B actin	5'- GAA GAT CAA GAT CAT TGC TCC T -3'	5'-TAC TCC TGC TTG CTG ATC CA -3'

CHAPTER III

RESULTS

3.1 Aim 1

Aim 1 was to evaluate whether phenotypic changes occurred in A549 cells when exposed to 0.05% Tween 80™, the nanoparticle Control Vehicle, known as Control, or exposed to either 25 μg/ml (Low) or 250 μg/ml (High) concentrations of AL_2O_3 and CeO_2 nanoparticles. These exposure concentrations are consistant throughout this study. Cell pellet samples were collected and assayed at 0 hour exposure, and then at 22, 44, 66 and 88 hours of incubation, allowing for 4 cell divisions. The health of the nanoparticle-exposed and Control cells was further evaluated by measuring their ability to rid their microenvironment of superoxides. This was accomplished directly using a xanthine/xanthine oxidase method for total oxidase enzyme activity and indirectly using qPCR to measure the expression of the Super Oxide Dismutase 1 (*SOD1*) gene in Control cells and exposed cells at 22 and 88 hours incubation.

3.2 alamarBlue™ Assay

The alamarBlue® Assay was utilized to determine cellular viability based on the cells' ability to reduce the dye resazurin. The alamarBlue® Assay is a standard oxidation/reduction indicator often used in nanotechnology publications. This assay ascertains the viability of cells via their ability to reduce resazurin dye into the fluorescent product resorufin.

Data was calculated for significance via one way anova, two way anova, and TukeyHSD tests computed in R 3.5. Diamonds indicate significance via two-tailed t-test.

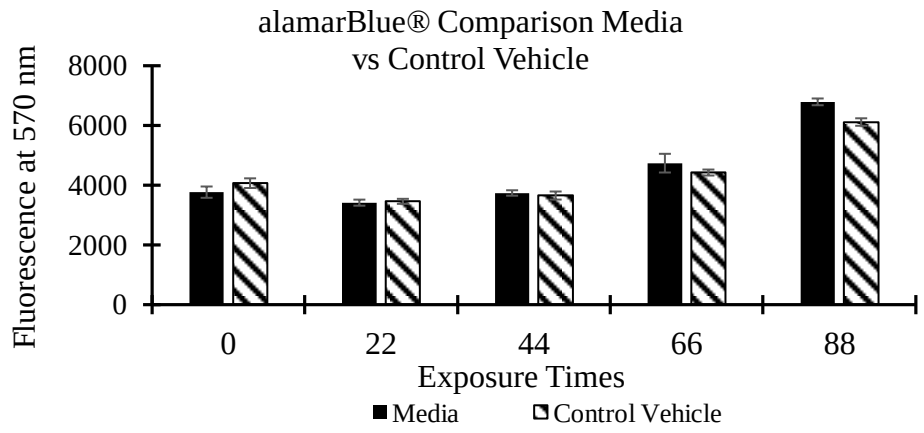

Figure 1. alamarBlue® Assay Comparison of Media vs Control Vehicle. alamarBlue® Assay comparison of cell viability between media and control vehicle (media with 0.05% Tween 80™ nanoparticle vehicle). N=6 except Media 88 and Control 88=11, Media 44 and Media 66=5.

No significance was found in comparisons of both conditions at all five time points.

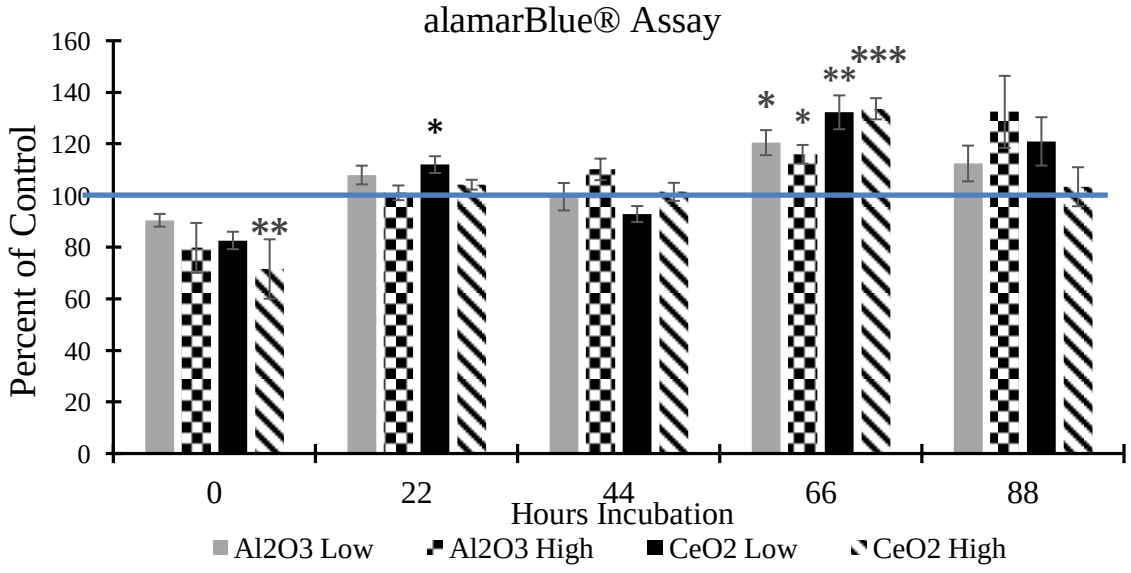

Figure 2. alamarBlue® Assay Exposed Cells. This assay determined cell viability. Cells were exposed to both Low and High concentrations of AL_2O_3 and CeO_2 nanoparticles. Comparison of exposed cell to unexposed cell cultures as a percent of control fluorescence at 570 nm. N=6 except Al High 88=4, Control 88=11, Al Low 0 and Ce High 0=5. Asterisks indicate significance (* $p < 0.05$, ** $p< 0.01$, *** $p<0.001$) from the control. Blue line =100% Control.

At 66 hours incubation, all nanoparticle-exposed conditions proved significantly different from the control indicating an increase in normal cell reduction-oxidation activity. All cells at these same conditions lowered close to the control by the next division at 88 hours, possibly the cells' attempt to stabilize metabolism. None of the gene expressions at this time point were measured. Additionally, the CeO_2 High concentration at 0 hour showed a decrease in reduction although at this time point, the nanoparticles had only a few hours during the assay incubation period to affect cellular function and could have resulted from a lower starting concentration of total cells. The significant rise in the reduction activity of cells exposed to CeO_2 Low 22 hour exposure may indicate increased cellular activity.

3.3 Flow Cytometry

Flow cytometry is a technique used to both visualize and determine live versus dead cell counts in mixed populations.

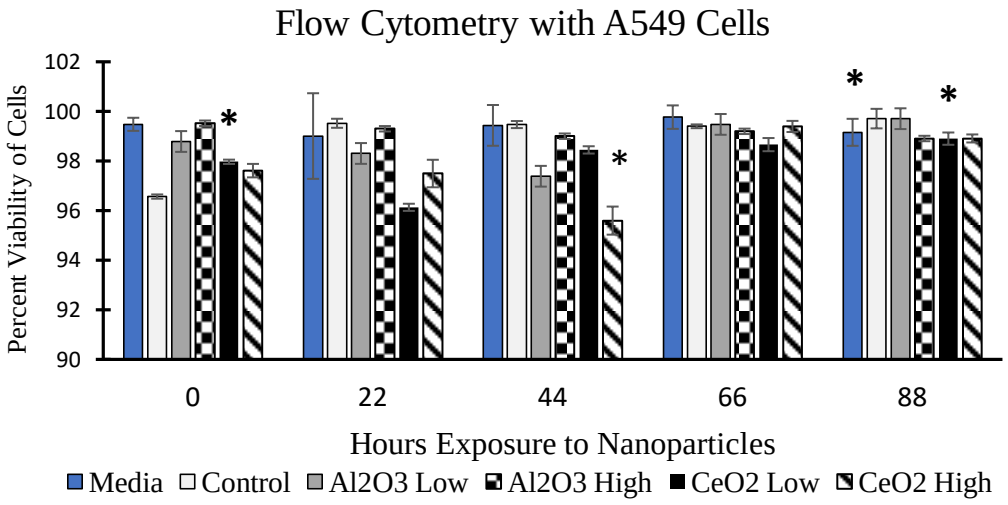

Figure 3. Flow Cytometry with A549 Cells. Exposure to both Low and High concentrations of both nanoparticles. Live counts divided by total counts indicate Percent Viability of Cells. N=3 except Control 22=2 and Media 88, Control 88, Ce Low 88 and Ce High 88=4. Asterisks indicate significance (* $p < 0.05$) as compared to the Control at that same time point.

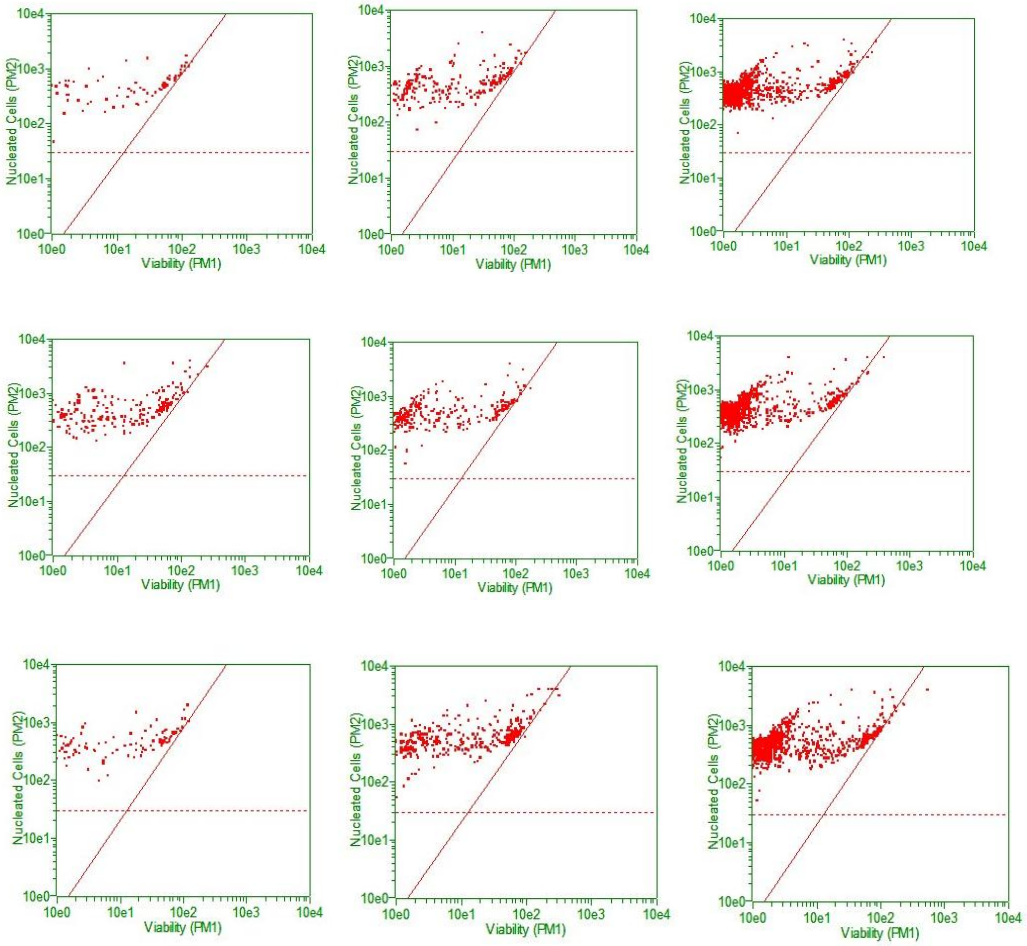

Figure 4. Flow Cytometry Anaylsis of Cell Populations.
Top three graphs are Control cells at 0, 22 and 88 hours incubation in Vehicle Carrier, 0.05% Tween™ 80.
Middle three graphs are Al_2O_3 exposed cells at 0, 22 and 88 hours.
Bottom three graphs are CeO_2 exposed cells at 0, 22 and 88 hours.

Flow cytometry results showed significant differences in viable cell populations (Fig 3 and 4). At 88 hours, the media and CeO_2 Low exposed cells had lower viable populations than the Control cells at 88 hours, and at 44 hours, the CeO_2 Low cells had a lower viable population than the Control and at 0 hour. The lowest percent of viable cells was 95.6%, the CeO_2 at 44 hours. Figure 4 shows the remarable similarity in the sequence and make-up of three cell populations, Control, Al_2O_3 and CeO_2 through 0 hour, 22 hour and 88 hours exposure.

Aim 1 further evaluated the health of the nanoparticle-exposed and Control cells by measuring their ability to rid their microenvironment of superoxides. This was accomplished directly using a xanthine/xanthine oxidase method for total oxidase enzyme activity and indirectly using qPCR to measure the expression of the Super Oxide Dismutase 1 (*SOD1*) gene in Control cells and exposed cells at 22 and 88 hours incubation.

3.4 Total SOD Assay for Al_2O_3 Exposed Cells

The Total SOD Assay evaluated the Al_2O_3 nanoparticle exposed and non-exposed A549 cell population health, by measuring their ability to break down superoxide with SOD1, SOD2 and SOD3. Cell pellet samples were collected and assayed at 22 hours exposure and then at 88 hours of incubation with nanoparticles. BioAssay System's EnzyChromTM Superoxide Dismutase Assay Kit (ESOD-100) was utilized according to the manufacturer's protocol.

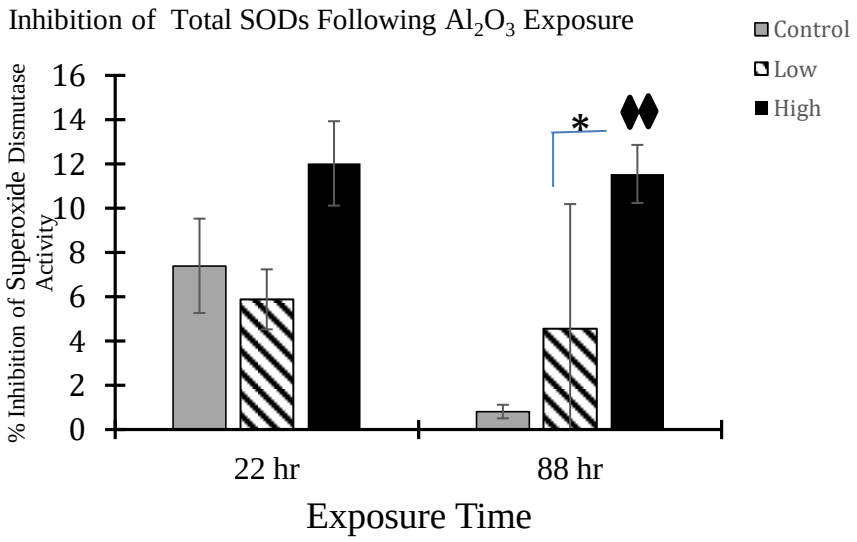

Figure 5. Inhibition of Total SODs Following Al_2O_3 Exposure. All three families of superoxide dismutases were measured in Control and Low and High concentrations of AL_2O_3 nanoparticle exposed cells using a xanthine/ xanthine oxidase test. N=3. Asterisks indicate significance (* $p < 0.05$). Double diamond indicates two-tailed t-test significance ($p< 0.01$) as compared to the control.

The cells exposed to the High 88 of Al_2O_3 nanoparticles showed a significant inhibition in Total SOD as compared to the control and the Low 88 suggesting inhibition of the cells' ability to utilize the three families of SOD enzymes: cytosolic Cu/Zn (SOD1), mitochondrial Fe/Mn (SOD2), and the extracellular nickel type (SODNi) to breakdown the superoxide radical.

3.5 Total SOD Assay for CeO_2 Exposed Cells

The Total SOD BioAssay System's EnzyChromTM Superoxide Dismutase Assay Kit (ESOD-100) measuring Total SODs was repeated for cells exposed to CeO_2 nanoparticles, according to the manufacturer's protocol.

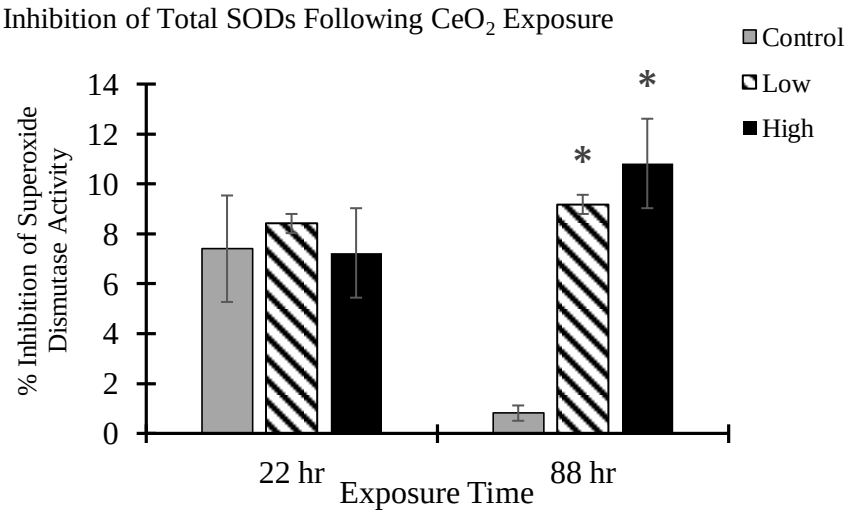

Figure 6. Inhibition of Total SOD Following CeO_2 Exposure. All three families of superoxide dismutases were measured in Control and Low and High concentrations of CeO_2 nanoparticle exposed cells using a xanthine/xanthine oxidase test. N=3. Asterisks indicate significance (* $p < 0.05$) as compared to control.

Both concentrations of 88 hour CeO_2 exposed nanoparticles showed a significant decrease in their ability to breakdown superoxide using the three types of Superoxide Dismutase: cytosolic Cu/Zn (SOD1), mitochondrial Fe/Mn (SOD2), and the extracellular nickel type (SODNi) over the Control cells.

3.6 Expression of ROS Enzyme Gene *SOD1* in Al_2O_3 Exposed Cells

Super Oxide Dismutase 1 (*SOD1*) gene expression was measured indirectly using qPCR to quantitate transcription in Control cells and Al_2O_3 exposed cells.

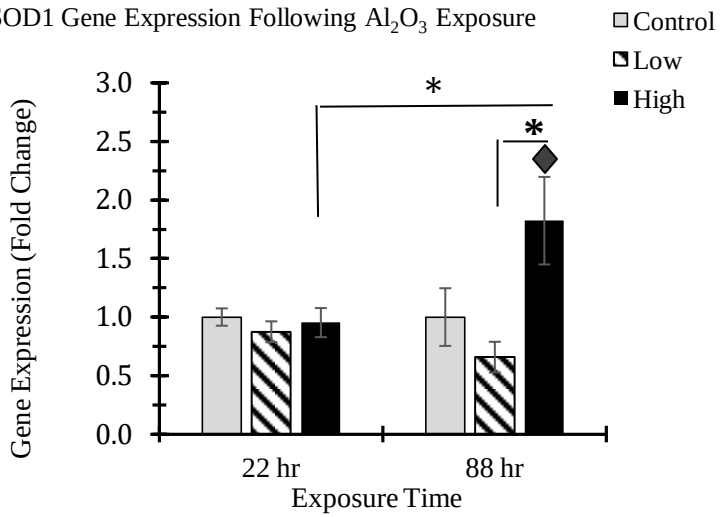

Figure 7. *SOD1* Gene Expression Following AL_2O_3 Exposure. qPCR results on Superoxide Dismutase 1 expression in cells exposed to Low and High concentrations of AL_2O_3 nanoparticles. N=6 except Control 88=8 and Control 22=13. Asterisks indicate significance (* $p < 0.05$). Diamond indicates two-tailed t-test significance ($p< 0.05$).

The High 88 hour CeO_2 exposed cells showed a significant increase in *SOD1* transcription as compared to the Control. There were differences between High 22 and High 88 as well as differences in Low 88 and High 88.

3.7 Expression of ROS Enzyme Gene *SOD1* in CeO_2 Exposed Cells

Super Oxide Dismutase 1 (*SOD1*) gene expression was measured indirectly using qPCR to measure gene transcription in Control cells and CeO_2 exposed cells.

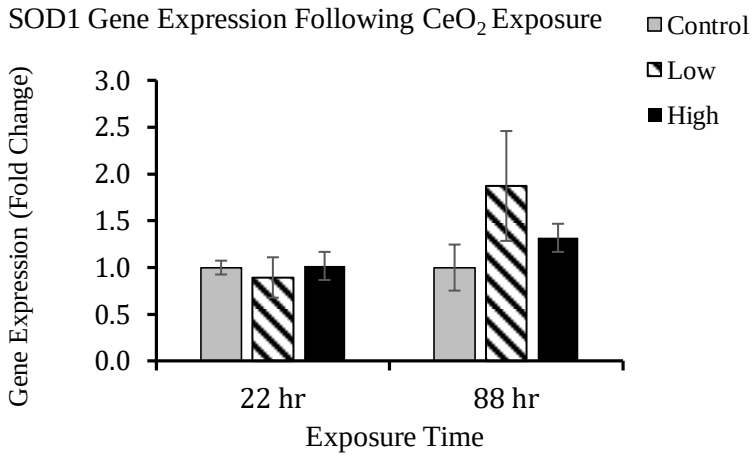

Figure 8. *SOD1* Gene Expression Following CeO_2 Exposure. qPCR results on Superoxide Dismutase 1 expression in cells exposed to Low and High concentrations of CeO_2 nanoparticles N=6 except Ce Low 88 and Ce High 88=7, Ce Low 22 and Control 88=8 and Control 22=13.

No cell groups differed significantly in gene expression.

3.8 Aim 2

Aim 2 was to examine the expression differences of 15 genes which regulate ROS breakdown and asthma, cancer responses, and DNA and histone methylation caused by Al_2O_3 and CeO_2 nanoparticle exposure as compared to Control cells using equivalent cDNA for quantitative polymerase chain reaction (qPCR). Results from 22 and 88 hour incubation time points are presented as fold change as compared to non-exposed Control cells.

Attempts to quantitate A549 cell transcription levels of TMPRSS4, CXCL11, CHI3L1 and CD 86 in A549 cells were unsuccessful.

3.9 Expression of ROS Response Genes *SESN3* and *iNOS* in Al_3O_2 Exposed Cells

These two genes are indicators of the ability to breakdown harmful ROS. Stress-induced Sestrin 3 reduces a variety of ROS and iNOS catalyzes NO-.

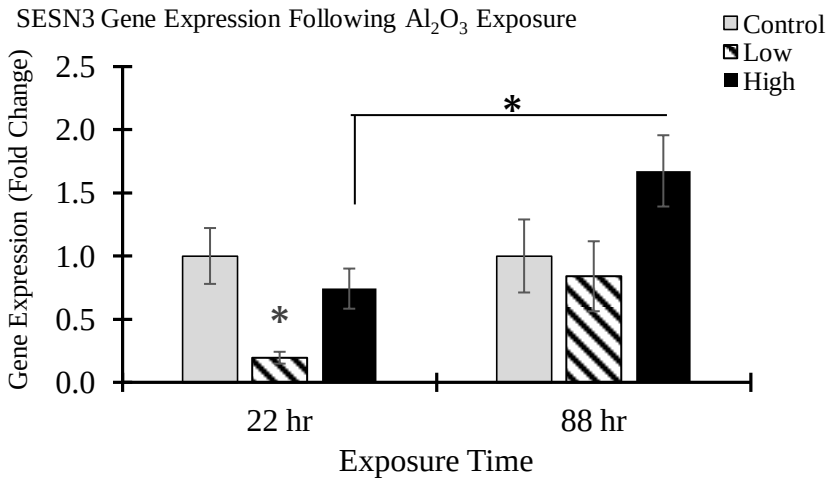

Figure 9. *SESN3* Gene Expression Following AL_2O_3 Exposure**.** qPCR results on Sestrin 3 expression in cells exposed to Low and High concentrations of AL_2O_3 nanoparticles. N=7 except Al High 22=5, Al Low 22 and Al High 88=6, Control 22=8 and Control 88=9. Asterisks indicate significance (* $p < 0.05$).

The Low 22 hours showed a significant lowering of the stress-induced protein Sestrin 3 expression as compared to the Control, which appears to increase toward the normal range in the next 66 hours. There is also a significant difference between the High 22 and 88 hour concentrations.

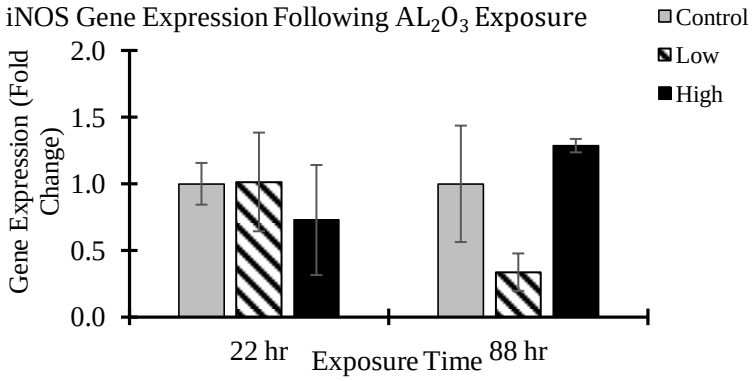

Figure 10. *iNOS* Gene Expression Following AL_2O_3 Exposure**.** qPCR results on Inducible Nitric Oxide Synthase expression in cells exposed to Low and High concentrations of AL_2O_3 nanoparticles . N=6 except Control 88=7 and Control 22 and Al Low 88=8.

No cell groups differed significantly in gene expression.

3.10 Expression of Asthmatic Response Genes *IL-6* and *IL-33* in Al_3O_2 Exposed Cells

Elevated levels of Interleukin 6 and33 are associated with asthma. These two cytokines can serve as either anti-inflammatory or pro-inflammatory signalers.

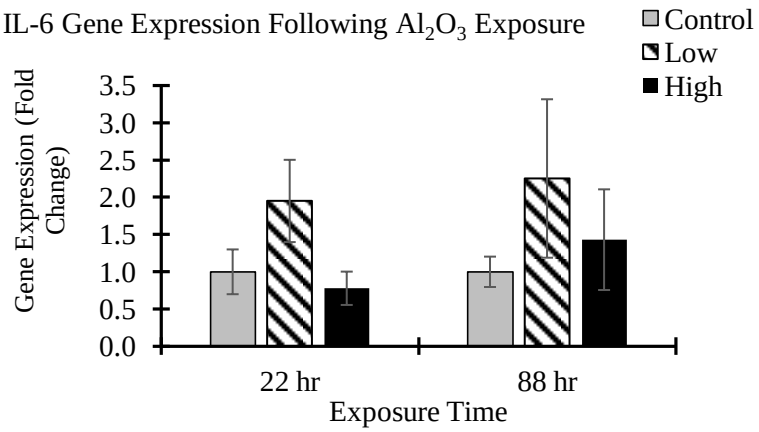

Figure 11. *IL-6* Gene Expression Following Al_2O_3 Exposure. qPCR results on Interleukin 6 expression in cells exposed to Low and High concentrations of CeO_2 nanoparticles. N=6 except Al Low 22 and Control 88=10 and Control 22=11.

No cell groups differed significantly in gene expression.

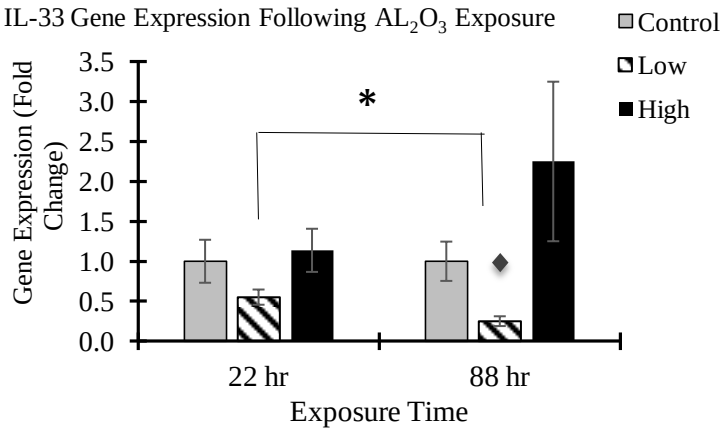

Figure 12. *IL-33* Gene Expression Following Al_2O_3 Exposure. qPCR results on Interleukin 33 expression in cells exposed to Low and High concentrations of Al_2O_3 nanoparticles. N=8 except Al Low 88 and Al High 88=7, Al Low 22=9, Control 88=11 and Control 22=12. Asterisks indicate significance (* $p< 0.05$). Diamond indicates two-tailed t-test significance ($p< 0.05$).

There was a significant decrease in the Low 88 cells when compared to the Control. This graph shows that decrease from the 22 hour concentration.

3.11 Expression of Cancer Genes *HLA-B, IRF8, CD44* and *TNFα* in Al_3O_2 Exposed Cells

All four of these genes have regulatory influence on neoplasm growth and metastasis.

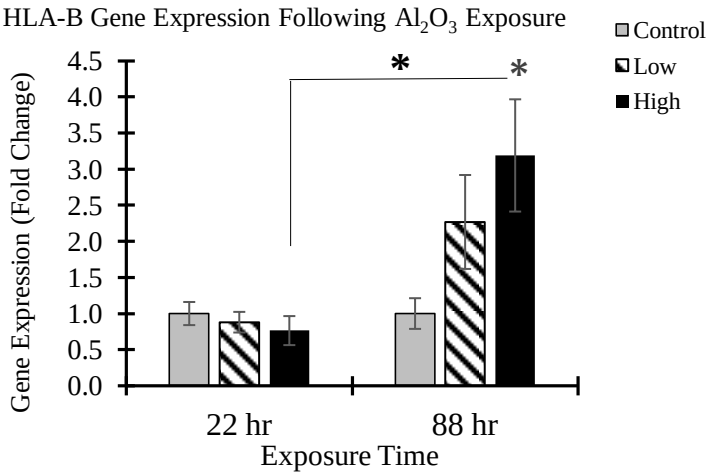

Figure 13. *HLA-B* Gene Expression Following AL_2O_3 Exposure. qPCR results on Human Leukocyte Antigen expression in cells exposed to Low and High concentrations of Al_2O_3 nanoparticles. N=6 except Al Low 88=7, Control 88=8, Al High 88=9 and Control 22=10. Asterisks indicate significance (* $p < 0.05$).

The High Concentration at 88 hours showed a significant upregulation of the *HLA-B* gene as compared to the Control. That increase in transcription is shown from the High 22 hour incubation gene expression.

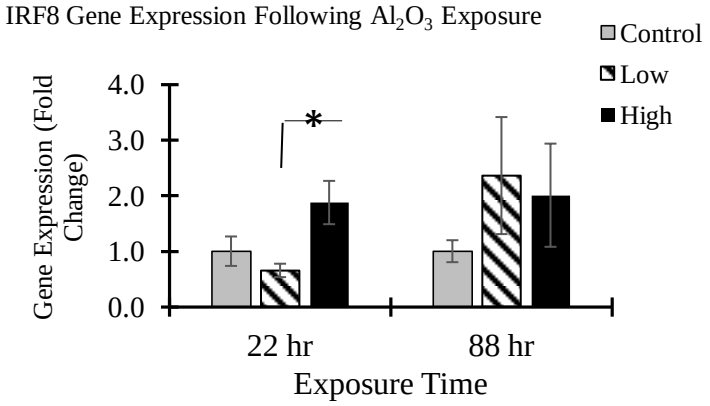

Figure 14. *IRF8* Gene Expression Following Al_2O_3Exposure. qPCR results on Interferon Regulatory Factor 8 expression in cells exposed toLow and High concentrations of Al_2O_3 nanoparticles. N=6 except Control 22, Al High 22 and Al High 88=7 and Control 88=11. Asterisks indicate significance (* $p < 0.05$).

There was a significant difference in the comparison of 22 hour Low and High exposed cells.

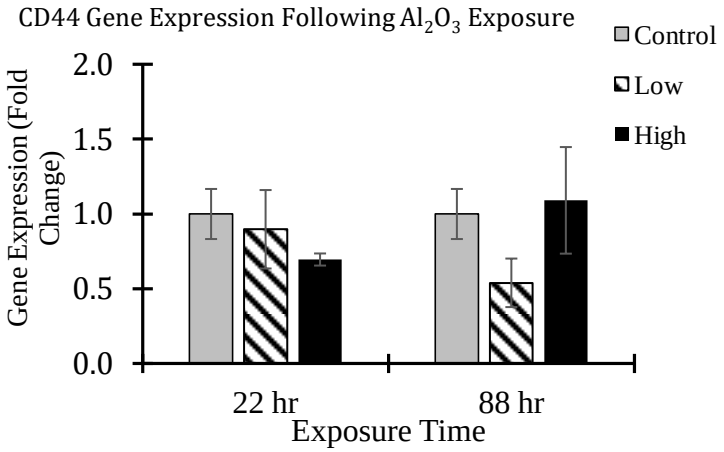

Figure 15. *CD44* Gene Expression Following Al_2O_3Exposure. qPCR results on The Cluster of Differentiation 44 antigen expression in cells exposed to Low and High concentrations of Al_2O_3 nanoparticles. N=6 except Al High 88=7, Control 22=8, Control 88=10.

No cell groups differed significantly in gene expression.

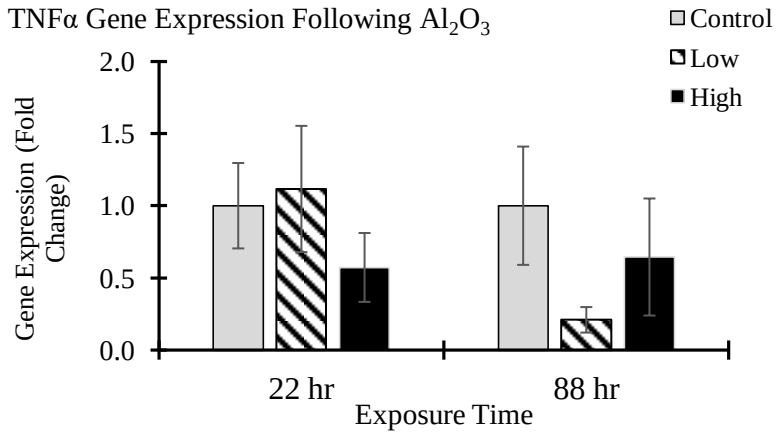

Figure 16. *TNF*α Gene Expression Following Al_2O_3 Exposure. qPCR results on Tumor Necrosis Factor α expression in cells exposed to Low and High concentrations of Al_2O_3 nanoparticles. N=6 except Control 22=10 and Control 88=12.

No cell groups differed significantly in gene expression.

3.12 Expression of ROS Response Genes *SESN3* and *iNOS* in CeO_2 Exposed Cells.

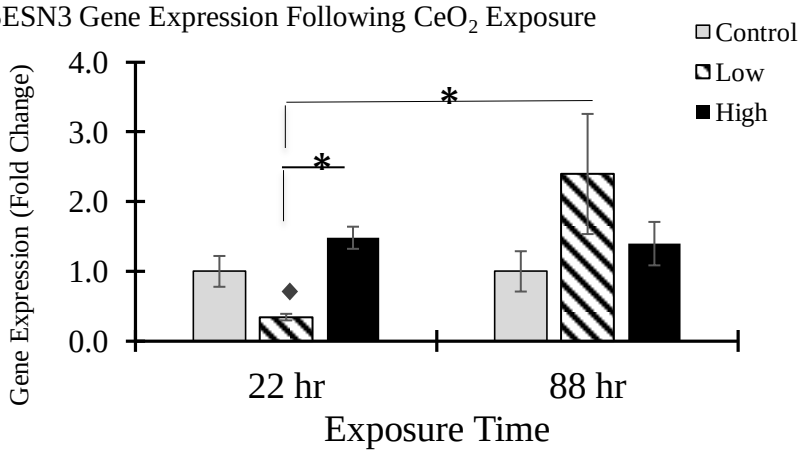

Figure 17. *SESN3* Gene Expression Following CeO_2 Exposure**.** qPCR results on Sestrin 3 expression in cells exposed to Low and High concentrations of CeO_2 nanoparticles N=7 except Control 2 and Ce Low 22=8 and Control 88=9. Asterisks indicate significance (* $p < 0.05$). Diamond indicates two-tailed t-test significance ($p< 0.05$).

The Low 22 hours of incubation showed a significant lowering of Sestrin 3 as compared to the Control. There were also increases between the Low 22 and the Low 88 and the Low 22 and High 22 levels.

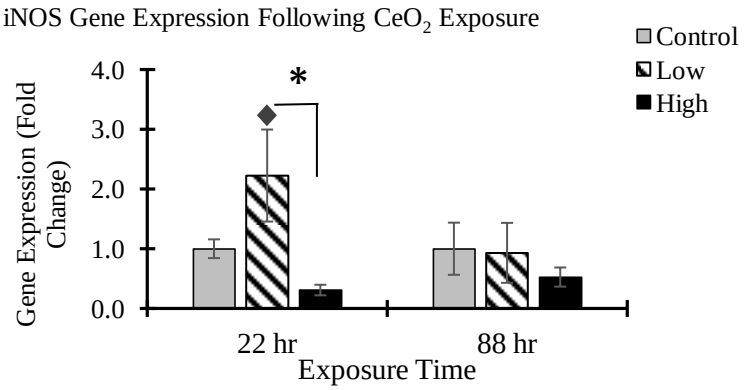

Figure 18. *iNOS* Gene Expression Following CeO_2 Exposure. qPCR results on inducible Nitric Oxide Synthase expression in cells exposed to Low and High concentrations of CeO_2 nanoparticles. N=6 except Control 88 and Ce High 88=7, Control 22 and Ce Low 22=8. Asterisks indicate significance (* $p< 0.05$). Diamond indicates two-tailed t-test significance (* $p < 0.05$).

The Low 22 cells showed a significantl increase in inducible Nitric Oxide Synthase transcription. as compared to the Control. The Low and High concentrations at 22 hours incubation showed a significant difference in level also.

3.13 Expression of Asthmatic Response Genes *IL-6* and *IL-33* in CeO_2 Exposed Cells.

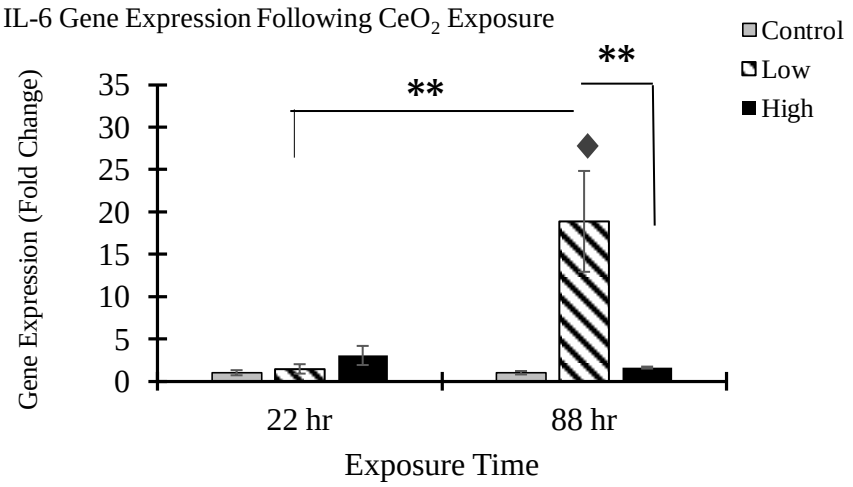

Figure 19. *IL-6* Gene Expression Following CeO_2 Exposure. qPCR results on Interleukin-6 expression in cells exposed to Low and High concentrations of CeO_2 nanoparticles. N=6 except Ce High 22=8, Ce Low 22=9, Control 88=10 and Control 22=11. Asterisks indicate significance (* $p< 0.05$, ** $p< 0.01$). Diamond indicates two-tailed t-test significance ($p< 0.05$).

The Low concentration at 88 hours incubation showed a significant increase in *IL-6* transcription as compared to the Control. The Low 22 and Low 88 expression levels are significantly different as are the Low and High 88.

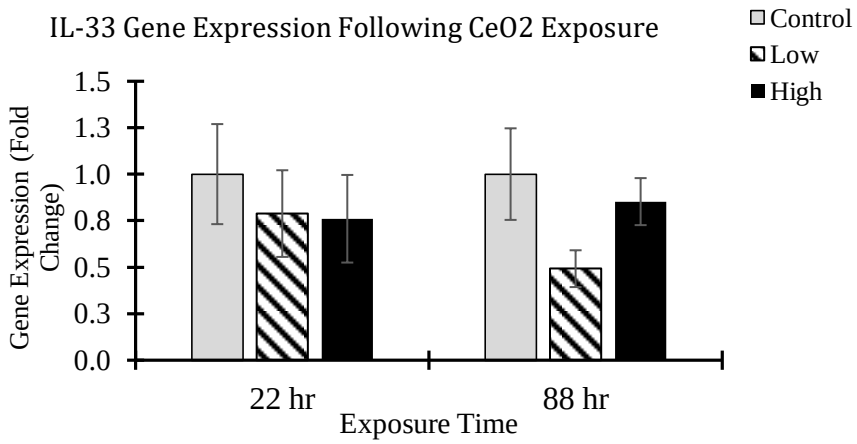

Figure 20. *IL-33* Gene Expression Following CeO_2 Exposure. qPCR results on Interleukin 33 expression in cells exposed to Low and High concentrations of CeO_2 nanoparticles. N=8 except Ce Low 88=6, Ce High 88=9, Control 88=11 and Control 22=12.

No cell groups differed significantly in gene expression.

3.14 Expression of Cancer Genes *HLA-B, IRF8, CD44* and *TNFα* in CeO_2 Exposed Cells.

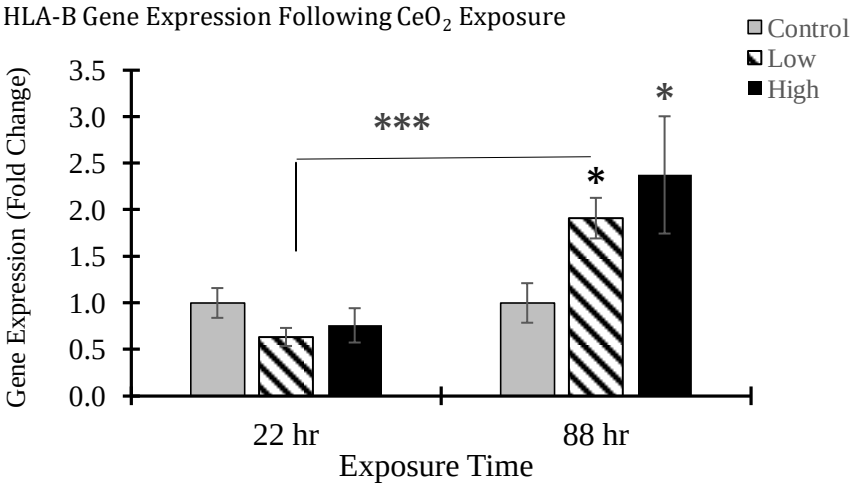

Figure 21. *HLA-B* Gene Expression Following CeO_2 Exposure. qPCR results on Human Leukocyte Antigen expression in cells exposed to Low and High concentrations of CeO_2 nanoparticles. N=6 except Control88=8 and Control 22=10. Asterisks indicate significance (* $p< 0.05$, *** $p< 0.001$).

Both the Low and High 88 Hour exposed cells showed a significant increase in Human Leukocyte Antigen-B expression over the Control cells. That significant increase can be viewed between the Low 22 and Low 88 exposed cell gene expression levels.

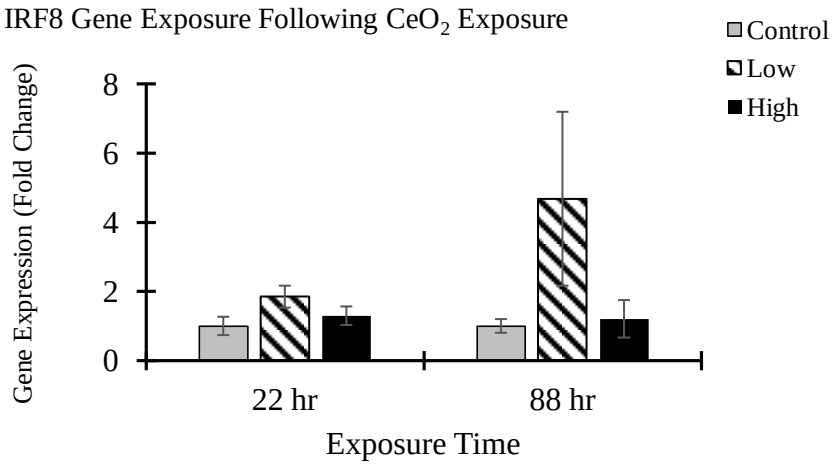

Figure 22. *IRF8* Gene Expression Following CeO_2 Exposure. qPCR results on Interferon expression in cells exposed to Low and High concentrations of CeO_2 nanoparticles. N=6 except Control 22, Ce Low 22 and Control 88=11.

No cell groups differed significantly in gene expression.

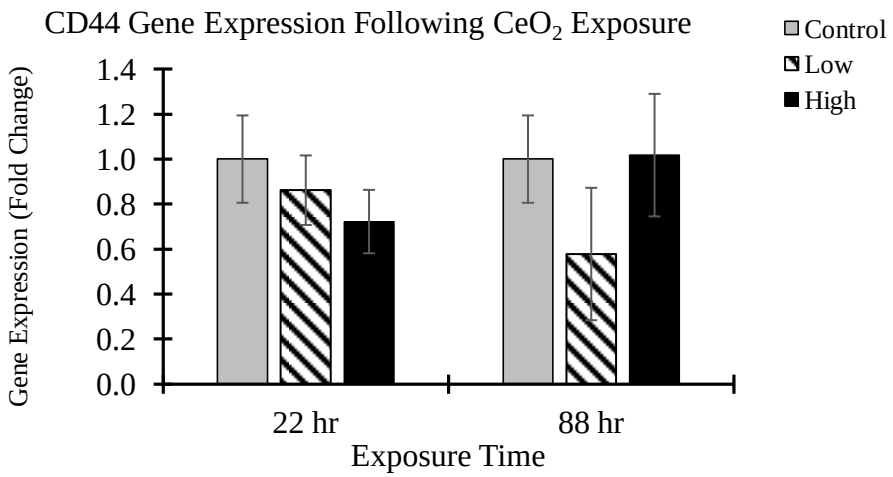

Figure 23. *CD44* Gene Expression Following CeO_2 Exposure. qPCR results on Cluster of Differentiation 44 expression in cells exposed to Low and High concentrations of CeO_2 nanoparticles. N=6 except Control 22 and Ce Low 22=8, Control 88=10.

No cell groups differed significantly in gene expression.

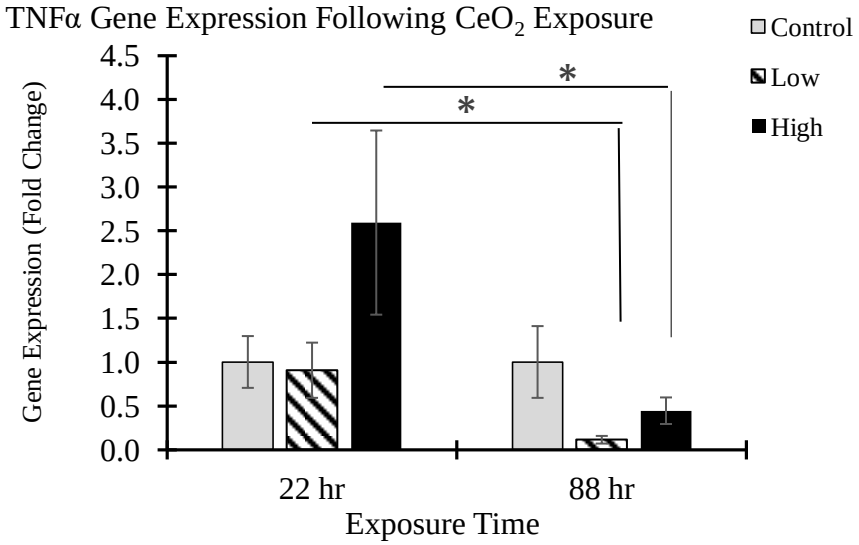

Figure 24. *TNF* α Expression Following CeO_2 Exposure. qPCR results on Tumor Necrosis Factor expression in cells exposed to Low and High concentrations of CeO_2 nanoparticles. N=6 except Ce High 88=9, Control 22=10 and Control 88=12. Asterisks indicate significance (* $p < 0.05$).

There was significance in the differences between TNFα expression levels of the Low 22 and Low 88, as well as the High 22 and 88.

3.15 Global DNA Methylation and DNA Methylation Genes *DNMT1* and *DNMT3A* in Al_2O_3 Exposed Cells

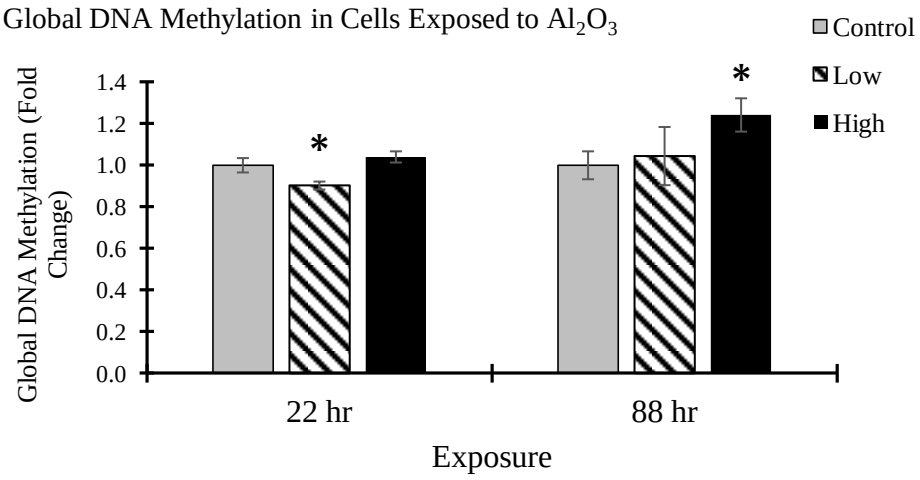

Figure 25. Global DNA Methylation in Cells Exposed to Al_2O_3 versus Control. ELISA technique on cells exposed to Low and High concentrations of AL_2O_3 nanoparticles. N=7 except Ce High 88=10, Control 22 and Control 88 = 11, Al High 22=13 and Al Lo 88=6. Asterisks indicate significance (* $p < 0.05$).

There was significant difference in Global DNA methylation in cells exposed to Low Concentration at 22 hours and in cells exposed to High Concentration at 88 hours as compared to Control.

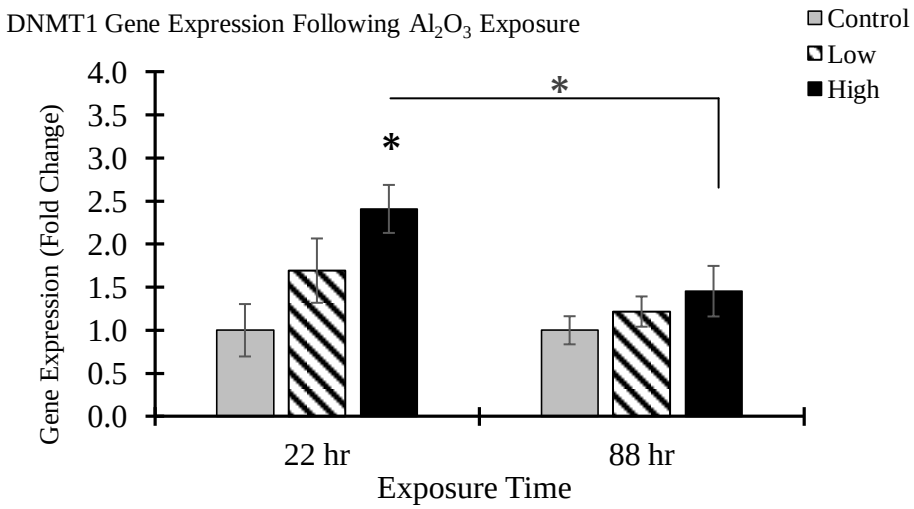

Figure 26. *DNMT1* Gene Expression Following Al_2O_3 Exposure. qPCR gene expression of DNA (cytosine-5)-Methyltransferase 1 in cells exposed to Low and High concentrations of AL_2O_3 nanoparticles. N=9 except Al Low 88=6, Al High 22 and Al High 88=7 and C88=15. Asterisks indicate significance (* $p < 0.05$).

There is a significant difference between the gene expression levels in the High 22 hour exposure as compared to Control, indicating increased transcription of DNA (cytosine-5)-Methyltransferase 1, the normal maintenance methylation enzyme. There is also a significant difference between that High 22 and High 88.

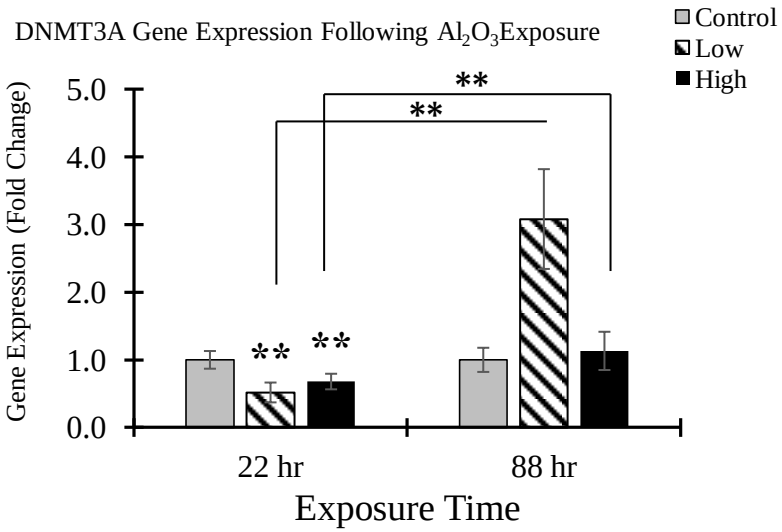

Figure 27. *DNMT3A* Gene Expression Following Al_2O_3 Exposure. qPCR results on expression of DNA (cytosine-5)-Methyltransferase 1 in cells exposed to Low and High concentrations of Al_2O_3 nanoparticles. N=6 except Al High 22 and Al High 88=9, Control 22=11 and Control 88=12. Asterisks indicate significance (**p <0.01).

Significance was observed in decreased *DNMT3A* levels, the de novo methylation enzyme, in both Low and High Concentration at 22 hours as compared to the Control. There were also significant differences between the Low 22 and 88 hour incubation cells and between the High 22 and 88 hour incubation cells.

3.16 Histone Methylation Genes *EZH1, KMT2D, EHMT1* and *DOT1L* in Al_2O_3 Exposed Cells.

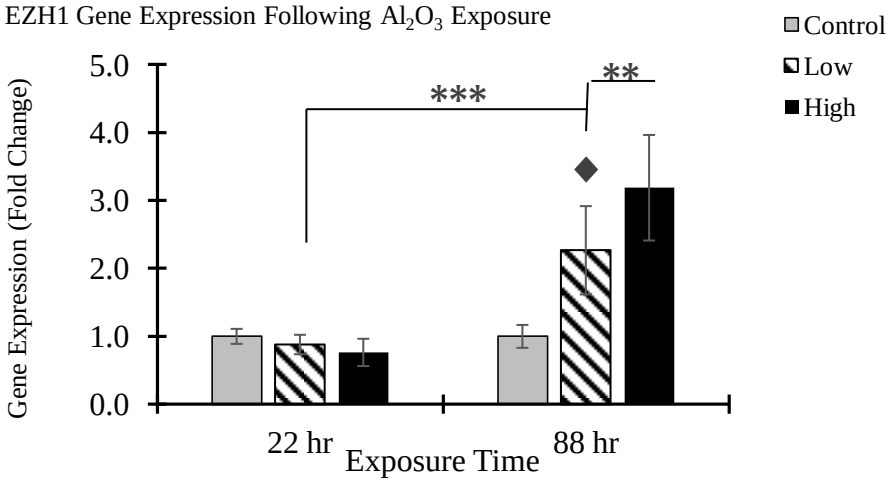

Figure 28. *EZH1* Gene Expression Following Al_2O_3 Exposure. qPCR results on expression of Euchromatic Histone Lysine Methyltransferase in cells exposed to Low and High concentrations of Al_2O_3 nanoparticles. N=6 except Al Low22 and Al High 88=7, Control 22=11 and Control 88=10. Asterisks indicate significance (**p< 0.01, ***p< 0.001). Diamond indicates two-tailed t-test significance (p< 0.05).

There was a significant increase in this histone methylation gene in the Low 88 cells as compared to the Control. That rise can be viewed from the Low 22 cell expression and there is a significant difference between Low 88 and High 88 exposed cell gene levels also.

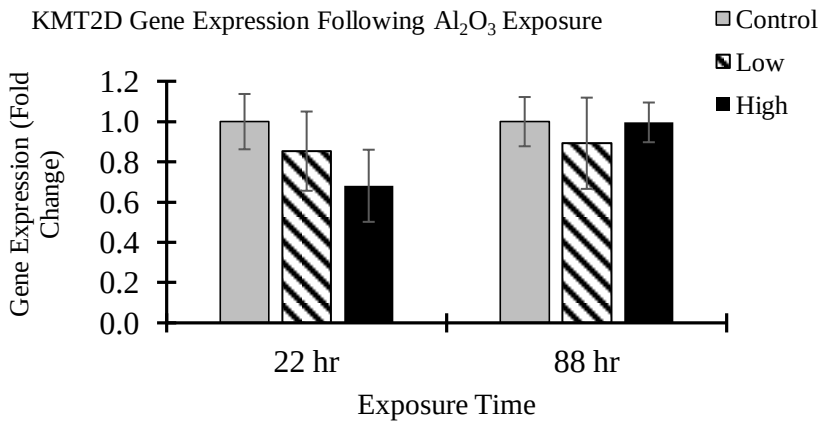

Figure 29. *KMT2D* Gene Expression Following Al_2O_3 Exposure. qPCR results on expression of Histone Lysine N –Methyltransferase 2D in cells exposed to Low and High concentrations of Al_2O_3 nanoparticles. N=6 except Al Low22 and Al High 88=7, Control 22=11 and Control 88=10.

No cell groups differed significantly in gene expression.

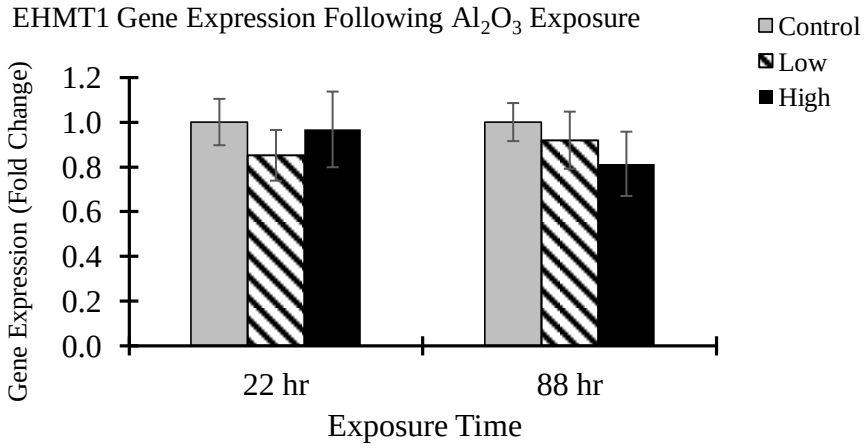

Figure 30. *EHMT1* Gene Expression Following Al_2O_3 Exposure. qPCR results on expression of Euchromatic Histone Lysine N- Methyltransferase 1 in cells exposed to Low and High concentrations of Al_2O_3 nanoparticles. N=6 except Al High 22 and Al Low 88=7, Control 22 and Control 88=13.

No cell groups differed significantly in gene expression.

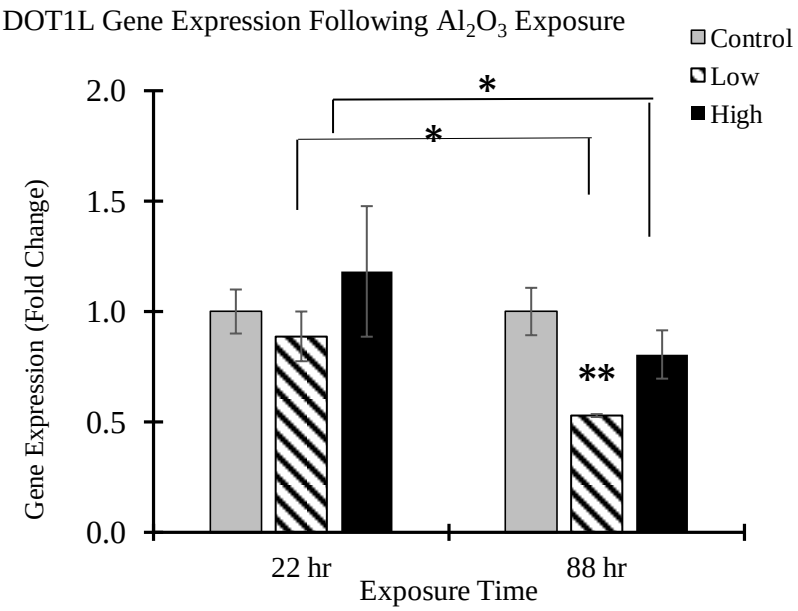

Figure 31. *DOT1* Gene Expression Following Al_2O_3 Exposure. qPCR results on expression of Histone H3K79 methyltransferase in cells exposed to Low and High concentrations of Al_2O_3 nanoparticles. N=6 except Al High 88=7, Control 22=13, Control 88=14. Asterisks indicate significance (* $p < 0.05$, ** $p< 0.01$).

There was a significant decrease between the Al_2O_3 Low 88 hour exposed cells and the Control in *DOT1L* expression. There were also significant differences between Low 22 and 88 cells and High 22 and 88 cells.

3.17 Global DNA Methylation and DNA Methyltransferase Genes *DNMT1, DNMT3A* in CeO_2 Exposed Cells

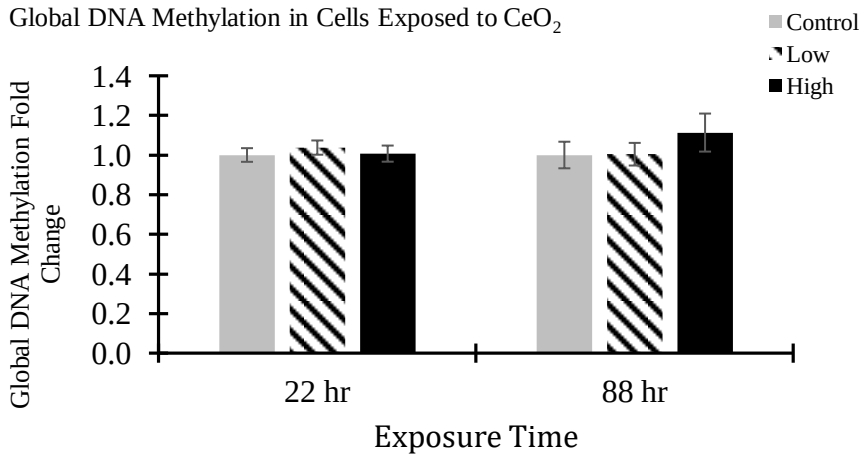

Figure 32. Global DNA Methylation in Cells Exposed to CeO_2 versus Control. ELISA technique on cells exposed to Low and High concentrations of CeO_2 nanoparticles. Control 22 and Control 88=11, Ce High 88=10, Ce High 22, Ce Low 22 and Ce Low 88=7.

No cell groups differed significantly in gene expression.

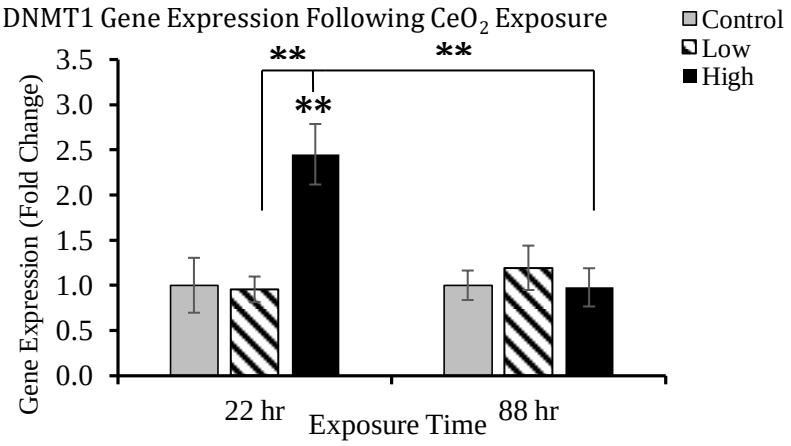

Figure 33. *DNMT1* Gene Expression Following CeO_2 Exposure. qPCR gene expression of DNA (cytosine-5)-Methyltransferase 1 in cells exposed to High and Low concentrations of CeO_2 nanoparticles. N=9 except Ce Low 22=7, Ce High 22 =10 and Control 88 =15. Asterisks indicate significance (** $p<0.01$).

There was a significant difference between the High 22 hour exposed cells and the Control in maintenance DNA methylation. There were also significant differences between Low 22 and High 22 and between High 22 and High 88.

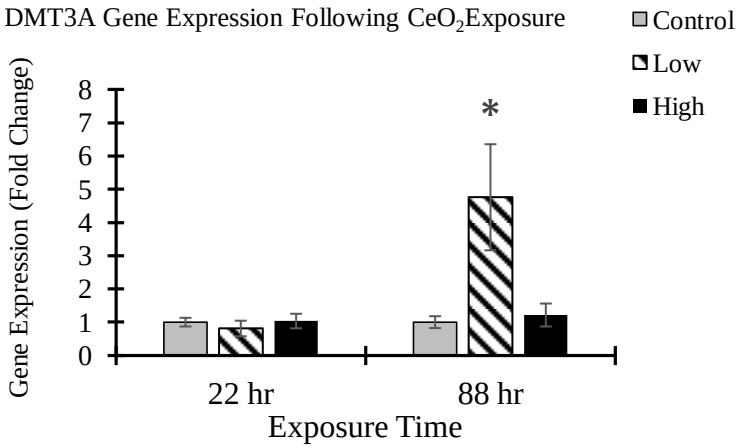

Figure 34. *DNMT3A* Gene Expression Following CeO_2 Exposure. qPCR gene expression of DNA (cytosine-5)-Methyltransferase 3A in cells exposed to Low and High concentrations of CeO_3 nanoparticles. N=6 except Ce Low 22=7, Ce High 22=9, Ce High 88=10, Control 22=11, Control 88=12. Asterisks indicate significance (* $p < 0.05$).

There was a significant increase in the Low 88 hour exposed cells in *de novo* DNA methylation over the Control cell levels.

3.18 Histone Methylation Genes *EZH1, KMT2D, EHMT1* and *DOT1L* in CeO_2 Exposed Cells

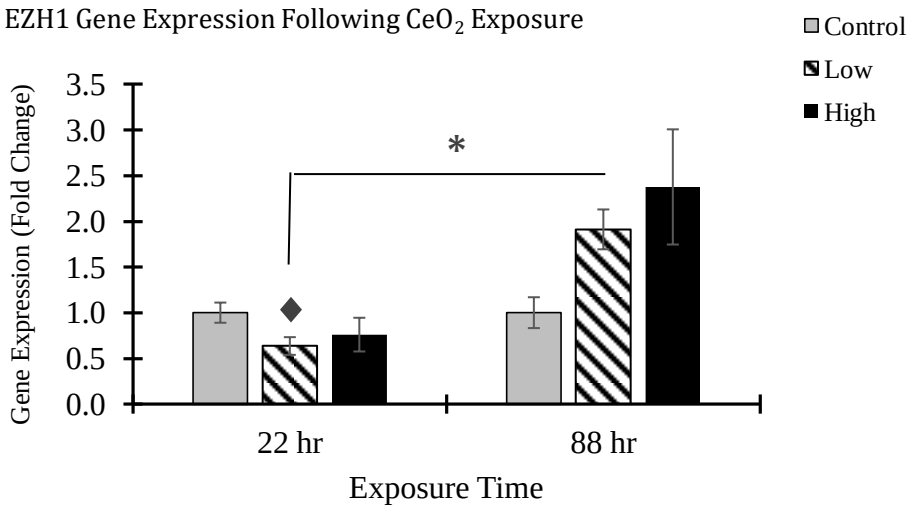

Figure 35. *EZH1* Gene Expression Following CeO_2 Exposure. qPCR gene expression of Euchromatic Histone-Lysine N-Methyltransferase in cells exposed to High and Low concentrations of CeO_2 nanoparticles. N=6 except Ce High 22 and Ce Low 88=7, Control 22=11 and Control 88=10. Asterisks indicate significance (* $p < 0.05$). Diamond indicates two-tailed t-test significance against control ($p< 0.05$).

There was a significant decrease in Low 22 cell transcription of this histone methylator as compared to the Control. There was a significant increase from that Low 22 hour to the Low 88 hour exposed cell expression.

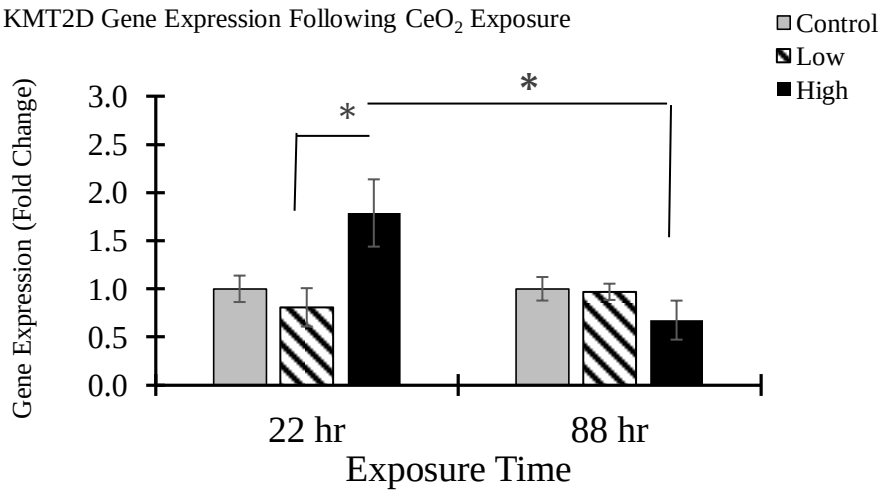

Figure 36. *KMT2D* Gene Expression Following CeO_2 Exposure. qPCR gene expression of Histone-Lysine N-Methyltransferase 2D in cells exposed to Low and High concentrations of CeO_3 nanoparticles. N=6 except Ce Low 22=7, Control 22=12, Control 88=10. Asterisks indicate significance (* $p < 0.05$).

There was a significant difference between the Low 22 and High 22 hour and High 22 and High 88 exposed cells.

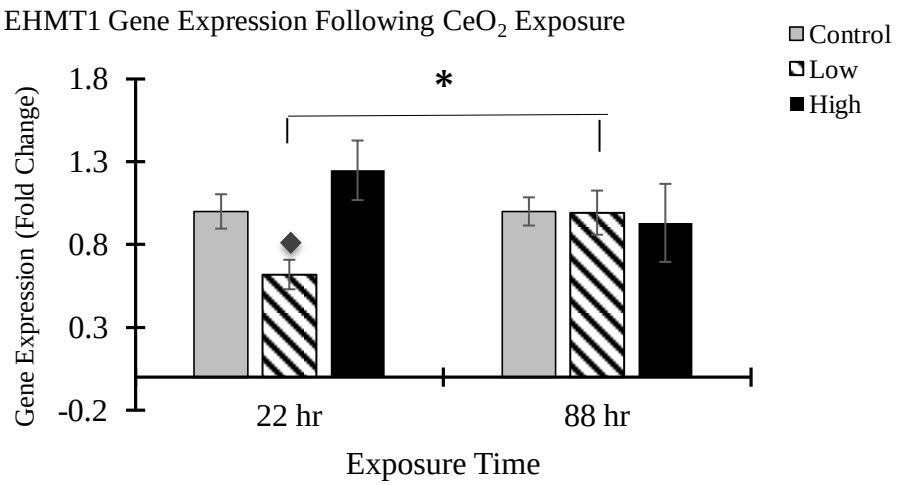

Figure 37. *EHMT1* Gene Expression Following CeO_2 Exposure. qPCR gene expression of Euchromatic Histone Lysine Methyltransferase 1 in cells exposed to Low and High concentrations of CeO_3 nanoparticles. N=6 except Ce High 22=7, Control 22 and Control 88=13. Asterisks indicate significance (* $p < 0.05$). Diamond indicates two-tailed t-test significance ($p< 0.05$) as compared to the control.

There was a significant decrease of *EHMT1* histone methylation as compared to the Control. At 88 Hours, that level significantly increased.

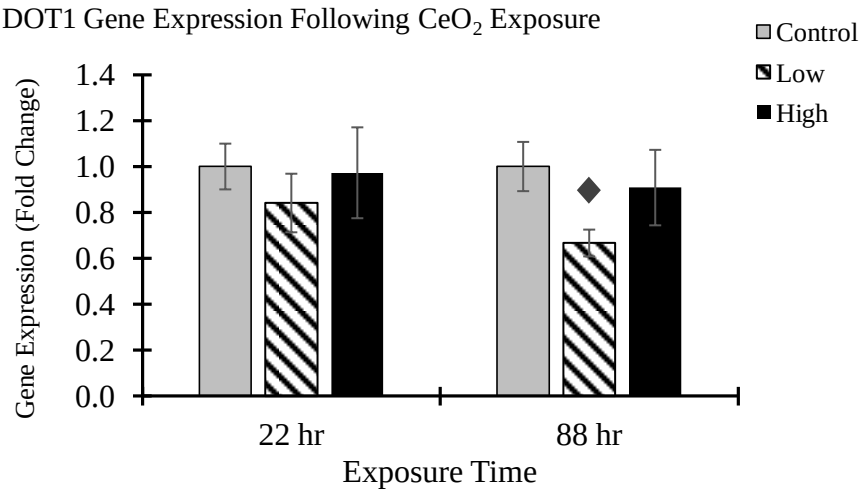

Figure 38. *DOT1L* Gene Expression Following CeO_2 Exposure. qPCR gene expression of Euchromatic Histone-Lysine Methyltransferase 1 in cells exposed to Low and High concentrations of CeO_3 nanoparticles. N=6 except Ce High 22 and Ce Low 88=7, Control 22=11, and Control 88=10. Diamond indicates two-tailed t-test significance ($p<0.05$) as compared to the control.

There was a significant difference between the Low 88 hour exposed cells and the control in *DOT1L* histone methylation expression.

CHAPTER IV

DISCUSSION

The present study examined the effects of 30 nm aluminum oxide and 15-30 nm cerium oxide nanoparticle exposure on alveolar cells (A549) at the cellular and epigenetic levels. Concentrations of 25 μg/ml (Low) and 250 μg/ml (High) were used. The Control Vehicle (Media with 0.05% Tween 80^{TM}) was not toxic to A549 cells. Neither aluminum oxide nor cerium oxide nanoparticles altered cell viability during an 88-hour exposure period. When the untreated control has 100% viability, greater than 70% viability shows a treatment is not toxic (Spezatti *et al* 2017). In the present study, the lowest viability demonstrated was 95.6% in the High CeO_2 at 44 hours. Inhalation of environmental nanoparticles may escalate as nanomaterial becomes increasingly utilized in manufacturing processes, food appilications, cosmetics and pharmaceuticals. Nanoparticles can even accumulate in the lungs and chronically slow down the body's ability to clear them (Moller *et al* 2008). In a cell culture condition, pinocytosis of nanoparticles occurs within 6 hours of culture. A study by Simon-Deckers *et al* (2008) found a variety of different sized and different composition of nanoparticles, including 13 nm Al_2O_3, aggregated into lysosomes, with no free nanoparticles seen after 48 hours exposure (Simon-Deckers *et al* 2008). Although endocytosis depends on concentration, time and energy, this indicates that nanoparticles can enter the cell without physically damaging the cells and altering viability (Kim *et al* 2003, Ma *et al* 2013, Meng *et al* 2011).

In contrary, some studies observed significant cell death *in vitro* due to Al_2O_3 exposure when different culture conditions than in the present study were used. Use of high concentrations of superheated Al_2O_3 nanoparticles, concentrations double the one in this study, or

1 mg/ml of 0.7 nm Al_2O_3 dust proved harmful (Jordan *et al* 2009, Li *et al* 2016b, Roh *et al* 2011). In one study, 25 ug/ml AL_2O_3 made 400-800 nm agglomerates but was not toxic to A549 cells in artificial lung surfactant in RPMI media with heat-inactivated serum, but was toxic to a co-culture with alveolar human phagocytes. Aggregates proved toxic when 25μg/ml concentrations of 13-25 nm AL_2O_3 nanoparticles without a dispersing agent were added to A549 cells (Lin *et al* 2008). A low concentration (0.05%) of Tween 80™, a non-ionic surfactant, was utilized in this study to alleviate nanoparticle clumping. The wells contained 0.0125% total Tween 80™ concentration. Tween 80™ concentrations of up to 1% usually are not toxic to mammalian cells (Stavrovskaya *et al* 1975). Plant cells and human peripheral blood lymphocytes proved susceptible to DNA strand breaks and oxidative stress when subjected to AL_2O_3 particles (De *et al* 2016, Sliwenska *et al* 2015).

This study used a Low concentration of 25 μg/ml and a High concentration of 250 μg/ml which are relevant to environment and human exposure. Based on past publications, it was plausible to assume that cells exposed to these concentrations could survive, undergo endocytosis and proceed to mitosis to observe gene expression changes. Earlier studies showed physical DNA damage in 68-390 μg/ml of <50 nm Al_2O_3 nanoparticle exposure in human BEAS-2B and 80 μg/ml of <25 nm CeO_2 nanoparticle exposure in A549 cells (Kim *et al* 2009, Kain *et al* 2012).

Because of their small size and large surface area to volume ratio, nanomaterials have shown more chemical activity leading to the increased production of ROS in a variety of cells (Caruthers *et al* 2007, Choi and Hu 2008, Zoroddu *et al* 2014). In this study, both High 88 dose nanoparticles significantly increased oxidative stress as indicated by the inhibition of total superoxide dismutase activity, the sum of SOD1, SOD2 and SOD3 activity. Interestingly, in contrast, the prolonged exposure (88 hours) of Low CeO_2 and High Al_2O_3 concentrations resulted

in increased SOD1 gene expression indicating the possibility for a decrease in SOD2 and SOD3expressions. The ability of aluminum nanoparticles to cause oxidative stress has previously been demonstrated. In HBE cell culture and mouse lung tissue 100 ug/ml and 500 ug/ml concentrations of 37-64 nm Al_2O_3 caused mitochondrial gene suppression and increased cellular ROS (Li *et al* 2016b). In human intestinal caco-2 cells, 200ug/ml nanoalumina was not cytotoxic but some oxidative stress pathways were activated (Braeuning *et al* 2018). In human lymphocyte cell culture, ROS was induced and their defenses: lipid peroxidation, catalase, glutathione, and superoxide dismutase, were reduced by the aluminum based nanoparticles (Rajiv *et al* 2016). In the fresh water fish, *Carassius auratus*, 0.01μg/ml 0.1 μg/ml concentrations of 20 nm Al_2O_3 nanoparticles over 14 days exposure caused catalase (which reduces the ROS hydrogen peroxide) and SOD activity to increase in the gills and livers *(*Benevides *et al* 2016). *In vivo* experiments have revealed oxidative damage in mice and algae (Shah *et al* 2015, Park *et al* 2015).

CeO_2 exposed cells had decreased levels of SOD, suggesting oxidative stress was elevated in these cells due to nanocerium exposure. Literature suggests that nanoceria do not appear as cytotoxic as nanoalumina, possibly because of the coexistence of both Ce^{3+}/Ce^{4+} on their surfaces (Sun *et al* 2012). Ceria-containing nanoparticles have shown the ability to scavenge harmful ROS to reduce oxidative stress and are being studied for possible therapuetic applications even with the existence of conflicting experimental results (Babu *et al* 2007, Tarnuzzer *et al* 2005, Xia *et a*l 2008). In spite of their promise in therapeutic applications, cerium oxide nanoparticles can be toxic to algae (Rohder *et al* 2014), plants (Majundar *et al* 2014, Tumburu *et al* 2017), earthworms (Lahive *et al* 2014), rodents (Aalapati *et al* 2014, Hirst *et al* 2013) and human cells (Kumari *et al* 2014, Mittal and Pandy 2014). In a 2014 study, A549 cells were exposed to100 μg/ml of 8-40 nm cuboidal CeO_2 nanoparticles in water, which led to DNA damage and an initial increase in ROS, which subsided within 24 hours of exposure (Mittal and

Pandy 2014). Conversley, cardiac progenitor cells exposed to 50 μg/ml of 5-8 nm CeO_2 proved viable and and cable of decomposing H_2O_2 to O_2 and H_2O (Pagliari *et al* 2012*).* *In vivo* studies have shown lung injury and cytokine increase, including IL-6 and TNFα, in mice inhalation tests, but no overt toxicity when administered orally, intraveneously or intrperitoneally (Aalapati *et al* 2014, Hirst *et al* 2011). However, in this study, the CeO_2 exposed cells did show a decrease in total SOD.

Expression of genes encoding the alarmin Sestrin protein (SESN3), which inhibits oxidative stress in alveolar cells, is decreased by both aluminum and cerium nanoparticles during 22 hour exposure, suggesting an early increased oxidative stress to the cells. Sixty-six hours later, levels had returned, with the cells leading an effort to counteract that oxidative stress. Some toxicants induce an over production of nitric oxide and reactive oxygen species, causing oxidative stress and cell death (Beckman and Koppenol 1996). Inducible Nitric Oxide Synthase levels may have been varied slightly and differentially by the nanoparticles but this important bioactive molecule is involved in the immune response at specific concentrations and dysregulation could have dangerous holistic consequences (Kelly *et al* 1994, Ikeda and Shimada 1997, Vannini *et al* 2015).

In the present study, both aluminum and cerium exposure caused an increase in the expression of *IL-6*, an asthma exacerbation indicator. Since clinical trials of an IL-33 suppressor shows promise as a treatment for asthma, it is of note that *IL-33* transcription is lowered in the 4th doubling of exposed cells in the Low Concentration. It should be pointed out, however, that both of these interleukins are both pro-inflammatory and anti-inflammatory agents. Most cytokines have dual roles to both activate and repress identical processes depending on stimulation due to co-factors, competitors, isoforms, and pathways enabled. Since cytokines can adsorb onto nanoparticles, it was important to measure them indirectly via gene expression dysregulation

(Pailleux *et al* 2013). Al_2O_3 nanoparticle exposure to rats led to an increase in IL-6 and white blood cells (Park et al 2015). In another study, TNF and IL-6, as measured by ELISA, were downregulated without significance over 4-6 hours incubation with nanoparticles and methicillin-resistant *Staphylococcus aureus* (MRSA) (Braydich-Stolle *et al* 2010).

Cancer proliferation is often preceded by variations in transcription of Human Leukocyte Antigen B (*HLA-B*), Interferon 8 (*IRF8*), Cluster of Differentiation (*CD44*) and Tumor Necrosis Factor Alpha (*TNF*α). Although there were no significant changes in the transcription levels of *IRF8*, *CD44* or *TNFα* in the present study, *HLA-B* transcription levels increased after exposure, which allows for an increase in tumor incidence and metastastis of lung cancer (Bremnes *et al* 2011, Bowness 2015). In another study, AL_2O_3 nanoparticles decreased the tumor regulator tyrosine-protein phosphatase non-receptor type (*Ptpn6*) gene transcription in A549 cells (Li *et al* 2016a). Also in A549 cells, silver nanoparticles have been observed to downregulate the cancer suppressor gene *P53* and caspase (important in programmed cell death) and increase DNA and histone methylation (Blanco *et al* 2017). Accumulating evidence shows that generalized chronic inflammation is associated with an increased cancer risk (Del Prete *et al* 2011). So the present study, together with existing literature suggests that the prolonged exposure to aluminum and cerium nanoparticles may induce activation of one or more cancer pathways.

One of the major objectives of this study was to examine epigenetic effects in A549 cells caused by Al_2O_3 and CeO_2 nano particles. The idea is if the nanoparticles cause epigenomic changes, the changes should be observed in the form of gene expression or global DNA methylation. Nanoaluminum exposure induced expression of DNA methyltransferase I (*DNMT1*) gene after 22 hours of exposure and at the same time tended to suppress *DNMT3A* expression and global methylation, suggesting the first wave of global hypomethylation followed by hypermethylation of genome due to nanoaluminum exposure.

The major protein of chromatin consists of histones, which control how much DNA can be accessed for transcription (Strahl and Allis 2000, Tan *et al* 2011). This study's DNA methylation adjustments are further supported by the decreased expression of the markers of active chromatin state (*DOT1*) and increased expression of the marker of closed chromatin (*EZH1*) upon prolonged exposure. On the other hand, nanocerium particle exposure led to the increased state of *DNMT1* expression with no significant alteration in global DNA methylation which could be compensated for by the decreased expression histone markers of closed chromatin (*EHMT1*) and decreased expression of open chromatin marker (*DOT1*). Taken together, the present study suggests that nanoaluminum and nanocerium particles induce oxidative stress and epigenetic alterations in alveolar A549 cells and provide insights into respiratory health risks by their exposure in humans. There was no significant change in the transcription of the *KMT2D* gene, the disregulation of which has been implicated in errant DNA repair, cell growth and cancers. Altered methylation processes can lead to the silencing of tumor suppressor genes, which in turn causes increased cell proliferation, the ability to metastasize to adjacent or distant sites and changes in programmed apoptosis (Plass and Smiraglia 2006). The use of this gene expression technique is valuable for the prediction of effects nanoparticles may have on the health of organisms.

In summary, this study found that both Al_2O_3 and CeO_2 nanoparticles have the capability of reducing human alveolar cell defenses to protect themselves from damaging reactive oxygen species, increasing HLA-B, a glycoprotein marker for lung cancer metastasis, and increasing the tail methylation of core histone H3. In addition, dysregulation of DNA methylation genes indicate exposure to the nanoparticles causes conformational changes to the cells' epigenetic markers which can further lead to disease states. Within the context of chromatin, DNA methylation does not function in isolation. Instead, there is a complex interplay between DNA

methylation and histone modifications, including acetylation, methylation and ubiquitylation (Rose and Klose 2014, Liu *et al* 2016, Vann and Kutateladze 2017, Smeenk and van Attikum 2013). So further histone examination is required as a follow-up to this project. Testing the co-mingling of CeO_2 and Al_2O_3 will realistically outline any threat to active duty military personnel as soldiers and sailors are exposed to both munitions and diesel exhaust. Without a doubt, additional gene expression assays will prove of interest in both cell lines and at varying nanoparticle exposure concentrations and additional time points. Effective immunity and a disease-free state depend on thousands of the soluble messenger proteinaceuos cytokines that affect the innate and acquired immune responses and there are a plethora to choose from for future testing. Since alveolar cells work in conjunction with alveolar macrophages, a co-culture experiment would make for an interesting sequel investigating effects on phagocytosis. *In vitro* genotoxicity should include the HPRT Gene Mutation Assay and the Mammalian Cell Micronucleus Test, which examine DNA damage (Elespuru *et al* 2018). *In vivo* testing could help define particle biokinetics, uptake and fate (Becker *et al* 2011). Therefore, future studies will be directed toward understanding long-term epigenotoxicity of these two nano-particles in respiratory cells *in vitro* and *in vivo*.

REFERENCES

Aalapati, S., Ganapathy, S., Manapuram, S. Anumolu, G., Prakya, B.M. 2014. Toxicity and bio-accumulation of inhaled cerium oxide nanoparticles in CD1 mice. *Nanotoxicology.* 8(7): 786–798.

Abel, K.J., Brody, L.C., Valdes, J.M., Erdos, M.R., McKinley, D.R., Castilla, L.H., Merajver, S.D., Couch, F.J., Friedman, L.S., Ostermeyer, E.A., Lynch, E.D., King, M.C., Welcsh, P.L., Osborne-Lawrence, S., Spillman, M., Bowcock, A.M., Collins, F.S., Weber, B.L. 1997. Characterization of EZH1, a human homolog of *Drosophila* enhancer of zeste near BRCA1. *Genomics*. 37(2): 161–71.

Ahmed, S.A., Gogal, Jr., R. M., Walsh, J.E. 1994. A new rapid and simple non-radioactive assay to monitor and determine the proliferation of lymphocytes: an alternative to [^{3}H]thymidine incorporation assay. *Journal of Immunological Methods*. 170(2): 211-224.

Almenier, H.A., Al Menshawy, H.H., Maher, M.M.,. Al Gamal, S.S. 2012. Oxidative stress and inflammatory bowel disease. *Front. Biosci*. 4: 1335-1344.

Alves C.S., Burdick, M.M., Thomas, S.N., Pawar, P., Konstantopoulos, K. 2008. The dual role of CD44 as a functional P-selectin ligand and fibrin receptor in colon carcinoma cell adhesion. *American Journal of Physiology. Cell Physiology*. 294(4): C907–16.

Amash, A., Wang, L., Wang, Y., Bhakta, V., Fairn, G.D., Hou, M., Peng, J., Sheffiled, W.P., Lazarus, A.H. 2016. CD44 antibody inhibition of macrophage phagocytosis targets Fcγ receptor-and complement receptor 3-dependent mechanisms. *J. Immunol.* 196: 3331–3340.

American Cancer Society. 2018. Key statistics for Lung Cancer. www.cancer.org/cancer/non-small-cell-lung-cancer.

American Lung Association, Editorial Staff. 2016. 15 Years Later: Looking at the respiratory impacts of the Sept. 11, 2001 attacks. Each breath, a blog by the American Lung Association.

Anderson, T. 2015. Diesel On The Ground – A Look At NATO Fuels And Vehicles.Diesel Army .www.dieselarmy.com/features/history/diesel-on-the-ground-a-look-at-nato-fuels-and-vehicles.

Arand, D., Spieler, T., Karius, M.R., Branco, Meilinger, D., Meissner, A., Jenuwein, T., Xu, G., Leonhardt, H., Wolf, V., Walter, J. 2012. In vivo control of CpG and non-CpG DNA methylation by DNA methyltransferases. *PLoS Genetics*. 8: e1002750.

Ardeshir-Larijani, F., Bhateja, P., Lipka, M.B., Sharma, N., Fu, P., Dowlati, A. 2018. KMT2D mutation is associated with poor prognosis in non–small-cell lung cancer. *Clinical Lung Cancer*. 19(4): e489-e501.

Babu, S., Velez, A., Wozniak, K, Szydlowska, J., Seal, S. 2007. Electron paramagnetic study on radical scavenging properties of ceria nanoparticles. *Chem. Phys. Lett*. 442: 405–408.

Baedke, J. 2018. *Above the Gene, Beyond Biology: Toward a Philosophy of Epigenetics*. Pittsburgh, Pa.: University of Pittsburgh Press.

Bahrami, M.S., Movahedi, M., Aryan, Z., Bahar, M.A., Rezaei, A., Sadr, M., Rezaei, N. 2015. Serum IL-33 is elevated in children with asthma and is associated with disease severity. *International Archives of Allergy and Immunology*. 168(3): 193–6.

Becker, H., Herzberg, F., Schulte, A., Kolossa-Gehring, M. 2011. The carcinogenic potential of nanomaterials, their release from products and options for regulating them, *Int. J. Hyg. Environ. Health*. 214: 231–238.

Beckman, J.S., Beckman, T.W., Chen, J., Marshall, P.A., Freeman, B.A. 1990. Apparent hydroxyl radical production by peroxynitrite: implications for endothelial injury from nitric oxide and superoxide. *Proc. Natl. Acad. Sci. USA*, 87(4): 1620–1624.

Beckman, J.S., Koppenol, W.H. 1996. Nitric oxide, superoxide, and peroxynitrite: the good, the bad, and ugly. *Am. J. Physiol*. 271(5) P1: C1424–C1437.

Belyanskaya L., Manser P., Spohn P., Bruinink A., Wick P. 2007. The reliability and limits of the MTT reduction assay for carbon nanotubes-cell interaction. *Carbon* 45: 2643–2648.

Benavidas, M., Fenandez-Lodiero, J., Coelho, P., Lodiero, C., Diniz, M. 2016. Single and combined effects of aluminum (Al_2O_3) and zinc (ZnO) oxide nanoparticles in a freshwater fish, *Carassius auratus*. *Environ. Sci. Pollut. Re.s* 23: 24578–24591.

Bierkandt, F., Leibrock, L., Wagener, S., Laux, P., Luch, A. 2018. The impact of nanomaterial characteristics on inhalation toxicity. *Toxicology Research*. 7: 321-346.

Blanco, J., Lafuente, D., Gómez, M., García, T., Domingo, J., & Sánchez, D. 2017. Polyvinyl pyrrolidone-coated silver nanoparticles in a human lung cancer cells: Time- and dose-dependent influence over p53 and caspase-3 protein expression and epigenetic effects. *Archives of Toxicology. 91*(2): 651-666.

Bowness, P. 2015. HLA-B27. *Annual Review of Immunology*, 33: 29-48.

Braeuning, S.H., Kunz, C., Daher, B., Kästner, H., Krause, B.C., Meyer, T., Jalili, P., Hogeveen, K., Bohmert, L., Lichenstein, D., Burel, A., Clevance, S., Jungnickel, H., Tentschert, J., Laux, P., Braeuning, A., Gauffre, F., Fessard, V., Meijer, J., Estrela-Lopis, I., Thunemann, A.F., Luch, A. Lampen, A. 2018. Uptake and molecular impact of aluminum-containing nanomaterials on human intestinal caco-2 cells. *Nanotoxicology, 22:* 1-22.

Braydich-Stolle, L.K., Speshock, J.L., Castle, A., Smith, M., Murdock, R.C., Hussain, S.M. 2010. Nanosized Aluminum Altered Immune Function. www.acsnano.org. 4(7): 3661–3670.

Bremnes R.M., Al-Shibli, K., Donnem, T., Sirera, R., Al-Saad, S., Andersen, S., Stenvold, H., Camps, C., Busund, L.-T. 2011. The role of tumor-infiltrating immune cells and chronic inflammation at the tumor site on cancer development, progression, and prognosis: emphasis on non-small cell lung cancer. *J. Thoracic Oncol*. 6: 824–833.

Brightling, C.E., Ammit, A.J., Kaur, D., Black, J.L., Wardlaw, A.J., Hughes, J.M., Bradding, P. 2005. The CXCL10/CXCR3 axis mediates human lung mast cell migration to asthmatic airway smooth muscle. *Am. J. Respir. Crit. Care Med.* 171: 1103–8.

Bugeon, L., Dallman, M. 2000. Costimulation of T Cells. *American Journal of Respiratory and Critical Care Medicine*, 162(3): S164-S168.

Campanero, M.R., Armstrong, M.I., Flemington, E.K. 2000. CpG methylation as a mechanism for the regulation of E2F activity. *Proc. Natl. Acad. Sci. USA.* 97: 6481-6486.

Carswell, E.A., Old, L.J., Kassel, R.L., Green, S., Fiore, N., Williamson, B. 1975. An endotoxin-induced serum factor that causes necrosis of tumors. *Proc. Natl. Acad. Sci. USA*. 72: 3666–3670.

Caruthers, S.D., Wickline, S.A., Lanza, G.M. 2007. Nanotechnological applications in medicine. *Curr. Opin. Biotechnol*. 18(1): 26–30.

Casas, A.I., Dao, V.T.-V., Daiber, A., Maghzal, G.J., Di Lisa, F., Kaludercic, N., Leach, S., Cuadrado, S., Jaquet, V., Seredenina, T., Krause, K.H., López, M.G., Stocker, R., Ghezzi, P., Schmidt, H.H.H.W. 2015. Reactive oxygen-related diseases: therapeutic targets and emerging clinical indications. *Antioxid. Redox Signal*., 23 (14): 1171–1185.

CDC. 2011. Asthma in the US. *CDC Vital Signs*. www.cdc.gov/vitalsigns/asthma.

Chan, S.W., Henderson, I.R., Jacobsen, S.E. 2005. Gardening the genome: DNA methylation in *Arabidopsis thaliana*. *Nat. Rev. Genet*. 6: 351–360.

Chen, A., Huang, G. 2015. Chapter 20 - Animal Model Study of Epigenetic Inhibitors. *Epigenetic Technological Applications*. Academic Press. 447-477.

Chen, C.H., Armstrong, S.A. 2015. Targeting *DOT1L* and *HOX* gene expression in *MLL*-rearranged leukemia and beyond. *Exp. Haematology*. 43(8): 673-684.

Chen, Z., Fillmore, C.M., Hammerman, P.S., Kim, C.F., Wong, K.-K. 2014. Non-small-cell lung cancers: a heterogeneous set of diseases. *Nat. Rev. Cancer*, 14: 535-546.

Chen Z.X., Riggs A.D. 2011. DNA methylation and demethylation in mammals. *J. Biol. Chem*. 286: 18347-53.

Choi, O., Hu, Z. 2008. Size dependent and reactive oxygen species related nanosilver toxicity to nitrifying bacteria. *Environ. Sci.Technol*. 42(12): 4583–4588.

Choi, S.J, Oh, J.M., Choy, A.H. 2009. Toxicological effects of inorganic nanoparticles on human lung cancer a549-cells. *Journal of Inorganic Biochemistry* 103(3): 463-71.

Cole K.E., Strick, C.A., Paradis, T.J., Ogborne, K.T., Loetscher, M., Gladue, R.P., Lin, W., Boyd, J.G., Moser, B., Wood, D.E., Sahagan, B.G., Neote, K. 1998. Interferon-inducible T cell alpha chemoattractant (I-TAC): a novel non-ELR CXC chemokine with potent activity on activated T cells through selective high affinity binding to CXCR3. *The Journal of Experimental Medicine*, 187(12): 2009–21.

Consumer Products Inventory (CPI): An inventory of nanotechnology-based consumer products introduced on the market, http://www.nanotechproject.org/cpi/.

Dale, J.G., Cox, S.S., Vance, M.E., Marr, L.C., Hochella, Jr., M.F. 2017. Transformation of cerium oxide nanoparticles from a diesel fuel additive during combustion in a diesel engine. *Environ. Sci. Technol*. 51(4): 1973–1980.

Dalgliesh, G.L., Furge, K., Greenman, C., Chen, L., Bignell, G., Butler, A., Davies, H., Edkins, S., Hardy, C., Latimer, C., Teague, J., Andrews, J., Barthorpe, S., Beare, D., Buck, G, Campbell, P.J., Forbes, S., Jia, M., Jones, D., Knott, H., Kok, C.Y., Lau, K.W., Leroy, C., Lin, M.-L., McBride, D.J., Maddison, M., Maguire, S., McLay, K., Menzies, A., Mironenko, T., Mulderrig, L., Mudie, L., O'Meara, S., Pleasance, E., Rajasingham, A., Shepherd, R., Smith, R., Stebbings, L., Stephens, P., Tang, G., Tarpey, P.S., Turrell, K., Dykema, K.J., Khoo, S.K., Petillo, D., Wondergem, D., Anema, J., Kahnoski, R.J., Teh, B.T., Stratton, M.R., Futreal, P.A. 2010. Systematic sequencing of renal carcinoma reveals inactivation of histone modifying genes. Nature. 463: 360-363.

Das, M. Patil, S., Bhargava, N., Kang, J.F., Riedel, L.M., Seal, S., Hickman, J.J. 2007. Auto-catalytic ceria nanoparticles offer neuroprotection to adult rat spinal cord neurons. *Biomaterials*, 28(10): 1918-1925.

De, A., Chakrabarti, M., Ghosh, I., Mukherjee, A. 2016. Evaluation of genotoxicity and oxidative stress of aluminium oxide nanoparticles and its bulk form in *Allium cepa* . *Nucleus.* 59: 219–225.

Deaton, A.M., Bird, A. 2011. CpG islands and the regulation of transcription. *Genes Dev*. 25(10): 1010–1022.

DeBaun, M.R., Niemitz, E.L., McNeil, D.E., Brandenburg, S.A., Lee, M.P., Feinberg, A.P. 2002. Epigenetic alterations of H19 and LIT1 distinguish patients with Beckwith-Wiedemann syndrome with cancer and birth defects. *Am. J. Hum. Genet*. 70: 604-11.

Del Prete, A., Allavena, P., Santoro, G., Fumarulo, R., Corsi, M.M., Mantovani, A**.** 2011**.** Molecular pathways in cancer-related inflammation. *Biochemia Medica* 21(3): 264-275.

De Marzi, L., Monaco, A., De Lapuente, J., Ramos, D., Borras, M., Gioacchino, M.D., Santucci, S.,Poma, A. 2013. Cytotoxicity and genotoxicity of cerianano particles on different cell lines in vitro. *Int. J. Mol.Sci*. 14(2): 3065–3077.

Department of Veterans Affairs. 2017. Profile of Veterans: 2015. Data from the American Community Survey. www.census.gov/programs-surveys/acs/

Dinerello, C.A. 2017. IL-1 Superfamily and Inflammasome. Cavaillon, J.-M., Singer, M. (eds). *Inflammation: From Molecular and Cellular Mechanisms to the Clinic.* Wiley-VCH

Dlott, D.D. 2006. Thinking big (and small) about energetic materials. *Materials Science and Technology*, 22(4): 463-473.

Donaldson, K., Seaton, A. 2012. A short history of the toxicology of inhaled particles. *Part. Fibre Toxicol*. 9: 13.

Donaldson, K., Stone, V., Tran, C.L., Kreyling, W., Borm, P.J.A. 2004. Nanotoxicology. *Occup. Environ. Med*. 61(9): 727:728.

Duffin , R., Tran, L., Brown, D., Stone, V. , Donaldson, K. 2007. Proinflammogenic effects of low - toxicity and metal nanoparticles *in vivo* and *in vitro*: highlighting the role of particle surface area and surface reactivity. *Inhal. Toxicol*. 19: 849–856.

Dunn, E. 2010. Endothelial nuclear hormone receptors in atherosclerosis . (Doctoral dissertation, University of California, San Diego, 2010). University of California, San Diego.

Elespuru, R., Pfuhler, S., Aardema, M., Chen, T., Doak, S., Doherty, A., Farabaugh, C., Kenny, J., Manjanatha, M., Mahadevan, B., Moore, M., Ouédraogo, G., Stankowski, L., Tanir, J. 2018. Genotoxicity assessment of nanomaterials: recommendations on best practices, assays, and methods. *Toxicological Sciences* 164(2): 391-416.

Eom, H.J., Cho, J. 2009. Oxidative stress of silica nanoparticles in human bronchial epithelial cell, Beas-2B. *Toxicol. In Vitro*. 23: 1326-1332.

Exley, C. 2004. The pro-oxidant activity of aluminum. *Free Radic. Biol. Med*. 36: 380–387.

Farooq, Z., Banday, S., Pandita, T.K., Altaf M. 2016. The many faces of histone H3K79 methylation. *Mutat. Res. Rev. Mutat. Res.* 768: 46–52.

Feinberg, A.P. 2018. The key role of epigenetics in human disease prevention and mitigation. *The New Eng. J. Med*. 378: 1323:1334.

Feinberg, A.P., Oshimura, M., Barrett, J.C. 2002. Epigenetic mechanisms in human disease. *Cancer Res.* 62: 6784–6787.

Felix, L.C., Ortega, V.A., Ede, J.D., Goss, G.G. 2013. Physicochemical characteristics of polymer-coated metal-oxide nanoparticles and their toxicological effects on zebrafish (*Danio rerio*) development. *ASC Environ. Sci. Technol.* 47: 6589–6596.

Fridovich, I. 1995. Superoxide radical and superoxide dismutases. *Annu. Rev. Biochem*. 64: 97–112.

Gates, A. 2006. Buildings Rise from Rubble while Health Crumbles, *The New York Times*, September 11, 2006, reporting on the documentary by Heidi Dehncke-Fisher, "Dust to Dust: The Health Effects of 9/11".

Gehr, P., Bachofen, M., Weibel, E. R. 1978. The normal human lung: ultrastructure and morphometric estimation of diffusion capacity. Respir. Physiol., 32: 121–140.

Goll, M.G., Kirpekar, F., Maggert, K.A., Yoder, J.A., Hsieh, C.L., Zhang, X., Golic, K.G., Jacobsen, S.E., Bestor, T.H. 2006. Methylation of tRNA by the DNA methyltransferase homolog Dnmt2. *Scienc*e. 311 (5759): 395–398.

Gordon, T., Chen, L.C., Cohen, B.S. 2008. Final Report: Role of particle agglomeration in nanoparticle toxicity. https://cfpub.epa.gov/ncer_abstracts/index.cfm/fuseaction/display.highlight/abstract/7814/report/F.

Granger, G.A., Shacks, S.J., Williams, T.W., Kolb, W.P. 1969. Lymphocyte in vitro cytotoxicity (specific release of lymphotoxin-like materials from tuberculin-sensitive lymphoid cells). *Nature*. 221: 1155–1157.

Grasso, C.S., Wu, Y.M., Robinson, D.R., Cao, X., Dhanasekaran, S.M., Khan, A.P., Quist,M.J., Jing, X., Lonigro,R.J., Brenner, J.C., Asangani, I.A., Ateeq, B., Chun, S.Y.,Siddiqui, J., Sam, L., Anstett, M., Mehra, R., Prensner, J.R. Palanisamy, N., Ryslik, G.A., Vandin, F., Raphael, B.J., Kunju, L.P., Rhodes, D.R., Pienta, K.J., Chinnaiyan, A.M., Tomlins, S.A. 2012. The mutational landscape of lethal castration-resistant prostate cancer. *Nature*, 487: 239-243.

Greenwood, N.N., Earnshaw, A. 1984. *Chemistry of the Elements*. Oxford: Pergamon Press.

Greer, E. L., Shi, Y. 2012. Histone methylation: a dynamic mark in health, disease and inheritance. *Nature Reviews Genetics*. 13: 343–57.

Grulke, E., Reed, K., Beck, M., Huang, X., Cormack, A., Seal, S. 2014. Nanoceria: factors affecting its pro-and antioxidant properties. *Environ. Sci.: Nano* 1(5): 429−444.

Salbert, S., Weber, M. 2013. Current Topics in Developmental Biology. Epigenetics and Development Chapter Two - Functions of DNA Methylation and Hydroxymethylation in Mammalian Development, 104:47-83.

Han, M., Grunstein, M. 1988. Nucleosome loss activates yeast downstream promoters *in vivo*. *Cell*. 55: 1137–45.

Hanley, W.D., Burdick, M.M., Konstantopoulos, K., Sackstein, R. 2005. CD44 on LS174T colon carcinoma cells possesses E-selectin ligand activity. *Cancer Research*. 65 (13): 5812–7.

Hankin, S.M., Poland, C.A. 2013. Nanoparticle Cell Penetration, Chapter 9. Aerosols handbook : measurement, dosimetry, and health effects , Taylor & Francis Pertual ebooks. Boca Raton: CRC Press, 2013.

Hayyan, M., Hashim, M.A., Al Nashef, I.M. 2016. Superoxide ion: generation and chemical implications. *Chemical Reviews*. 116 (5): 3029–85.

Head, J.A. 2014. Patterns of DNA methylation in animals: an ecotoxicological perspective. *Intergr. Comp. Bio.* 54(1):77-86.

Heckert, E.G., Karakoti, A.S., Seal, S., Self, W.T. 2008. The role of cerium redox state in the SOD mimetic activity of nanoceria. *Biomaterials*, 29(18): 2705-2709.

Henz, B.J., Hawa, T., Zachariah, M. 2010. Molecular dynamics simulation of the kinetic reaction of nickel and aluminum nanoparticles. Army Research Laboratory Report, March 2010.

Hirst, S.M., Karakoti, A., Singh, S., Self, W., Tyler, R., Seal, S., Reilly, C. 2013.Bio-distribution and in vivo antioxidant effects of cerium oxide nanoparticles in mice. *Environmental Toxicology.* 28(2): 107–118.

Holbrook, R.D., Galyean, A.A., Gorham, J.M., Herzingy, A. Pettibone, J. 2015. Overview of nanomaterial characterization and metrology. *Front. Nanosci*. 8: 47–87.

Hu, X., Yang, D., Zimmerman, M., Liu, F., Yang, J., Kannan, S., Burchert, A., Szulc, Z., Bielawska, A., Ozato, K.., Bhalla, K., Liu, K. 2011. IRF8 regulates acid ceramidase expression to mediate apoptosis and suppresses myelogeneous leukemia. *Cancer Res*. 71 (8): 2882–91.

Iguchi-Ariga, S.M., Schaffner, W. 1989. CpG methylation of the cAMP-responsive enhancer/promoter sequence TGACGTCA abolishes specific factor binding as well as transcriptional activation. *Genes and Development*, 3: 612-619.

Ikeda, U., Shimada, K. 1997. Nitric oxide and cardiac failure. *Clin. Cardiol*. 20: 837-841.

Jiang, R., Shen, H., Piao, Y. 2010. The morphometrical analysis on the ultrastructure of A549 cells. *Romanian Journal of Morphology and Embryology = Revue Roumaine De Morphologie Et Embryologi.* 51(4): 663-7.

Jeffery, E.H., Abreo, K., Burgess, E., Cannata, J., Greger, J.L. 1996. Systemic aluminum toxicity: effects on bone, hematopoietic tissue, and kidney. *J. Tox.Environ. Health*. 48(6): 649-665.

Johnstone, A.L., O'Reilly, J.J., Patel, A.J., Guo, Z., Andrade, N.S., Magistri, M., Nathanson, L., Esanov, R., Miller, B.H., Turecki, G., Brothers, S.P., Zeier, Z., Wahlestedt, C. 2018. EZH1 is an antipsychotic-sensitive epigenetic modulator of social and motivational behavior that is dysregulated in schizophrenia. *Neurobiology of Disease.* 119: 149-158.

Jordan, J.A., Verhoff, A.M., Morgan, J.E., Fischer, D.G. 2009. Assessing the in vitro toxicity of the lunar dust environment using respiratory cells exposed. *In Vitro Cellular & Developmental Biology. Animal*. 45(10): 602-613.

Jung, C.K., Kim, Y., Jeon, S., Jo, K., Lee, S., Bae, J.S. 2018. Clinical utility of *EZH1* mutations in the diagnosis of follicular-patterned thyroid tumors. *Human Pathology*. 81:9-17.

Kadar, A., Rauch, T.A. 2012. Chapter 7 Epigenetic Reprogramming in Lung Carcinomas. Minarovits, J., & Niller, H. *Patho-epigenetics of disease*. New York, NY: Springer.

Kain, J., Karlsson, H.L., Möller, L. 2012. DNA damage induced by micro- and nanoparticles – interaction with FPG influences the detection of DNA oxidation in the comet assay. *Mutagenesis*. 27(4): 491–500.

Kelly, R.A., Balligand, J.L., Smith, T.W. 1994. Nitric oxide and cardiac function. *Circ. Res*. 79: 363-380.

Khan, B.V., Harrison, D.G., Olbrych, M.T., Alexander, R.W., Medford, R.M. 1996. Nitric oxide regulates vascular cell adhesion molecule 1 gene expression and redox-sensitive transcriptional events in human vascular endothelial cells. *Proc. Natl. Acad. Sci. USA*. 93: 9114–9119.

Kilbourn, B.T. 2004. Cerium and cerium compounds. A. Seidel (Ed.) (fifth ed.), Kirk–Othmer Encyclopedia of Chemical Technology, vol. 5, Wiley Interscience, Hoboken, NJ, 670-692.

Kim, J., Kollhoff, A., Bergmann, A., Stubbs, L. 2003. Methylation-sensitive binding of transcription factor YY1 to an insulator sequence within the paternally expressed imprinted gene, *Peg3*. *Human Molecular Genetics*. 12: 233-245.

Kim, Y.-J., Choi, H.S., Song, M.-K., Youk, D.-Y., Kim, J.-H., Ryu, J.-C. 2009. Genotoxicity of aluminum oxide (Al_2O_3) nanoparticle in mammalian cell lines. *Mol. Cell. Toxicol*. 5(2): 172–178.

Kitchin, K.T., Grulke, E., Robinette, B.L., Castellon, B.T. 2014. Metabolomic effects in HepG2 cells exposed to four TiO_2 and two CeO_2 nanomaterials. *Environ. Sci.: Nano*, 1(5): 466−477.

Kondo, Y. 2009. Epigenetic cross-talk between DNA methylation and histone modifications in human cancers. Y*onsei Medical Journal.* 50(4): 455-63.

Korani, M., Rezayat, S.M., Bidgoli, S. A. 2013. Subchronic dermal toxicity of silver nanoparticles in guinea pig: special emphasis to heart, bone and kidney toxicities. *Iran. J. Pharm. Res*. 12: 511–519.

Kreyling, W.G., Semmler, M., Erbe, F., Mayer, P., Takenaka, S., Schulz, H. 2002. Translocation of ultrafine insoluble iridium particles from lung epithelium to extra pulmonary organs is size dependent but very low. *J. Toxicol. Environ. Health*. 65: 1513–1530.

Kreyling, W.G., Semmler-Behnke, M., Seitz, J., Scymczak, J., Wenk, A., Mayer, P., Takenaka, S., Oberdörster, G. 2009. Size dependence of the translocation of inhaled iridium and carbon nanoparticle aggregates from the lung of rats to the blood and secondary target organs. *Inhalation Toxicol*. 21: 55–60.

Kroll A., Pillukat M.H., Hahn D., Schnekenburger J. 2009. Current in vitro methods in nanoparticle risk assessment: limitations and challenges. *Eur. J. Pharm. Biopharm*. 72: 370–377.

Kumari, M., Singh, S.P., Chinde, S., Rahman, M.F., Mahboob, M., Grover, P. 2014. Toxicity study of cerium oxide nanoparticles in human neuroblastoma cells. *Int. J. Toxicol*. 33: 86**–**97.

Kundakovic, M., Chen, Y., Guidotti, A., Grayson, D.R. 2009. The reelin and GAD67 promoters are activated by epigenetic drugs that facilitate the disruption of local repressor complexes. *Molecular Pharmacology*. 75 (2): 342–54.

Kuthan H., Houssmann, H.J., Werringloer, J. 1986. A spectrophotometric assay for superoxide dismutase activities in crude tissue fractions. *Biochem J*. 237: 175-80.

Lahive, E., Jurkschat, K., Shaw, B.J., Handy, R.D., Spurgeon, D.J., Svendsen, C. 2014. Toxicity of cerium oxide nanoparticles to the earthworm *Eisenia fetida*: subtle effects. *Environ Chem* 11: 268–278.

Lankoff, A., Sandberg, W.A., Wegierek-Ciuk, A., Lisowska, H., Refsnes, M., Sartowska, B., Schwarze, P.E., Meczynska-Wielgosz, S., Wojewodzka, M., Kruszewski, M. 2012. The effect of agglomeration state of silver and titanium dioxide nanoparticles on cellular response of HepG2, A549 and THP-1 cells. Toxicol. Lett. 208: 197–213.

Law, J.A., Jacobsen, S.E. 2010. Establishing, maintaining and modifying DNA methylation patterns in plants and animals. *Nat. Rev. Genet*. 11: 204–220.

Lee, J.H., Budanov, A.V., Karin, M. 2013. Sestrins orchestrate cellular metabolism to attenuate aging. *Cell Meta*. 18: 792–801.

Lee, S., Oh, S., Jeong, K., Jo,H., Choi,Y., Seo,H.D., Kim,M., Choe,J., Kwon,C.S., Lee,D. 2018. Dot1 regulates nucleosome dynamics by its inherent histone chaperone activity in yeast. *Nat. Commun*. 9: 240.

Leonhardt, A., Page, A.W., Weier, H.U., Bestor, T.H. 1992. A targeting sequence directs DNA methyltransferase to sites of DNA replication in mammalian nuclei. *Cell*. 71: 865-873.

Li, N., Sioutas, C., Cho, A., Schmitz, D., Misra, C., Sempf, J., Wany, M., Oberley, T., Froines, J., Nel, A. 2003. Ultrafine particulate pollutants induce oxidative stress and mitochondrial damage. *Environ. Health Perspect*. 111: 455–460.

Li, X., Zhang, C., Bian, Q., Gao, N., Zhang, X., Meng, Q., Wu, S., Wang, Xia, Y., Chen, R. 2016a. Integrative functional transcriptomic analyses implicate specific molecular pathways in pulmonary toxicity from exposure to aluminum oxide nanoparticles. Nanotoxicology. 10(7): 957-969.

Li, X., Zhang, C., Zhang, X., Wang, S., Meng, Q., Wu, S., Yang, H., Xia, Y., Chen, R. 2016b. An acetyl-L-carnitine switch on mitochondrial dysfunction and rescue in the metabolomics study on aluminum oxide nanoparticles. *Particle and Fibre Toxicology*. 13: 4.

Lieber, M, Smith, B., Szakal, A., Nelson-Rees, W., Todaro, G. 1976. A continuous tumor-cell line from a human lung carcinoma with properties of type II alveolar epithelial cells. 17(1): 62-70.

Lim, S.S., Vos, T., Flaxman, A.D., Danaei, G., Shibuya, K., Adair-Rohani, H., Amann, M., Anderson, H.R., Andrews, K.G., Aryee, M., Atkinson, C., Bacchus, L.J., Bahalim, A.N., Balakrishnan, K., Balmes, K., Barker-Collo, S., Baxter, A., Bell, M.L., Blore, J.D., Blyth, F., Bonner, C., Borges, G., Bourne, R., Boussinesq, M., Brauer, Brooks, M.P., Bruce, N.G., Brunekreef, B., Bryan-Hancock, C., Bucello, C., Buchbinder, R., Bull, F., Burnett, R.T., Byers, T.E., Calabria, B., Carapetis, J., Carnahan, E., Chafe, Z., Charlson, F., Chen, H., Chen, J.S., Cheng, A.T., Child, J.C., Cohen, A., Colson, K.E., Cowie, B.C., Darby, S., Darling, S., Davis, A., Degenhardt, L., Dentener, F., Des Jarlais, D.C., Devries, K., Dherani, M., Ding, E.L., Dorsey, E.R., Driscoll, T., Edmond, K., Ali, S.E., Engell, R.E., Erwin, P.J., Fahimi, S., Falder, G., Farzadfar, F., Ferrari, A., Finucane, M.M., Flaxman, S., Fowkes, F.G., Freedman, G., Freeman, M.K., Gakidou, E., Ghosh, S., Giovannucci, E., Gmel, G., Graham, K., Grainger, R., Grant, B., Gunnell, D., Gutierrez, H.R., Hall, W., Hoek, H.W., Hogan, A., Hosgood, 3rd, H.G., Hoy, D., Hu, H., Hubbell, B.J., Hutchings, S.J., Ibeanusi, S.G., Jacklyn, G.L., Jasrasaria, R., Jonas, J.B., Kan, H., Kanis, J.A., Kassebaum, N., Kawakami, N., Khang, Y.H., Khatibzadeh, S., Khoo, J.P., Kok, C., Laden, F., Lalloo, R., Lan, Q.,

Lathlean, T., Leasher, J.L., Leigh, J., Li, Y., Lin, J.K., Lipshultz, S.E., London, S., Lozano, R., Lu, Y., Mak, J., Malekzadeh, R., Mallinger, L., Marcenes, W., March, L., Marks, R., Martin, R., McGale, P., McGrath, J., Mehta, S., Mensah, G.A., Merriman, T.R., Micha, R., Michaud, C., Mishra, V., Mohd Hanafiah, K., Mokda, A.A., Morawska, L., Mozaffarian, D., Murphy, T., Naghavi, M., Neal, B., Nelson, P.K., Nolla, J.M., Norman,R., Olives, C., Omer, S.B., Orchard, J., Osborne, R., Ostro, B., Page, A., Pandey, K.D., Parry, C.D., Passmore, E., Patra, J., Pearce, N., Pelizzari, P.M., Petzold, M., Phillips, M.R., Pope, D., Pope, 3rd, C.A., Powles, J., Rao, M., Razavi, H., Rehfuess, E.A., Rehm, J.T., Ritz, B., Rivara, F.P., Roberts, T., Robinson, C., Rodriguez-Portales, J.A., Romieu, I., Room, R., Rosenfeld, L.C., Roy, A., Rushton, L., Salomon, J.A., Sampson, U., Sanchez-Riera, L., Sanman, E., Sapkota, A., Seedat, S., Shi, P., Shield, K., Shivakoti, R., Singh, G.M., Sleet, D.A., Smith, E., Smith, K.R., Stapelberg, N.J., Steenland, K., Stockl, H., Stovner, L.J., Straif, K., Straney, L., Thurston, G.D., Tran, J.H., Van Dingenen, R., van Donkelaar, A., Veerman, J.L., Vijayakumar, L., Weintraub, R., Weissman, M.M., White, R.A., Whiteford, H., Wiersma, S.T., Wilkinson, J.D., Williams, H.C., Williams, W., Wilson, N., Woolf, A.D., Yip, P., Zielinski, J.M., Lopez, A.D., Murray, C.J., Ezzat, M., Almazaroa, M.A., Memish, Z.A. 2012. A comparative risk assessment of burden of disease and injury attributable to 67 risk factors and risk factor clusters in 21 regions, 1990-2010: a systematic analysis for the Global Burden of Disease Study 2010. *Lancet* 380: 2224–2260.

Lin, W., Stayton, I., Huang, Y.-W., Zhou, X.-D., Ma, Y. 2008. Cytotoxicity and cell membrane depolarization induced by aluminum oxide nanoparticles in human lung epithelial cells A549. *Tox. Environ. Chem*. 90(5): 983-996.

Liu, K., Liu, Y., Lau, J., Min, J. 2016. Epigenetic targets and drug discovery Part 2: Histone demethylation and DNA methylation. *Pharm. Thera*. 151: 121-140.

López, G.Y., Grant, G.A., Fuchs, H.E., Leithe, L.G., Gururangan, S., Bigner, D.D., Yan, H., McLendon, R.E., He, Y. 2014. Clinico-pathological description of three paediatric medulloblastoma cases with *MLL2/3* gene mutations. *Neuropathol. Appl. Neurobiol*., 40: 217-220

Lorch, Y., LaPointe, J.W., Kornberg, R.D. 1987. Nucleosomes inhibit the initiation of transcription but allow chain elongation with the displacement of histones. *Cell*. 49(2): 203–10.

Lukas, M. 2010 Inflammatory bowel disease as a risk factor for colorectal cancer. *Dig. Dis*. 28: 619–624.

Ma, B., Herzog, E.L, Moore, M., Lee, C.M., Na, S.H., Lee, C.G., Elias, J.A. 2016. RIG-like helicase regulation of chitinase 3-like 1 axis and pulmonary metastasis. *Scientific Reports*. 6: 26299.

Ma, N., Ma, C., Li, C., Wang, T., Tang, Y., Wang, H., Moul, X., Chen, Z., Hel, N. 2013. Influence of nanoparticle shape, size, and surface functionalization on cellular uptake. *J. Nanosci. Nanotechnol*. 13(10): 6485–6498.

Ma, Y., Kuang, L., He, X., Bai, W., Ding, Y., Zhang, Z., Zhao, Y., Chai, Z.. 2010. Effects of rare earth oxide nanoparticles on root elongation of plants. *Chemosphere*. 78(3): 273−279.

Maegawa, S., Gough, S.M., Watanabe-Okochi, N., Lu, Y., Zhang, N., Castoro, R.J., Estecio, M.R., Jelinek, J., Liang, S., Kitamura, T., Aplan, P.D., Issa, J.P. 2014. Age-related epigenetic drift in the pathogenesis of MDS and AML. *Genome Res*. 24: 580-91.

Majumdar, S., Peralta-Videa. J.R., Bandyopadhyay, S., Castillo-Michel, H., Hernandez-Viezcas, J., Sahi, S., Gardea-Torresdey, J.L. 2014. Exposure of cerium oxide nanoparticles to kidney bean shows disturbance in the plant defense mechanisms. *J. Hazard. Mater*. 278: 279–287.

Maynard, A. D., Aitken, R.J. 2007. Assessing exposure to airborne nanomaterials: Current abilities and future requirements, *Nanotoxicology*. 1: 26–41.

McAuliffe, M. E., Perry, M. J. 2007. Are nanoparticles potential male reproductive toxicants? A literature review. *Nanotoxicology*. 1: 204–210.

McCord, J. M., and Fridovich, I. 1969. Superoxide dismutase: an enzymic function for erythrocuprein (hemocuprein). *J. Biol. Chem*. 244: 6049–6055.

McDowell, E.M., Barrett, L.A., Glavin, F., Harris, C. C. Trump, B.F. 1978. The respiratory epithelium. I. Human bronchus. *J. Natl. Cancer Inst*. 61: 539–549.

McLean, C.M., Karemaker I.D., van Leeuwen F. 2014. The emerging roles of DOT1L in leukemia and normal development. *Leukemia*. 28: 2131–2138.

McGough, J.M., Yang, D., Huang, S., Georgi, D., Hewitt, S.M., Röcken, C., Tänzer, M., Ebert, M.P., Liu, K. 2008. DNA methylation represses IFN-gamma-induced and signal transducer and activator of transcription 1-mediated IFN regulatory factor 8 activation in colon carcinoma cells. *Mol. Cancer Res*. 6(12): 1841–51.

Meng, H., Yang, S., Li, Z., Xia, T., Chen, J., Ji, Z., Zhang, H., Wang, X., Lin, S., Huang, C., Zhou, Z.H., Zink, J.I., Nel, A.E. 2011. Aspect ratio determines the quantity of mesoporous silica nanoparticle uptake by a small GTPase-dependent macropinocytosis mechanism. *A.C.S. Nano* 5(6): 4434–4447.

Miller, J.A., Ding, S.L. Sunkin, S.M. Smith, K.A., Ng, L., Szafer, A., Ebbert, A., Riley, Z.L., Royall, J.J., Aiona, K., Arnold, J.M., Bennet, C., Bertagnolli, D., Brouner, K., Butler, S., Caldejon, S., Carey, A., Cuhaciyan, C., Dalley, R.A., Dee, N., Dolbeare, T. A., Facer, B. A. C., Feng, D., Fliss, T. P., Gee, G., Goldy, J., Gourley, L., Gregor, B. J., Gu, G., Howard, R. E., Jochim, J. M., Kuan, C.L., Lau, C., Lee, C.-K., Lee, F., Lemon,

T.A., Lesnar, P., McMurray, B., Mastan, N., Mosqueda, D., Naluai-Cecchini, N., Ngo, N.-K., Nyhus, J. Oldre, A., Olson, E., Parente, J., Parker, P., Parry, S. E., Stevens, A., Pletikos, M., Reding, M., Roll, K., Sandman, D., Sarreal, M., Shapouri, S., Shapovalova, N.V., Shen, E.H., Sjoquist, N., Slaughterbeck, C. R., Smith, M., Sodt, M. J., Williams, D., Zo¨llei, L., Fischl, B., Gerstein, M.B., Geschwind, D. H., Glass, I. A., Hawrylycz, M. J., Hevner, R., Huang, H., Jones, A. R., Knowles, J. A., Levitt, P., Phillips, J. W., Sestan, N., Wohnoutka, P., Dang, C., Bernard, A., Hohmann, J. G., Lein, E. S. 2014. Transcriptional landscape of the prenatal human brain. *Nature*, 508 (7495): 199-206.

Mittal, S., Pandey, A. K. 2014. Cerium oxide nanoparticles induced toxicity in human lung cells: Role of ROS mediated DNA damage and apoptosis. Bio. Med. Res.Int. 2014: 891934.

Moller, W., Felten, K., Sommerer, K., Scheuch, G., Meyer, G., Meyer, P., Haussinger, K., Kreyling, W. G. 2008. Deposition, retention, and translocation of ultrafine particles from the central airways and lung periphery. *Am. J. Respir. Crit. Care Med.* 177: 426–432.

Moncada, S., Herman, A.G., and Vanhoutte, P. 1987. Endothelium-derived relaxing factor is identified as nitric oxide. *Trends Pharmacol. Sci*. 8 (10): 365–368.

Morin, R.D., Mendez-Lago, M., Mungall, A.J., Goya, R., Mungall, K. L., Corbett, R. D., Johnson, N. A., Severson, T. M., Chiu, R., Field, M., Jackman, S., Krzywinski, M., Scott, D. W., Trinh, D. L., Tamura-Wells, J., Li, S., Firme, M. R., Rogic, S., Griffith, M., Chan, S., Yakovenko, O., Meyer, I. M., Zhao, E. Y., Smailus, D., Moksa, M., Chittaranjan, S., Rimsza, L., Brooks-Wilson, A., Spinelli, J. J., Ben-Neriah, S., Meissner, B., Woolcock, B., Boyle, M., McDonald, H., Tam, A., Zhao, Y., Delaney, A., Zeng, T.,Tse, K., Butterfield, Y., Birol, I., Holt, R., Schein, J., Horsman, D. E., Moore, R., Jones, S. J. M., Connors, J. M., Hirst, M., Gascoyne, R. D., Marra, M. A. 2011. Frequent mutation of histone-modifying genes in non-Hodgkin lymphoma. *Nature*, 476: 298-303.

Muehlinghaus, G., Cigliano, L., Huehn, S., Peddinghaus, A., Leyendeckers, H., Hauser, A.E., Hiepe, F., Radbruch, A., Arce, S., Manz, R.A. 2005. Regulation of CXCR3 and CXCR4 expression during terminal differentiation of memory B cells into plasma cells. *Blood*. 105: 3965–71.

Naor, D., Nedvetzki, S., Golan, I., Melnik, L., Faitelson, Y. 2002. CD44 in cancer. *Critical Reviews in Clinical Laboratory Sciences*. 39 (6): 527-579.

Nguyen, A.T., Zhang, Y. 2011. The diverse functions of Dot1 and H3K79 methylation. *Genes Dev*. 25: 1345–1358.

Ober, C., Tan, Z., Sun, Y., Possick, J.D., Pan, L., Nicolae, R., Radford, S., Parry, R.R., Heinzmann, A., Deichmann, K.A., Lester, L.A., Gern, J.E., Lemanske, R.F., Nicolae, D.L., Elias, J.A., Chupp, G.L. 2008. Effect of variation in CHI3L1 on serum YKL-40 level, risk of asthma, and lung function. *The New England Journal of Medicine*. 358 (16): 1682–91.

Oberdörster, G. 2001. Pulmonary effects of inhaled ultrafine particles. *Int. Arch. Occup. Environ. Health.* 74: 1–8.

Oberdörster, G., Oberdörster, E., Oberdörster, J. 2005. Nanotoxicology: an emerging discipline evolving from studies of ultrafine particles. *Environ. Health Perspect*. 113: 823–839.

Ochs, M., Weibel, E. R. 2008. *Functional Design of the Human Lung for Gas Exchange*. New York: McGraw – Hill.

O'Dell, T.J., Hawkins, R.D., Kandel, E.R., Arancio, O. 1991. Tests of the roles of two diffusible substances in long-term potentiation: evidence for nitric oxide as a possible early retrograde messenger. *Proc. Natl. Acad. Sci. USA*. 88: 11285–11289.

Official US Department of Defense (DOD) website. www.defense.gov.

Ohmori, Y., Wyner, L., Narumi, S., Armstrong, D., Stoler, M., Hamilton, T.A. 1993. Tumor necrosis factor-alpha induces cell type and tissue-specific expression of chemoattractant cytokines in vivo. *Am. J. Pathol.* 142: 861–70.

Ohmori, Y., Schreiber, R.D., Hamilton, T.A. 1997. Synergy between interferon-gamma and tumor necrosis factor-alpha in transcriptional activation is mediated by cooperation between signal transducer and activator of transcription 1 and nuclear factor kappa B. *J. Biol. Chem.* 272: 14899–907.

Okano, M, Bell, D.W., Haber, D.A., Li, A. 1999. DNA methyltransferases DNMT3A and Dnmt3b are essential for de novo methylation and mammalian development *Cell*. 99: 47-257.

Pagliari, F., Mandoli, C., Forte, G., Magnani, E., Pagliari, S., Nardone, G., Licoccia, S., Minieri, M., Di Nardo, P., Traversa, E. 2012. Cerium oxide nanoparticles protect cardiac progenitor cells from oxidative stress. *ACS Nano. 6* (5): 3767-3775.

Pailleux M., Boudard D., Pourchez J., Forest V., Grosseau P., Cottier M. 2013.New insight into artifactual phenomena during in vitro toxicity assessment of engineered nanoparticles: study of TNF-α adsorption on alumina oxide nanoparticle. *Toxicol. In Vitro*. 27: 1049–1056.

Palmer, R.M.J., Ferrige, A.G., and Moncada, S. 1987. Nitric oxide release accounts for the biological activity of endothelium-derived relaxing factor. *Nature.* 327 (6122): 524–526.

Parente, M. 2018. Methylation. *Genetics Vol. 3. 2nd ed*. Farmington Hills, MI: Gale. 75-80.

Park, B; Donaldson, K., Duffin, R., Tran, L., Kelly, F., Mudway, I., Morin, J.P., Guest, R., Jenkinson, P., Samaras, Z., Giannouli, M., Kouridis, H., Martin, P. 2008. Hazard and risk assessment of a nanoparticulate cerium oxide-based diesel fuel additive—a case study. *Inhalation Toxicology*, 20(6): 547-566.

Park, E.J., Sim, J., Kim, Y., Han, B.S., Yoon, C. Lee, S., Cho, M.H., Lee, B.S., Kim, J.H. 2015. A 13 week repeated-dose oral toxicity and bioaccumulation of aluminum oxide nanoparticles in mice. *Arch .Tox*. 89(3): 371-379.

Park, E.J., Lee, G.H., Yoon, C., Jeong, U., Kim, Y., Cho, M., Kim, D. 2016. Biodistribution and toxicity of spherical aluminum oxide nanoparticles. *Journal of Applied Toxicology*, 36 (3): 424-433.

Park, J.W., Lee, I.C., Shin, N.R., Jeon, C.M., Kwan, O.K., Ko, J.W., Kim, J.C., Oh, S.R., Shin, I.S., Ahn, K.S. 2016. Copper oxide nanoparticles aggravate airway inflammation and mucus production in asthmatic mice via MAPK signaling. *Nanotoxicology*. 10(4): 445:452.

Parmigiani, A., Budanov, A.V. 2016. Sensing the environment through Sestrins: implications for cellular metabolism. *Int. Rev. Cell Mol. Biol.* 327: 1–42.

Peters, A., Wichmann, H. E., Tuch, T., Heinrich, J., Heyder, J. 1997. Respiratory effects are associated with the number of ultrafine particles. *Am. J. Respir. Crit. Care Med*. 155: 1376–1383.

Peters, M.C., McGrath, K.W., Hawkins, G.A., Hastie, A.T., Levy, B.D., Israel, E., Phillips, B.R., Mauger, D.T., Comhair, S.A., Erzurum, S.C., Johansson, M.W., Jarjour, N.N., Coverstone, A.M., Castro, M., Holguin, F., Wenzel, S.E., Woodruff, P.G., Bleecker, E.R., Fahy, J.V. 2016. Plasma interleukin-6 concentrations, metabolic dysfunction, and asthma severity: a cross-sectional analysis of two cohorts. *The Lancet Respiratory Medicine.* 4(7*): 574–84*.

Peterson, C.L., Laniel, M.A. 2004. Histories and histone modifications. *Curr. Biol.* 14(14): R546–R551.

Peyravian, N., Gharib, E., Moradi, A., Mobahat, M., Tarban, P., Azimzadeh, P., Nazemalhosseini-Mojarad, E., Aghdaei, H. 2017. Evaluating the expression level of co-stimulatory molecules CD 80 and CD 86 in different types of colon polyps. *Cur. Res. Trans. Med*. 66(1): 19-25.

Plass C., Smiraglia D.J. 2006. Genome-wide Analysis of DNA Methylation Changes in Human Malignancies. In: Doerfler W., Böhm P. (eds) *DNA Methylation: Development, Genetic Disease and Cancer*. Current Topics in Microbiology and Immunology. 310. Springer, Berlin, Heidelberg.

Poland, C.A., Clift, M.J.D. 2013. Nanoparticle–Lung Interactions and Their Potential Consequences for Human Health. *Bio-Nanotechnology: A Revolution in Food, Biomedical and Health Sciences*, First Edition. Edited by Debasis Bagchi, Manashi Bagchi, Hiroyoshi Moriyama, and Fereidoon Shahidi. John Wiley & Sons, Ltd.

Ponta, H., Sherman, L., Herrlich, P.A. 2003. CD44: from adhesion molecules to signalling regulators. *Nat. Rev. Mol. Cell Biol. 4: 33–45.*

Pope, C.A., Dockery, D.W. 1999. Epidemiology of particle effects. In air pollution and health, eds. ST Holgate, JM Samet, HS Koren, RL Maynard, San Diego: Academic Press. 673–705.

Porter, J. 2008. Defense Nanotechnology: Research and Development. DOD publication.

Powers, W., Paul L. Carpinone, Kerry N. Siebein. 2012. Characterization of Nanomaterials for Toxicological Studies, Nanotoxicity: Methods and Protocols. *Methods in Molecular Biology.* Clifton, N.J. 13-32.

Prasad, R., Zhadanov, A.B., Sedkov, Y., Bullrich, F., Druck, T., Rallapalli, R., Yano, T. Alder, H., Croce, C. M., Huebner, K., Mazo, A., Canaani, E. 1997. Structure and expression pattern of human ALR, a novel gene with strong homology to ALL-1 involved in acute leukemia and to *Drosophila trithorax*. *Oncogene*. 15 (5): 549–60.

Priest, N. D., Newton, D., Talbot, B., McAughey, J., Day, P., Fifield, K. 1998. Industry-sponsored studies on the biokinetics and bioavailability of aluminium in man. In Health in the aluminium industry, eds. N. D. Priest and T. V. O'Donnell, London: Middlesex University Press. 105–129.

Pujadas E., Feinberg A.P. 2012. Regulated noise in the epigenetic landscape of development and disease. *Cell*. 148: 1123.

Rajiv, S., Jerobin, J., Saranya, V., Nainawat, M., Sharma, A., Makwana, P., Gayathri, C., Bharath, L., Singh, M., Kumar, M., Mukherjee, A., Chandrasekaran, N. 2016. Comparative cytotoxicity and genotoxicity of cobalt (II, III) oxide, iron (III) oxide, silicon dioxide,and aluminum oxide nanoparticles on human lymphocytes in vitro. *Human and Experimental Toxicology*. 35(2): 170–183.

Reinhardt, K, Winkler, H. 2003. Cerium mischmetal, cerium alloys, and cerium compounds A. Seidel (Ed.) (sixth ed.), *Illmann's Encyclopedia of Industrial Chemistry, Vol. 7*, Wiley-VCH Verlag GmbH & Co. KGaA, Weinheim, Germany, 285-300.

Richards, E.J., Elgin, S.C. 2002. Epigenetic codes for heterochromatin formation and silencing: rounding up the usual suspects. *Cell*. 108: 489-500.

Roh, J.Y., Park, Y.K., Park, K., Choi, J. 2010. Ecotoxicological investigation of CeO_2 and TiO_2 nanoparticles on the soil nematode *Caenorhabditis elegans* using gene expression, growth, fertility, and survival as endpoints. *Environ Toxicol Pharmacol*. 29: 167–172.

Roh, H.S., Choi, G.K., An, J.S., Cho, C.M., Kim, D.H., Park, I.J., Noh, T.H., Kim, D.-W., Hong, K.S. 2011. Size-controlled synthesis of monodispersed mesoporous alumina spheres by a template-free forced hydrolysis method. *Dalton Trans.* 40: 6901–6905.

Röhder, L.A., Brandt, T., Sigg, L., Behra, R. 2014. Influence of agglomeration of cerium oxide nanoparticles and speciation of cerium (III) on short term effects to the green algae *Chlamydomonas reinhardtii. Aquat. Toxicol.* 152: 121–130.

Rose, N.R, Klose, R.J. 2014. Understanding the relationship between DNA methylation and histone lysine methylation. *Biochimica et Biophysica Acta*, Elsevier Pub. Co, Dec. 2014.

Salbert, S., Weber, M. 2013. Current Topics in Developmental Biology. Epigenetics and Development Chapter Two - Functions of DNA Methylation and Hydroxymethylation in Mammalian Development, 104: 47-83.

Saptarshi, S.R., Duschl, A., Lopata, A. 2013. Interaction of nanoparticles with proteins: relation to bio-reactivity of the nanoparticle. *Journal of Nanobiotechnology*. 11: 26.

SCCP. The European Commission's Scientific Committee on Consumer Products (SCCP). 2007. Opinion on safety of nanomaterials in cosmetic products. Brussels.

SCENIHR. The European Commission's Scientific Committee on Emerging and Newly Identified Health Risks (SCENIHR). 2007. Opinion on the scientific aspects of the existing and proposed definitions relating to products nanoscience and nanotechnologies. Brussels.

Schuman, E.M., Madison, D.V. 1991. A requirement for the intercellular messenger nitric oxide in long-term potentiation. *Science*. 254: 1503–1506.

Serfozo, N., Ondráček, J., Glytsos, T., Lazaridis, M. 2018. Evaluation of nanoparticle emissions from a laser printer in an experimental chamber and estimation of the human particle dose. *Environmental Science and Pollution Research*. 25 (13): 13103–13117.

Shah, S.A., Yoon, G.H., Ahmad, A., Ullah, F., Amin, F.U., Kim, M.O. 2015. Nanoscale alumina induces oxidative stress and accelerates amyloid beta protein production in ICR female mice. *Nanoscale.* 37: 15225-15237.

Simon-Deckers, A., Gouget, B., Mayne-L'Hermite, M., Herlin-Boime, N., Reynaud, C., Carrière, M. 2008. *In vitro* investigation of oxide nanoparticle and carbon nanotube toxicity and intracellular accumulation in A549 human pneumocytes. *Toxicology.* 253: 137–146.

Sjögren, B., Ulfvarson, U. 1985. Respiratory symptoms and pulmonary function among welders working with aluminum, stainless steel and railroad tracks. *Scandinavian Journal of Work, Environment & Health*. 11(1): 27-32.

Sliwinska, A., Kwiatkowski, D., Czarny, P., Milczarek, J., Toma, M., Korycinska, A., Szemraj, J., Sliwinski, T. 2015. Genotoxicity and cytotoxicity of ZnO and Al_2O_3 nanoparticles. *Toxico.l Mech. Methods.* 25(3): 176–183.

Smeenk, G., van Attikum, H. 2013. The chromatin response to DNA breaks: leaving a mark on genome integrity. *Ann. Rev. Biochem.* 82: 55-80.

Smith, M.N. 2016. The number of cars worldwide is set to double by 2040. World Economic Forum, Business Insider. www.weforum.org/agenda/2016/04/the-number-of-cars-worldwide-is-set-to-double-by-2040.

Smith, Z.D., Meissner, A. 2013. DNA methylation: roles in mammalian development. *Nat. Rev. Genet.* 14: 204–220.

Soria-Valles, C., Osorio, F.G., López-Otín, C. 2015. Reprogramming aging through DOT1L inhibition. *Cell Cycle*. 14 (21): 3345–3346.

Soshnev, A.A., Josefowicz, S.Z., Allis, C.D. 2016. Greater than the sum of parts: complexity of the dynamic epigenome. *Mol. Cell*. 62: 681-94.

Spezzati, G., Fant, K., Ahniyaz, A., Lundin-Johnson, M., Hensen, E., Langermans, H., & Hofmann, J. 2017. Synthesis, physicochemical characterization, and cytotoxicity assessment of ceo_2 nanoparticles with different morphologies. *European Journal of Inorganic Chemistry*. 2017(25): 3184-3190.

Stafford, N. 2008.Newer diesel engines emit more harmful nanoparticles. Chemistry World. www.chemistryworld.com/news/newer-diesel-engines-emit-more-harmful-nanoparticles.

Stavrovskaya, A.A., Potapova, T.V., Rosenblat, V.A., Serpinskaya, 1975. The effect of non-ionic detergent Tween 80 on colcemid-resistant transformed mouse cells in vitro. Int. J. Cancer.15: 665-672.

Stefaniak, A.B., Hackley, V.A., Roebben, G., Ehara, K., Hankin, S., Postek, M.T., Lynch, I., Fu, W.E., Linsinger T.P.J., Thunemann, A.F. 2013. Nanoscale reference materials for environmental, health and safety measurements: needs, gaps and opportunities. *Nanotoxicology*. 7: 1325–1337.

Stone, V., Shaw, J., Brown, D. M., MacNee, W., Faux, S. P., Donaldson, K. 1998. The role of oxidative stress in the prolonged inhibitory effect of ultrafine carbon black on epithelial cell function. *Toxicol. In Vitro*, 12: 649–659.

Strahl B.D. Allis, C.D. 2000. The language of covalent histone modifications. *Nature*. 403: 41–5.

Sun, C., Li, H., Chen, L. 2012. Nanostructured ceria-based materials: synthesis, properties, and applications. *Energy Envir. Sci.* 5: 8475-8505.

Szakal, C., Roberts, S. M., Westerhoff, P., Bartholomaeus, A., Buck, N., Illuminato, I., Canady, R., Rogers, M. 2014. Measurement of nanomaterials in foods: integrative consideration of challenges and future prospects. *ACS Nano.* 8: 3128–3135.

Tan, M., Luo, H., Lee, S., Jin, F., Yang, J. S., Montellier, E., Buchou, T., Cheng, Z., Rousseaux, S., Rajagopal, N., Lu, Z., Ye, Z., Zhu, Q., Wysocka, J., Ye, Y., Khochbin, S., Ren, B., Zhao, Y. 2011. Identification of 67 histone marks and histone lysine crotonylation as a new type of histone modification. *Cell*. 146(6): 1016-28.

Tanaka, T., Narazaki, M., Kishimoto, T. 2017. IL-6 Superfamily. Cavaillon, J.-M., Singer, M. (eds). *Inflammation: From Molecular and Cellular Mechanisms to the Clinic*. Wiley-VCH.

Tarnuzzer, R.W., Colon, J., Patil, S., Seal, S. 2005 Vacancy Engineered Ceria Nanostructures for Protection from Radiation-Induced Cellular Damage. *Nano Letters. 5*(12): 2573-2577.

Teschendorff A.E., West J., Beck S. 2013. Age associated epigenetic drift: implications, and a case of epigenetic thrift? *Hum. Mol. Genet.* 22(R1): R7-R15.

Thirlwell, C., Eymard, M., Feber, A., Chestendorff, A., Pearce, K., Lechner, M., Widschwendter, M., Beck, S. 2010. Genome-wide DNA methylation analysis of archival formalin-fixed paraffin-embedded tissue using the Illumina Infinium Human Methylation 27 Bead Chip. *Methods*. 52: 248-54.

Trovarelli, A. 1996. Catalytic properties of ceria and CeO_2-containing materials. *Catal. Rev.*: *Sci. Eng*. 38(4): 439−520.

Tumburu, L., Andersen, C., Rygiewicz, P., Reichman, J., 2017. Molecular and physiological responses to titanium dioxide and cerium oxide nanoparticles in *Arabidopsis.* Environmental Toxicology and Chemistry. 36(1): 71–82.

Upadhyay, S., Sharma, N., Gupta, K.B., Dhiman, M. 2018. Role of immune system in tumor progression and carcinogenesis. *J. Cell Biochem.* 119**:** 5028–5042.

U.S. Department of Energy (USDOE), Energy Information Administration (EIA). 2014 Diesel Fuel Explained. Available at http://www.eia.gov.

Vakana, E., Arslan, A.D., Szilard, A., Altman, J.K., Platanias, L.C. 2013. Regulatory effects of sestrin 3 (SESN3) in BCR-ABL expressing cells. *PLoS ONE*. 8(11): e78780.

Valero-Jime´nez, A., Zuniga, J., Cisneros, J., Becerril, C. , Salgado, A., Checa, M., Buendı´a-Rolda´n, I., Mendoza-Milla, C., Gaxiola, M., Pardo, A., Selman, M. 2018. Transmembrane protease, serine 4 (*TMPRSS4*) is upregulated in IPF lungs and increases the fibrotic response in bleomycin-induced lung injury. *PloS one*. 13(3): e0192963.

Valko, M., Leibfritz, D., Moncol, J., Cronin, M. T. D., Mazur, M., Telser, J. 2007. Free radicals and antioxidants in normal physiological functions and human disease. *International Journal of Biochemistry & Cell Biology*. 39(1): 44–84.

Vandiver, A.R., Irizarry, R.A., Hansen, K.D., Garza, L.A., Runarsson, A., Li, X., Chien, A.L., Wang, T.S., Leung, S.G.,Kang, S., Feinberg, A.P. 2015. Age and sun exposure-related widespread genomic blocks of hypomethylation in nonmalignant skin. *Genome Biol.* 16: 80.

Van Hoecke, K., Quik, J.T.K., Mankiewicz-Boczek, J., De Schamphelaere, K.C., Elsaesser, A., Van der Meeren, P. 2009. Fate and effects of CeO_2 nanoparticles in aquatic ecotoxicity tests. *Environ. Sci. Technol.* 43: 4537–4546.

Van Meerbeeck, J.P., Fennell, D.A., De Ruysscher, D.K.M. 2011. Small-cell lung cancer. *Lancet*, 378: 1741-1755.

Vann, K.R., Kutateladze, T.G. 2017. Histone H3 dual ubiquitylation mediates maintenance DNA methylation. *Mol. Cell.* 68(2): 261-262.

Vannini, F., Kashfi, K., Nath, N. 2015. The dual role of iNOS in cancer. *Redox Biol*. 6: 334-43.

Van'T Hof, R. J., Ralston, S. H. 2001. Nitric oxide and bone. *Immunology*. 103: 255-261.

Vlaming, H., van Leeuwen, F. 2016. The upstreams and downstreams of histone H3K79 methylation by *Dot1L*. *Chromosoma*. 125: 593-605.

Voelcker, J. 2014. 1.2 Billion vehicles on world's roads now, 2 billion by 2035: Report. Green Car Reports.

Waddington, C.H. 1942. The epigenotype. *Endeavour*. 1:18-20.

Wang, X., Chen, C.W., Armstrong, S.A. 2016. The role of *DOT1L* in the maintenance of leukemia gene expression. *Curr. Opin. Genet. Dev*. 36: 68–72.

Wang, Y, Xiong, L., Tang, M. 2017. Toxicity of inhaled particulate matter on the central nervous system: neuroinflammation, neuropsychological effects and neurodegenerative disease. *J. Appl. Toxicol*. 37: 644–667.

Watanabe, S., Limori, M., Chan, D.V., Hara, E., Kitao, H., Maehara, Y. 2018. MDC1 methylation mediated by lysine methyltransferases EHMT1 and EHMT2 regulates active ATM accumulation flanking DNA damage. Scientific Reports, Nature Publisher Group: London 8: 1-12.

Xia, T., Kovochich, M., Liong, M., Mädler, L., Gilbert, B., Shi, H., Yeh, J.I., Zink, J.I., Nel, A.E. 2008. Comparison of the mechanism of toxicity of zinc oxide and cerium oxide nanoparticles based on dissolution and oxidative stress properties. *ACS Nano*. *2* (10): 2121-2134.

Xiong, Y., Li, F., Babault, N. Dong, A., Zeng, H., Wu, H.,, X., Arrowsmith, C.H., Brown, P.J., Liu, J., Vedadi, M., Jin, J. 2017. Discovery of potent and selective inhibitors for G9a-like protein (GLP) lysine methyltransferase. *J. Med. Chem*. 60(5): 1876-1891.

Yang, W., Peters J. I., Williams, R.O. 2008. Inhaled nanoparticles - A current review. *Int. J. Pharm*. 356: 239–247.

Yang, D., Thangaraju, M., Greeneltch, K., Browning, D.D., Schoenlein, P.V., Tamura, T., Ozato, K., Ganapathy, V., Abrams, S.I., Liu, K. 2007. Repression of IFN regulatory factor 8 by DNA methylation is a molecular determinant of apoptotic resistance and metastatic phenotype in metastatic tumor cells. *Cancer Res*. 67(7): 3301–9.

Yang, Z., Li, C., Liu, H., Zhang, X., Cai, Z., Xu, L., Luo, J., Huang, Y., He, L., Liu, C., Wu, S., 2017. Single-cell sequencing reveals variants in ARID1A, GPRC5A and MLL2 driving self-renewal of human bladder cancer stem cells. *Eur. Urol*. 71: 8-12.

Zamkov, M. A., Conner, R.W., Dlott, D.D. 2007. Ultrafast chemistry of nanoenergetic materials studied by time-resolved infrared spectroscopy: aluminum nanoparticles in Teflon. *The Journal of Physical Chemistry* C. 111(28): 10278-10284.

Zamkova, M. A., Khromova, N., Kopnin, B.P., Kopnin, P. 2013. Ras-induced ROS upregulation affecting cell proliferation is connected with cell type-specific alterations of HSF1/SESN3/p21Cip1/WAF1 pathways. *Cell Cycle*. 12(5): 826–36.

Zelco, I.N., Mariani, T.J., Folz, R.J. 2002.Superoxide dismutase multigene family: a comparison of the CuZn-SOD (SOD1), Mn-SOD (SOD2), and EC-SOD (SOD3) gene structures, evolution, and expression. *Free Rad. Bio. Med*. 33(3): 337-349.

Zhang, J., Lee, K.B., He, L., Seiffert, J., Subramaniam, P., Yang, L., Chen, S., Maguire, P., Mainelis, G., Schwander, S., Tetley, T., Porter, A., Ryan, M., Shaffer, M., Hu, S., Gong, J., Chung, K.F. 2016. Effects of a nanoceria fuel additive on the physicochemical properties of diesel exhaust particles. *Environmental Science: Processes & Impacts* 10: 1333-1342.

Zhou, Y., He, C.H., Yang, D.S., Nguyen, T., Cao, Y., Kamle, S., Lee, C.-M., Gochuico, B.R., Gahl, W.A., Shea, B.S., Lee, C.G., Elias, J.A. 2018. Galectin-3 interacts with the CHI3L1 axis and contributes to Hermansky–Pudlak Syndrome lung disease. *J. Immunol.* 200: 2140-2153.

Zhu, K., Devesa, S., Wu, H., Zham, S., Jatoi, I., Ander son, W., Peoples, G., Maxwell, L., Granger, E., Potter, J., McGlynn, K. 2009. Cancer incidence in the U.S. military population: comparison with rates from the SEER program. *Cancer Epidemiol. Biomarkers Prev.* 18(6): 1740-1745.

Zoroddu, M.A., Medici, S., Ledda, L., Nurchi, V.M., Lachowicz, J.I., Peana, M. 2014. Toxicity of nanoparticles. *Curr. Med.Chem*. 21(33): 3837–3853.